NTNU – Trondheim
Norwegian University of
Science and Technology

Multilevel Converters for a 10 MW, 100 kV Transformer-less Offshore Wind Generator System

Tor Martin Iversen

Master of Energy and Environmental Engineering
Submission date: June 2012
Supervisor: Tore Marvin Undeland, ELKRAFT
Co-supervisor: Sverre Skalleberg Gjerde, ELKRAFT

Norwegian University of Science and Technology
Department of Electric Power Engineering

Problem Description

Title: Multilevel Converters for a 10 MW, 100 kV Transformer-less Offshore Wind Generator System

Background

Offshore wind energy has a large potential, and power ratings in offshore wind turbines are reaching for 10 MW. When the turbine size increases, the nacelle weight reduction becomes a key element. A new module-based generator concept that omits both the gear box and the transformer, and by that creates a lightweight turbine solution, is under development in a PhD-project. The new concept utilizes a special permanent magnet synchronous generator with nine converter modules in series to obtain a 100 kV DC voltage output.

The basis for this master thesis is the master specialization project from the fall of 2011, which presents the modular multilevel converter (MMC) as the most interesting candidate for the proposed concept. To verify the MMC topology as a realistic candidate, further studies are required.

Expected outcome of the project:

The work should continue the comparison of the MMC and a conventional two-level converter, with respect to their suitability for the proposed concept. The list of criteria includes voltage quality, harmonic content, DC voltage ripple and filter demands. The simulations performed in the specialization projects were simplified and ideal. A natural delvelopment of these models should include control challenges revealed in the specialization project, i.e. voltage balancing control and redundancy. The MMC should also be implemented in the full scale simulation models from the PhD-project.

The student will work with PhD-candidate Sverre S. Gjerde, who will be the main contact person. He started his PhD-work during fall 2009.

Responsible supervisor will be professor Tore Undeland.

Abstract

Multilevel Converters for a 10 MW, 100 kV Transformer-less Offshore Wind Generator System

The size of offshore wind generators is increasing, and the trend is moving towards full converter gear-less solutions with permanent magnet synchronous generators (PMSG). The nacelle weight reduction is a key design criterion for offshore wind turbines. To overcome the weight challenge, a transformer-less concept is under development. This concept employs a special PMSG with an innovative high insulation level between the groups of windings. The generator supplies nine series connected converter modules, which results in a high voltage DC output of 100 kV, reducing the total weight of the system.

Conventional three phase 2-level voltage source converters, each with 11.1 kV output, are utilized in concept studies and simulations. However, other voltage source converter topologies are assumed to be more beneficial in terms of efficiency, voltage quality and reliability issues. This work compares multilevel converter topologies with regards to their suitability for the proposed concept.

The result of an initial study is that the modular multilevel converter (MMC) is the most promising candidate. The MMC adds more components and complexity to an already intricate system, but gives benefits that are in line with many of the ideas behind the proposed concept. A modular structure grants the easiest expansion to a high number of levels, providing a high-quality voltage with less demand for filters to save both volume and weight. The MMC also offers redundancy possibilities for higher reliability, which is important in offshore wind power installations.

PSCAD/EMTDC simulation models have been built, implementing voltage balancing and redundancy control. The simulations have also investigated the functionality of the converter in the proposed system. The results show that the MMC performs well in the full system, and is therefore considered as a viable candidate. The number of levels needed is at least five to avoid series connection of IGBTs. Further studies should find an optimal number of levels, depending on the generator specifications, the desired level of losses, voltage quality and a weighting of reliability versus complexity.

Sammendrag

Flernivåomformere for et 10 MW, 100 kV transformatorløst offshore vindgeneratorsystem

Ytelsen på vindkraftturbiner er i kontinuerlig vekst, og strekker seg i dag mot 10 MW. Trenden viser økt bruk av turbiner designet for variabel hastighet og permanentmagnet synkrongeneratorer (PMSG) med fullomformerløsninger. I design av store turbiner er nacellevekten avgjørende. Et helt nytt turbinkonsept er derfor under utvikling ved NTNU. Konseptet benytter en veldig spesiell PMSG og ni seriekoblede omformere, som til sammen gir en DC-spenning på 100 kV. En vektreduksjon oppnås ved å unngå både girboks og transformator i nacellen.

Konvensjonelle trefaset tonivåomformere er brukt i innledende studier og simuleringer av systemet med ni omformermoduler. Tonivåomformeren er mye brukt i systemer med lavere spenning, men på grunn av det høye spenningsnivået resulterer en bruk av tonivåomformere i en seriekobling av transistorer. Dette er uønsket. I tillegg er det grunnlag for å tro at andre omformertopologier har bedre egenskaper innen effektivitet, spenningskvalitet og pålitelighet.

Et forstudie har pekt ut en modulær multinivå omformer (MMC) som det mest interessante alternativet til konvensjonelle løsninger. MMC gir fordeler som økt spenningskvalitet, redusert filtrering, lavt harmonisk nivå og økt pålitelighet i form av redundans. Denne masteroppgaven omfatter en grundigere studie av MMC-omformeren og dens anvendbarhet i det nye turbinkonseptet. PSCAD-simuleringer er brukt i en grundig sammenligning mot tonivåomformeren, både i enkeltstående MMC-modeller og i et komplett vindturbinsystem. Utfordringer med spenningsbalansering og redundans har blitt nøye studert.

Resultatene viser at en MMC fungerer veldig godt i det foreslåtte turbinkonseptet, og bedre enn tonivåomformeren med tanke på spenningskvalitet og pålitelighet. På grunn av spenningsnivået behøves minst 5 nivå. Det optimale antall nivå avhenger av ønsket grad av redundans, generatorspesifikasjoner og en optimalisering og veining mellom ønsket spenningskvalitet, tap, vekt, volum og kompleksitet.

Preface

This master's thesis is the final part of the electrical power engineering master programme at NTNU. Looking back on my first years, I remember thinking of master students as very serious and hard-working, with no spare time for all the fun we as first year students had. And the infamous master thesis! At that time it seemed so terrifyingly far away, both in time and amount of knowledge. This master's thesis is therefore a proof of that I've made it through these five years, and a symbol of my great gratitude towards NTNU and Trondheim as a student city. The work has given me a good background in the field of power electronics, but also provided an important exercise in individual project discipline.

The fact that I find the topic very interesting has raised my motivation and eased the work. I would like to point out some people that have provided great inspiration and help in the writing of this thesis.

First I would like to thank my co-supervisor Sverre S. Gjerde for all the help and support in understanding the concept, help with paper-writing and presentations, and for being available and patient, despite all my silly questions.

Jon Are Suul has also been very supportive regarding programming and simulations in PSCAD. Thanks also to Pål Keim Olsen for explaining the generator concept. The other guys in the study room and my fellow master students all deserve big thanks for all the fun and support during my studies.

Finally, I sincerely thank Professor Tore Undeland, my supervisor. It was because of him and his introduction course in power electronics, that I got interested in this field of power engineering. He has been a true inspiration.

Trondheim, 20^{th} of June 2012

Tor Martin Iversen

Contents

List of Figures

List of Tables

Abbreviations

A-NPC Active Neutral Point Clamped

CHB Cascaded H-Bridge

CSC Current Source Converter

CTL Cascaded Two-Level

DFIG Doubly Fed Induction Generator

DQ Direct, Quadrature

FCC Flying Capacitor Converter

HVDC High Voltage Direct Current

MMC Modular Multilevel Converter

NPC Neutral Point Clamped

PCC Point of Common Coupling

PMSG Permanent Magnet Synchronous Generator

pu Per Unit

PWM Pulse Width Modulation

SHE Selective Harmonic Elimination

SVM Space Vector Modulation

THD Total Harmonic Distortion

VAr Volt Ampere reactive

VSC Voltage Source Converter

Chapter 1

Introduction

1.1 Background and motivation

The increasing demand for electricity, combined with the necessity of reducing the CO_2-emissions is one of the greatest challenges of this century. There is a need for green energy, and the worldwide energy sector faces a huge public responsibility. A responsibility of not only providing the possibility for continuous growth in living standards, but also securing that the growth has a certain sustainability. In addition to a greener utilization of fossil fuels like oil and gas, the use of renewable energy sources will be an important contribution to the energy mix.

The extraction of oil and gas has also given a positive contribution. It has pushed the technology in most disciplines of engineering. In electrical engineering the main results are increased power handling of electrical drives to provide power to offshore compressors and pumps, and a significant reliability improvement of many components. As a consequence of this technology advance in oil and gas, high quality components and systems are developed. These components are also fit for use in other fields - for instance renewable energy.

The idea of supplying offshore installations from shore is not only politically driven as a result of global warming. It also requires a certain willingness to make it happen. Oil companies made several attempts during the 80's and 90's, but it was a demanding political process, and failed due to big footprint [7]. The Troll A installation is now fully electrified from shore, being the largest oil platform in the North Sea this saves CO_2-emissions in the range of 100,000 to 150,000 tonnes per year [8].

Using renewable energy solutions like offshore wind, would give a green contribution to the electrification. One idea is to connect offshore wind farms and offshore installations.

1.1.1 Offshore wind

The world market for wind turbines in general continues with exponential growth, and it experienced another record in the year 2011. The total worldwide capacity of wind power worldwide has become 239 GW, which covers 3 % of the worlds electricity demand [5].

The planning of large-scale onshore wind farms have in many cases met great opposition, often due to the fact that onshore wind farms results in a significant footprint. In Norway, large plans have have been delayed or cancelled because of political protests and demonstrations.

Offshore wind is a relatively new approach to the generation of green electricity. Moving the electrical power generation offshore gives several benefits, but has a comprehensive list of challenges. This includes mechanical influence, fatigue, transport and assembly, electrical grid design and maintenance issues due to the scarce availability. As mentioned in section 1.1, several technical advancements in oil and gas applications have resolved challenges in offshore installations. Offshore wind power has because of this become even more technically and economically possible. The use of offshore wind is steadily increasing: 1.2 GW was installed in 2010, resulting in a worldwide total of 3.1 GW, and a share of 1.6 % of the total wind capacity [9].

Table 1.1: Countries with offshore wind 2010 [5]

Pos.	Country	Capacity [MW]	Added 2010 [MW]
1	United Kingdom	1341	653
2	Denmark	854	190.4
3	Netherlands	249	2
4	Belgium	195	165
5	Sweden	164	0
6	China	123	100
7	Germany	108.3	36.3
8	Finland	30	0
9	Ireland	25	0
10	Japan	16	15
11	Spain	10	0
12	Norway	2.3	0
	Total	3117.6	1161.7

Table 1.1 shows the twelve countries that have realized offshore wind projects. Noteworthy European offshore projects are Sheringham Shoal (U.K. 315 MW) and the many projects north of Germany; BorWin, DolWin, HelWin. Doggerbank (U.K. 9000 MW) is under develeopment. Even though Norway is on the bottom of the list in table 1.1, the two Norwegian companies Statoil and

Statkraft are involved heavily in both Sheringham Shoal and Doggerbank.

President Dr. He Dexin of the World Wind Energy Association has highlighted some of his observations [5]:

> *"Wind power has become - as a low-cost, low-risk and non-polluting energy option - a pillar of the energy supply in many countries. These countries have been able to create new industries and hundreds of thousands of jobs. Other countries should learn from this experience and also set up the right policies."*

Dr. Dexin includes a new point for consideration, namely the labour market. This is especially important in developing countries and countries with high unemployment rates. Other benefits of offshore wind generation are:

- The wind is stronger and more stable offshore than onshore because of the terrain topology.
- An increase in the average wind speed will give a significant increase in power [10]: $P_{wind} = \frac{1}{2}\rho A U^3$.
- Transportation is not dependent of a road network capable of handling huge loads as wind turbines are getting heavier. This reduces the ecological impact, and the footprint is smaller.
- An offshore wind farm is, because of the Earth's curvature, not visible from shore.
- The audible noise is not that prominent offshore.

The work of this thesis will not focus on the political or economical aspects of wind energy conversion systems. It is however important to point out that political support in the development is crucial. Examples of politically generated support is the green certificates [11], or government supported incentives in renewable energy.

1.2 Relation to the Specialization Project

This master thesis is a continuation from a specialization project, which was written during the fall of 2011. The specialization project report was titled "Converter Topologies for Enhanced Performance of Wind Turbine Generators". The span of this thesis grasps much of the same topic as the specialization project. Some of the material from the project report has therefore been used in order to form a more independent thesis. The actual sections are listed below.

- Section 2.4: DC Link and DC Grid
- Section 3.3: The Multilevel Concept
- Section 3.5: Multilevel Topologies

- Section 3.6: Comparison and Choice of Topology
- Section 3.4: Multilevel Modulation Strategies

Since the focus on this thesis has concentrated on the Modular Multilevel Converter (MMC) topology, this material includes much of the literature review on the other converter topologies. The description of the MMC have been updated and restructured.

1.3 Scope of work

When a specific converter topology was chosen during the specialization project for a more narrow study, some challenges and questions about the topology still remained. A superior goal for the continuation work of this master thesis has therefore been to study these challenges in depth. This section presents the selected focus points for the master thesis.

The proposed wind turbine concept presented in Chapter 2 includes a generator topology with nine series connected converters. The main argument for this topology is to create a reliable, low weight solution without transformer. It is worth to notice that the main focus of this work is on one of the converter modules, and its suitability to the proposed concept.

There is a focus on the control of the converter module. The simulation models have therefore been upgraded from those used in the specialization project. Challenges with drifting capacitor voltages are included, and a balancing block has been programmed in PSCAD. A redundancy case is also included in the simulations.

In the specialization project, an implementation of the selected converter topology into the full system is mentioned as a necessary next step. A full system simulation model is therefore included, to see if the MMC performs as expected in the proposed concept. The full model in PSCAD is limited by the educational licence. The tendencies are still believed to be representative for a complete simulation model.

The results from this work does not involve laboratory results, but are solely based on simulations in PSCAD. A consequence of this is the exclusion of loss calculations for comparison against real-life losses. Practical issues regarding detailed mechanical support structures is not thoroughly studied. Nor is detailed estimates of weight.

The report is organized as follows. Chapter 2 gives an overview of the proposed concept. In Chapter 3, the studied voltage source converter (VSC) topologies are described. A topology is chosen for further study, and a closer look at the most interesting topology is performed in Chapter 4. This gives the basis for

the simulations described in Chapter 5. Finally, the conclusions and scope of further work are summarized in Chapter 6 and 7.

1.4 Presentations and publication of results

A presentation of the specialization project, and some of the results from this master thesis, was given at the Technoport Renewable Energy Research Conference which took place in Trondheim 16-18th of April 2012. The abstract is printed in the conferences' book of abstracts [12]. See appendix D.

A paper based on this thesis was accepted for a lecture presentation at the EPE Joint Wind Energy and T&D Chapters Seminar in Aalborg, Denmark 28th and 29th of June 2012. The title is the same as this thesis, and the paper has the following co-authors: Sverre Skalleberg Gjerde (NTNU) and Tore Undeland (NTNU). The paper will be made available through the IEEE Explore website. See appendix E.

Chapter 2

The proposed turbine concept

This chapter presents first the conventional wind turbine drive train solution. The intention is to highlight some of the challenges with the conventional design in terms of weight and reliability. A new, lightweight and reliable concept is then presented.

2.1 The conventional solution

The doubly-fed induction generator (DFIG) is today the most popular generator solution in offshore wind applications, and stands for almost 50 % of all operational generators [13]. A sketch of the solution is shown in figure 2.1.

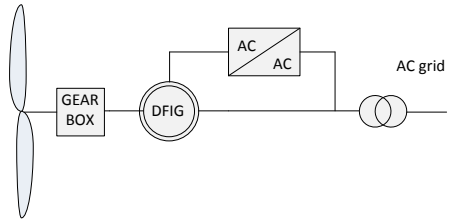

Figure 2.1: Standard DFIG structure

The DFIG solution consists of:

- A gear box to step down the rotational speed.
- A doubly fed induction generator.
- A proportionally rated AC/AC converter to control the excitation of the machine

- A step-up transformer, located either in the nacelle or in the foundation of the turbine.

The gear box has a reputation of being a troublesome component, especially in offshore wind turbines where the reliability is very important. In a swedish survey on failures in wind turbines between 1997 and 2005, the gear box is one of the main reasons for wind turbine failures. The gear box was in fact the cause for 20 % of the downtime for a typical turbine [14]. The average repair time for a gear box is said to be 256 hours, but the survey is concentrating on onshore systems where the availability is much better than offshore. The repair time of a gear box offshore is therefore believed to be longer. In addition, the gear box is a large and heavy mechanical unit, which has to be mounted and replaced in one piece. This means that one of few existing crane vessels has to be brought to the site. The repair time will not only influence large components like the gear-box. Electrical components that are relatively easy to replace manually in onshore turbines, will have a much longer repair-time offshore. The repair time will also depend on the weather conditions to a larger extent than onshore.

The gear box is therefore one of the reasons why the use of permanent magnet generator machines is increasing.

2.1.1 Trend towards permanent magnet machines

The average generator size in offshore wind turbines is increasing, and is today 3.8 MW [13]. The main reason for the increase in size, is that it is more convenient in terms of infrastructure, transport, assembly and maintenance, to use few large wind turbines instead of many small. The trend in offshore wind is leaning towards a permanent magnet synchronous generator (PMSG) solution [13]. The classical PMSG solution is shown in figure 2.2, and consists of:

- A permanent magnet synchronous generator.
- A full converter back-to-back.
- A step up transformer connected to the grid.

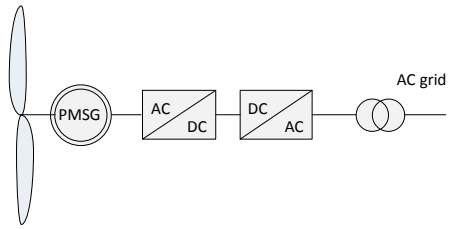

Figure 2.2: Standard PMSG structure

Using a permanent magnet machine offers some advantages that are very useful compared to a DFIG-solution:

- Direct driven without need for gearing.
- Less maintenance; no brushes nor slip-rings.
- Increased reliability.
- Increased efficiency in the whole range of wind speeds [13].

Firstly, because of the permanent magnet rotor excitation, the number of poles can be much higher than for the induction machine. The greater number of poles enables the direct driven low speed operation of the turbine. A gear box is therefore avoided. Equation 2.1 describes the relationship between the synchronous rotational speed n_{sync} in RPM, the electrical frequency f_e and the number of poles in the machine. If the electrical frequency is said to be constant, it is evident from equation 2.1 that the number of poles must increase when the rotational speed is decreased.

$$n_{sync} = \frac{120 f_e}{p} \tag{2.1}$$

Secondly, the PMSG has no slip-rings nor brushes that needs maintenance. Reducing the need for maintenance increases the time between service, which is beneficial since the accessibility is much worse offshore than onshore. In addition, a comparison in [13] show that both low-speed and medium-speed PMSGs have superior efficiency to the other generator solutions. The efficiency is also increased over a larger span in wind speeds.

The disadvantages with PMSGs are related to political and environmental issues, and the price. China is today the largest exporter of the material NdFeB, and the price is very high. A fair question is therefore; is the reliability advantage in gear-less turbine significant enough to justify the price.

If a standard PMSG solution is chosen, the system is more reliable and more efficient. For larger turbines, it is believed that the weight is reduced with PMSGs. This because the relative weight of a gear box increases more rapidly than for a permanent magnet generator when the torque and size increases. However, as seen in figure 2.2, the step-up transformer is still included. This is due to the large power handling of the generator, and the relatively low voltage. The standard industrial voltage of 690 V is low in the megawatt segment. This results in a very high current which needs to be transferred down the tower, see equation 2.2.

A simple calculation shows the maximal output current from a 10 MW generator with conventional 690 V output voltage:

$$I_{ac,0.690kV} = \frac{P}{\sqrt{3} \cdot U} = \frac{10 \text{ MW}}{\sqrt{3} \cdot 690 \text{ V}} = 8.4 \text{ kA} \tag{2.2}$$

As seen from equation 2.2, a considerable current has to be transferred, and bulky cables are needed if the transformer is to be mounted in the foundation. This is seldom practical, and therefore the transformer for large offshore turbines is placed in the nacelle. The use of bulky cables is not just a weight issue. Cables from the nacelle and down have to be flexible enough to handle the yaw control of the turbine.

The voltage output from the generator should therefore be increased in order to reduce the current, reduce the losses and to omit the transformer in the nacelle.

2.2 The low-weight, high voltage solution

To reduce the nacelle weight, a new generator concept is under development. This is presented in [15], [16], and a sketch of the concept is included in figure 2.3. The system consists of a special permanent magnet synchronous generator with nine sets of 3-phase windings. Each winding set is electrically separated from the others, and supplies a three phase converter module. Each converter module produces an output DC voltage of 11.1 kV, and the stack of modules are series connected to obtain a desired DC voltage of 100 kV.

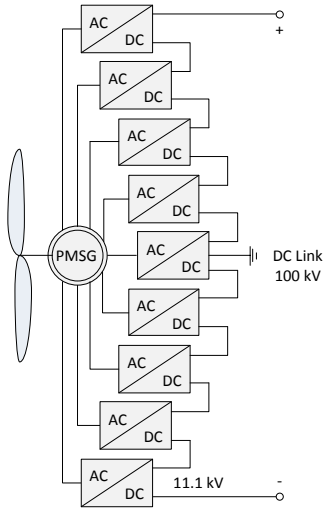

Figure 2.3: The proposed generator structure

As seen in figure 2.3, both the gear box and the step up transformer is now replaced by a special PMSG- and converter structure. The weight reduction is a direct result of the special solution. Even though the permanent magnet generator is large, and the concept introduces many more converters, the total weight is assumed to be significantly reduced. There are a few arguments for this:

- The transformer and gear is omitted.
- The generator is built by composite materials instead of cast steel, and is therefore lighter than a corresponding induction machine. The generator mass is typically 20-30 % of the equivalent iron-cored systems [17].

The structure is stripped for two heavy components, and is by that simpler. The converter part seems at first glance more complex, but it is actually not that intricate - compared to the alternative. Because of component limitations at the desired power and voltage rating, a single two-level full-converter structure would also need both series- and parallel connections to handle the power rating. So if a complex structure is unavoidable, the challenge is to make up for this complexity in a reliable design. This is indeed one of the intentions with the proposed system [18]. With a more complex system comes more complex support structures. A detailed study of weight and size is not included in this thesis. It is therefore difficult to estimate the details around the structural dimensioning of the wind turbine.

2.2.1 Reduced current

A simple calculation shows the current reduction achieved when introducing the high voltage output from the converter:

$$I_{dc,100kV} = \frac{P}{U} = \frac{10 \text{ MW}}{100 \text{ kV}} = 100 \text{ A} \tag{2.3}$$

As shown, the high DC-voltage results in a considerably lower current, thus reducing the cable size needed and the transmission losses. Smaller cables will also give a weight reduction, and simpler assembly.

2.3 Wind turbine control system

The aim in power electronic systems is to control the energy transfer from the source to the grid. To fully exploit the possibilities in any types of power electronics, good control strategies are needed. Types of control strategies are for instance mechanical control in variable speed turbines, or the balancing of the capacitor voltages in an MMC.

This chapter describes the control strategies used in the proposed wind turbine system.

2.3.1 Operation target

In the wind turbine system, the control system is constructed with basis on the following:

- Maximum Power Point Tracking (MPPT)
- Balanced DC link voltage
- Reduction of direct axis current to minimize the losses

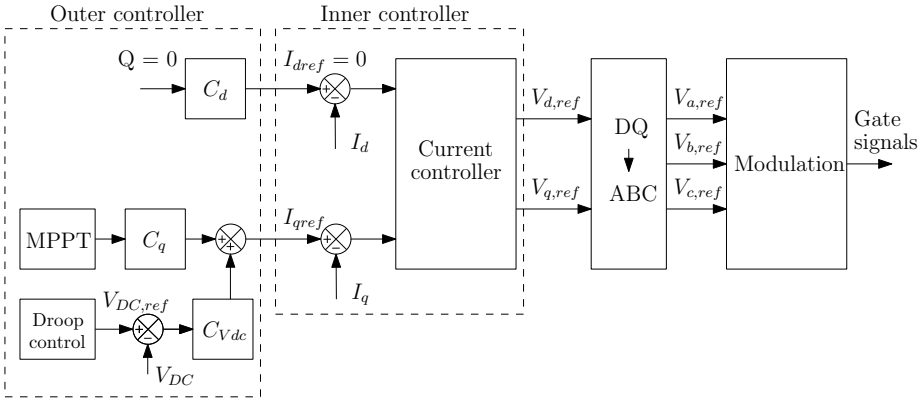

Figure 2.4: Overview of the complete control system for the proposed structure. Main elements: Voltage controller (outer controller), Current controller (inner controller) and the modulation block.

2.3.2 Outer controller

Controlling the turbine with an MPPT controller [19] is an alternative to more mechanical control methods, like pitch control with wind measurements. The MPPT method uses the rotor speed measurement as input, and calculates the optimal power output from the turbine. This is compared to the actual generator power output, and the error is used to control the quadrature axis current reference. Indirectly this controls the torque [20]. The MPPT implemented in the system, utilizes measurements of power output and rotational speed, so wind measurements are unnecessary. External components as anemometers are therefore avoided, thus increasing the reliability. Another benefit is that the control system follows the proposed system's idea of module-based construction, for simplified customization.

The balancing of the DC voltage of each converter module ensures the stable DC link voltage. This is added as an adjustment of $I_{q,ref}$ as seen in figure 2.4. A reference DC voltage, $V_{DC,ref}$, is compared to the measured DC voltage V_{DC}. The reference voltage calculation of each converter module should take into consideration the possibility of a module break down, i.e. operation with n-1 converters. Detailed description of the DC link controller is found in [15], while the droop control is described in [16].

To minimize resistive losses, and thus maximizing the efficiency of the turbine,

the current reduction is preferred. While the q-axis current controls the torque, the d-axis current reference is set to zero to minimize the current [20].

2.3.3 Current controller

The inner controller uses a conventional vector control principle with PI-controllers, which is extensively covered in literature [21], [22]. Figure 2.5 shows the inner controller, the current controller.

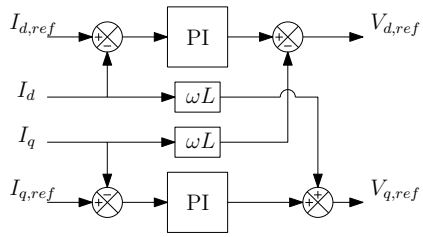

Figure 2.5: A more detailed block diagram of the inner controller of figure 2.4.

The tuning of inner PI current controllers follows the criterion of modulus optimum, as described in [23].

2.3.4 DQ-transformation to modulation

The inner controller gives the voltage reference signal referred to rotating direct and quadrature axes. This signal has to be transformed into a,b and c phase values before fed into the modulation block.

A principal description and derivation of DQ-transformation can be found in Appendix A.

The modulation block in figure 2.4, represents the last control operation in the converter. The input from the current controller is the reference voltage, $V_{abc,ref}$. The block can employ different modulation strategies, calculating the gate signals for the switches in the converter. Different modulation strategies are described in 3.4.

2.4 DC link and grid

HVDC transmission systems are increasing in popularity, and advanced converter technology is today included in long distance cable systems both onshore and offshore. The conventional connection to offshore wind farms is done with

AC, which is unproblematic when the wind farm is close to shore, and relatively small in size. In [24], the different challenges in connecting an offshore wind farm to shore are highlighted. With an increasing size and distance from shore, a DC connection is not only preferable but also necessary. The rating of AC-cables is limited, and Static VAr-compensation is needed both offshore and onshore. A converter station is then placed in the wind farm; normally connecting multiple AC feeds from the wind turbines, with a DC connection to shore.

A complete DC grid is also possible, and it is discussed whether a "DC supergrid" can be built or not. There are many challenges regarding DC breakers and fault handling, and the cost of such an offshore network would be enormous [24]. Since the proposed concept supplies a HVDC output, the converter station platform could be avoided, and the turbine directly integrated in a HVDC supergrid. A cost reduction is therefore possible, as the converter station is expensive.

The lack of DC-breakers has been a real argument against the DC grid. ABB claims the existence of DC breaker technology [25]. This is an indication of that the DC breaker might be commercially available in the future.

2.5 High voltage insulation

One of the challenges in many high voltage designs, and also this concept, is the electric insulation. This applies for both the generator and in every module. A high voltage difference between either the windings and ground, or one module and ground requires a good insulation to prevent breakdown. One benefit with this insulation screen is the size-reduction of the generator because of increased breakdown strength. The insulation system of the generator is described in [26].

Insulation design is not included in the scope of this work, but it is an important issue which needs further research - and therefore mentioned.

2.6 Converter module

The focus of this work is as mentioned in section 1.3, on one converter module in the proposed structure shown in figure 2.3. A standard two level VSC is utilized in preliminary studies, but this topology suffer from relatively poor voltage quality and a high capacitor volume. It does not include redundancy possibilities, so the reliability depends upon a well known and proven topology. Series connection of transistors is also necessary because of the high DC-voltage link.

Table 2.1 shows the most important specifications for one of the converter modules.

Table 2.1: The propoced concept - key specifications

Rated total generator power	10 MW
Rated converter module power	1.1 MW
# 3 phase moules	9
Converter rated voltage	11.1 kV
Total DC link voltage	100 kV
Generator insulation	±50 kV
Converter module insulation	±50 kV

Multilevel converter topologies could be a good alternative in this concept. They can provide an increased voltage quality, redundancy possibilities, less filtering and distributed capacitors.

With a great number of AC/DC converters in series, the voltage quality of the DC link is highly affected by the DC voltage quality in each converter. There is however a benefit of this. The ripple in the DC-link can be smoothed by shifting the voltage conversion between each of the converter modules in the stack. Since this work focuses on one converter module instead of the whole structure, this is not further discussed.

If a multilevel converter topology is to be a serious alternative to the conventional two-level converter, it must satisfy the following criteria:

- No series connection of IGBTs.
- High voltage quality, low harmonic distortion.
- High reliability, redundancy possibilities.
- Reduced DC-link capacity.
- Preserve the total generator-converter system responce.

Chapter 3

Voltage Source Converters

3.1 Introduction

The use of Voltage Source Converters (VSC) is the state-of-the-art method of converting and transmitting electrical power. Traditionally, Current Source Converters (CSC) were preferred in HVDC transmission because of lower losses and higher transmission capabilities. But due to recent advancements in component design, VSCs are now used in numerous power electronic applications, and give several benefits. Some of these are:

- Easier bidirectional power flow
- Faster responce because of active switches (IGBTs)
- Better control of active and reactive power

This chapter describes first the standard two-level VSC before introducing the concept of multilevel converters in section 3.3. A study of the most popular multilevel topologies is presented in section 3.5. A comparison, and a choice of converter topology for further study is summarized in section 3.6.

3.2 Standard two-level VSC

The standard two-level VSC is the baseline converter, and is widely used in numerous applications. It has the simplest structure of the three-phase converters, and consists of six IGBTs with diodes in anti-parallel. Figure 3.1 shows the basic structure of such a two-level VSC. As illustrated in the figure, the DC-link is split in two with capacitors to form a neutral point.

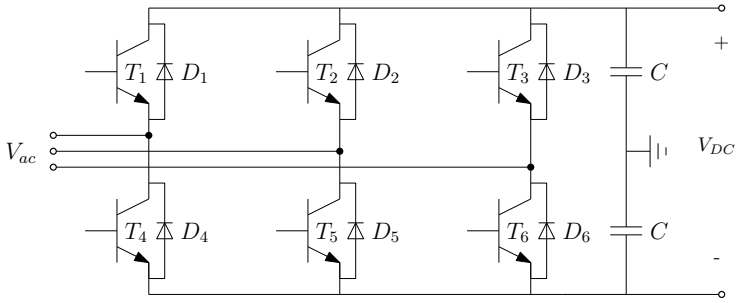

Figure 3.1: Principal drawing of a two-level voltage source converter.

By using active switches like IGBTs, both the turn-on and turn-off can be controlled. The benefit with active switching is the possibility to control both voltage phase and amplitude. This is preferred in contrast to thyristor turn-on-based converters, where only one commutation per period is possible. The phase voltage waveform switches between the two voltage levels V and -V, as shown in figure 3.2.

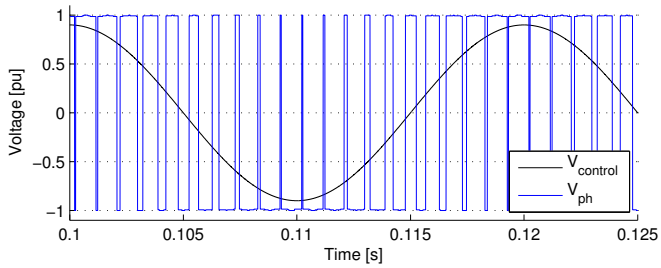

Figure 3.2: The phase voltage V_{ph} and the reference voltage $V_{control}$ of a two level converter, controlled with ordinary pulse width modulation

Different modulation techniques can be applied, but the carrier-based pulse width modulation (CB-PWM) is a common technique and is therefore used in the simulations presented in this work. To make the converter operate in all four quadrants, the PWM control signal's amplitude and the phase-shift in relation to the AC voltage is regulated [27].

The standard two-level VSC benefits with its simplicity, both in structure and control, and is a well-known technology. For low voltage and power ratings it is therefore very popular.

3.2.1 The troublesome series connection

With higher voltage and power ratings however, each phase arm has to withstand both a high voltage and a high current. Since each IGBT has limitations in voltage blocking and current leading capabilities [28], the following two requirements may be important:

- Series connection of IGBTs to meet the increased voltage stress on each switch.
- Parallel connection of IGBT branches to increase the current leading capability of the converter.

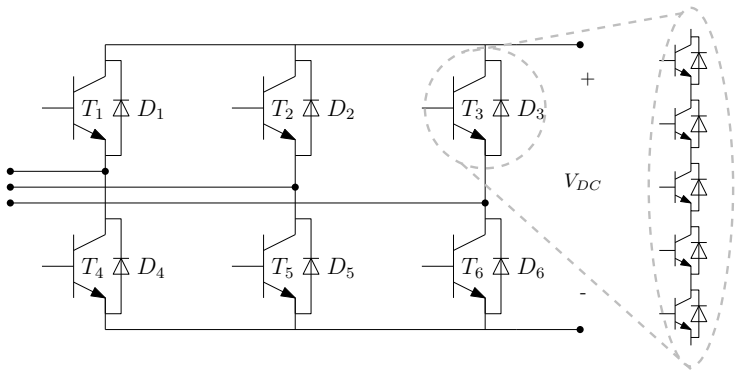

Figure 3.3: The principle of series connection of IGBTs in a two-level VSC

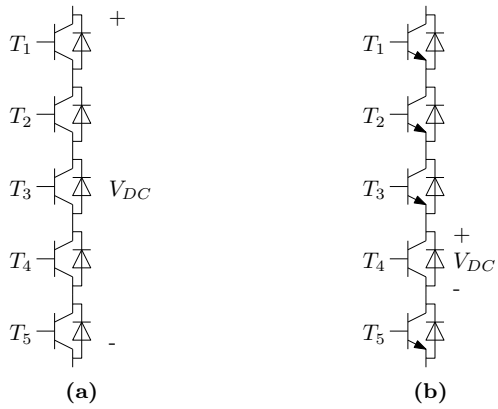

Figure 3.4: a) Desired operation: All IGBTs block simultaneously. b) Failure: Only T_4 block V_{DC}

The two level converter has been used in high voltage transmissions, but then with series connection of switches as shown in figure 3.3. In this figure, each

switch really consists of five IGBTs in series. IGBTs are available with blocking voltages up to 6.5 kV [28]. A vital criteria with series connection of IGBTs is the switch control. The switches have to be turned on or off at the exact same time to avoid IGBT failure.

Figure 3.4 illustrates the switch failure when the timing is not precise. In 3.4a) all five IGBTs block the voltage simultaneously. The voltage imposed on each of them is one fifth of the DC voltage, which is lower than their voltage rating. 3.4b) illustrates the case of a lag in the turn-off time for one of the IGBTs. T_4 is the only IGBT blocking the whole DC voltage. In series connection of IGBTs, the voltage rating of each switch is lower than the DC voltage, so the IGBTs will most probably short circuit - causing a breakdown of the converter.

The branch of IGBTs has to be able to switch simultaneously. This is however quite complicated, and the consequence of delayed switching in one part of the branch is severe. This is one of the reasons why multilevel converters have become popular. Another reason is the demand for filtering in two-level converters. This is a consequence from the high harmonic content of the phase voltage shown in figure 3.2.

3.3 The multilevel concept

A patent search done in [29], states that the first multilevel converter was patented as early as in 1975. This multilevel converter was a cascade inverter, and connected multiple converter cells in series to form the familiar staircase voltage waveform. The technology in multilevel converters has since then evolved over nearly 40 years, and multilevel converters are now the state-of-the-art solution for medium voltage level applications.

This chapter describes the idea behind multilevel converters, and specially why it is suitable for the proposed wind turbine concept described in Chapter 2.

3.3.1 Operation principle

Figure 3.5 shows a principle sketch of one leg in a three phase multilevel converter. The idea is to stack n-1 capacitors or voltage levels, and use controlled switching to obtain a desired n-level AC voltage. The amplitude of the voltage is then determined by the number of contributing capacitors [1].

Figure 3.6 compares the typical phase voltage shape of the two-level converter with multilevel converters. The upper graph shows the two-level phase voltage. This is an unfiltered voltage, switching between two levels. By introducing more levels, the phase voltage becomes more sinusoidal, and follows the voltage reference, normally a pure sinusoidal wave, more closely. The last graph of figure 3.6 illustrates this, with a 15 level phase voltage. The need for filtering

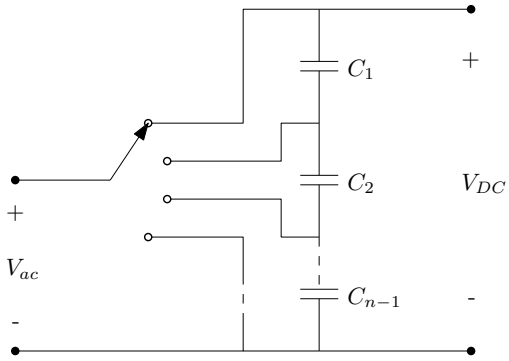

Figure 3.5: Principal drawing of an n-level converter phase leg

is greatly reduced, and the $\frac{dv}{dt}$ is much lower than for the two-level voltage. A low $\frac{dv}{dt}$ is beneficial for generator design, and especially the turn insulation.

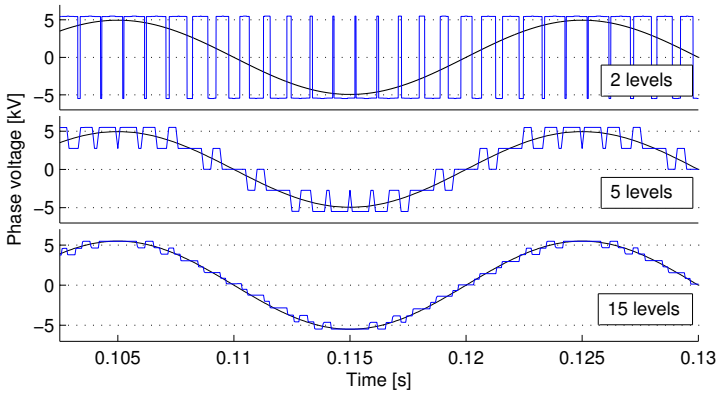

Figure 3.6: Phase voltages V_a and the voltage reference signal in a two level, five level and a 15 level converter

3.3.2 Advantages

Some of the advantages with multilevel converters are:

- The multilevel approach divides the total voltage into multiple levels, which results in a lower $\frac{dv}{dt}$.
- The losses in a converter include mainly conduction losses and switching losses [30]. Reduced switching frequency results in lower switching losses.

- The harmonic distortion is reduced, resulting in lower loss due to harmonic components.
- Some multilevel topologies make redundancy possibilities easier to implement. This makes component failures less critical for the operation of the converter.
- The filtering demand in multilevel configurations is reduced, reducing the volume and cost, and the losses due to filtering.

3.3.3 Possible drawbacks

- The investment cost increases with more complex structures and additional research and development.
- An increase in complexity could jeopardize the reliability.
- Extensive control strategies are needed. For instance, capacitor voltage balancing strategies are needed for most multilevel converters.

3.4 Multilevel modulation strategies

This section gives a short review of the different modulation strategies used in multilevel converters. The modulation strategies are divided into synchronous and asynchronous modulation strategies, as indicated in figure 3.7 below.

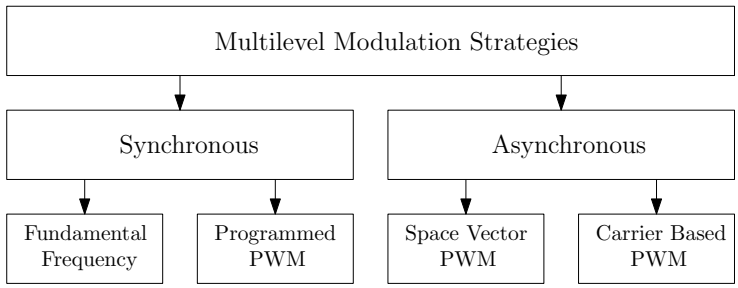

Figure 3.7: Different multilevel modulation strategies [1]

3.4.1 Fundamental frequency

As the title implies, Fundamental Frequency modulation is a slow switching modulation, i.e. synchronized with the reference voltage frequency. There is only one commutation per cycle. It is used for slow switching semiconductors such as gate turn-off thyristors (GTOs) [1].

The fundamental frequency modulation is appropriate for controlling multilevel converters, and because of half-wave symmetry only $\frac{1}{2}(n-1)$ firing angles have to be calculated for an n-level converter.

Since there is only one commutation per cycle, this modulation method introduces odd, harmonic components. The k^{th} harmonic of an n-level phase voltage is given by [31]:

$$F_k = \frac{4}{\pi k}\frac{U_{DC}}{2}\frac{2}{n-1}\sum_{i=1}^{m} cos(k\alpha_i) \tag{3.1}$$

In [31], an optimization algorithm is presented. It is an optimization of harmonic elimination, where the firing angles that results in the lowest harmonic content are calculated. These m firing angles have to be calculated for each modulation index m_f. Figure 3.8 shows the typical phase voltage in a three level converter, with the turn-on firing angle α_1. Because of symmetry, the turn-off angle is $\pi - \alpha_1$.

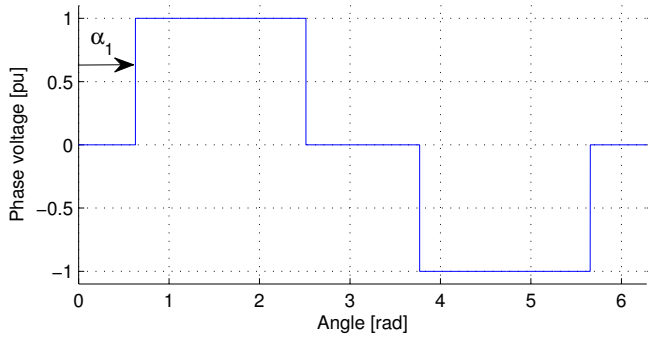

Figure 3.8: Fundamental Frequency PWM with the one turn-on angle α_1

3.4.2 Programmed PWM

The Programmed PWM technique is a more advanced fundamental frequency modulation, and is also called *Selective Harmonic Elimination (SHE)* [32]. The strategy is to eliminate more harmonic components by introducing additional notches between the turn-on and the turn-off angle mentioned in section 3.4.1. Each notch is specially designed to eliminate desired harmonic components, one harmonic component for each notch angle. The higher amount of angles, the more the voltage shape resembles a classical PWM pattern.

In figure 3.9 the addition of one notch is shown. The notch width and position is calculated in an optimization process to reduce the harmonic components. In the example from figure 3.9, three angles needs to be calculated: the fundamental turn-on angle α_1, and the two angles for the notch, α_2 and α_3. From

Fourier-analysis, the three non-linear equations that needs to be solved are [32]:

$$cos(\alpha_1) - cos(\alpha_2) + cos(\alpha_3) = \frac{4}{\pi} m_a \tag{3.2}$$

$$cos(5\alpha_1) - cos(5\alpha_2) + cos(5\alpha_3) = 0 \tag{3.3}$$

$$cos(7\alpha_1) - cos(7\alpha_2) + cos(7\alpha_3) = 0 \tag{3.4}$$

Where m_a is the modulation index. The angles are therefore dependent on the modulation index of the reference voltage signal. Here, the fifth and seventh harmonic components will be eliminated. The third harmonic is not included because of natural elimination in symmetric three phase systems.

Programmed PWM is a very effective way to reduce harmonic components when applying a low switching frequency. The number of switching operations is minimized to exactly the number needed for the desired harmonic elimination. In this way, the switching losses are minimized. A possible downside is the large data capacity needed to recalculate all the angles for each operating state, especially during transient states. Furthermore, the switching losses increase with the increasing number of notches created.

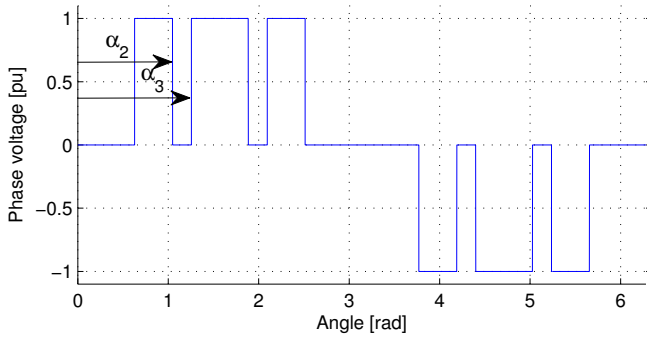

Figure 3.9: Selective harmonic elimination with Programmed PWM: Fundamental frequency output with one notch added for elimination of two harmonic components

3.4.3 Carrier based PWM

The classical carrier-based PWM is a widely used modulation technique, and it is used for both classical VSCs and for multilevel converters. In addition to the technique described in the following, two other carrier based variations are *sawtooth rotation* and *phase shifted carriers*. These multicarrier techniques are described in [33].

Figures 3.10 and 3.11 below show the modulation schemes for the two uppermost IGBTs in a phase of a five-level model simulated in PSCAD. With an n level

converter, $n-1$ triangle carriers are stacked from -1 to 1. The control signal for each phase, defined in equation 3.6, is then compared with all the triangle carriers, with the following criteria:

$$T_1 = \begin{cases} 1 & \text{if } V_{control} \geq V_{tri} \\ 0 & \text{if } V_{control} < V_{tri} \end{cases} \tag{3.5}$$

$$V_{control,i} = \begin{cases} m_a sin(\omega t) \\ m_a sin(\omega t - \frac{2\pi}{3}) \\ m_a sin(\omega t + \frac{2\pi}{3}) \end{cases} \quad \text{for } i = a, b, c \tag{3.6}$$

Only one of the four carrier signals is shown in the figure, and the switching of T_{1+} is marked in blue. The green graph is the a phase control signal with a modulation ratio $m_a = 0.8$.

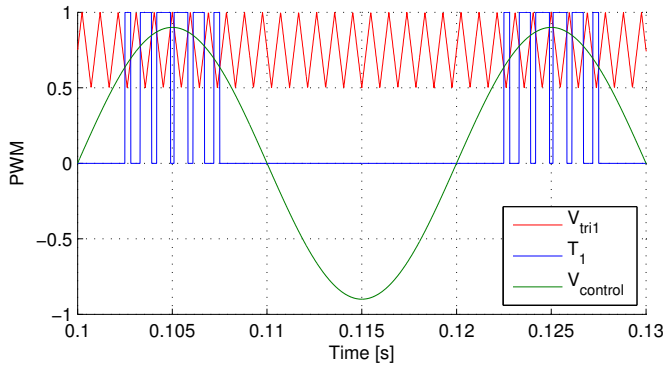

Figure 3.10: PWM for the five-level NPC, first IGBT

Figure 3.11 shows the switching signal for the second IGBT. It can be observed that the first IGBT switches more often, thus having larger switching losses.

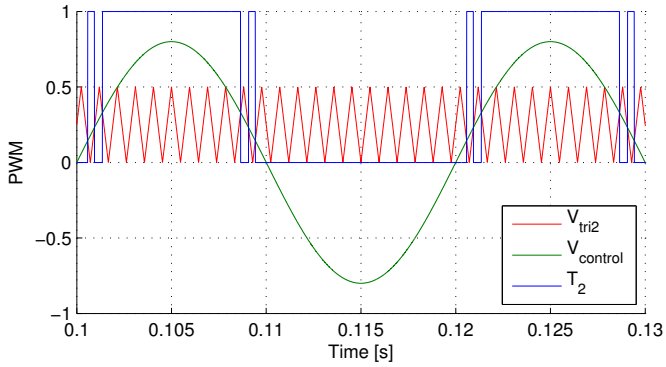

Figure 3.11: PWM for the five-level NPC, second IGBT

For a two level converter this is similar, but simpler. Figure 3.12 shows the two level PWM scheme. The modulation is done by comparing one sinusoidal control signal $V_{control}$, which has the same frequency as the system, with a triangle signal, V_{tri}. The gate trigger signal on the upper IGBT is then opposite of the gate trigger signal on the lower IGBT [27].

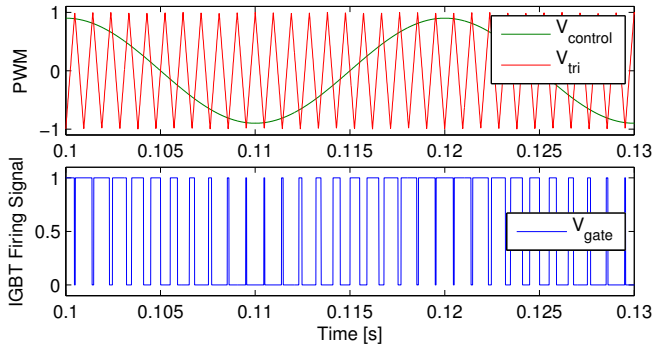

Figure 3.12: PWM firing for one of the IGBTs in a two-level converter

3.4.4 Space Vector PWM

The space vector modulation (SVM) technique was presented in the 1980s as an alternative to the classical PWM [1]. The SVM is used to determine the switching pulse widths, and has become very popular in the last years, much because of the digital implementation in today's control systems [1].

For an n-level converter there are n^3 switching combinations, resulting in 8 combinations for a 2-level converter. Two of these combinations short-circuits

the AC side of the converter, and are therefore called zero-states. The six other are defined as stationary vectors, and any arbitrary output vector can be synthesized from the stationary vectors $S\vec{V}_1$ - $S\vec{V}_6$. A space vector diagram for a two-level modulation is shown in figure 3.13. For a three level converter the number of space vectors is 27.

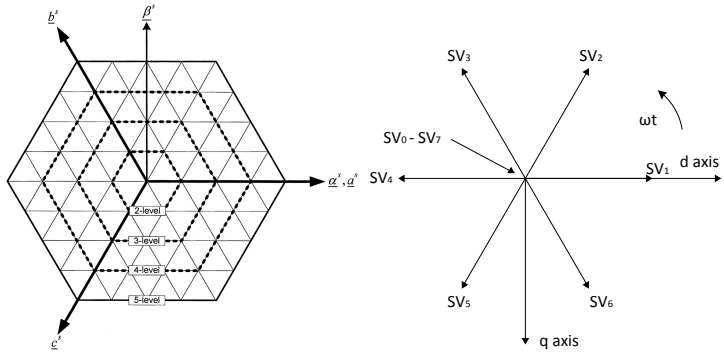

Figure 3.13: Space vector diagram: a) 5-level structure [1], b) 2-level SVM

Since each switching state corresponds to a space vector, the desired output is controlled by the duty cycle for each space vector [31].

Third harmonic injection

An injection of a third harmonic component to the control signal in the PWM modulation, reduces the peak of the control signal by 15%. This gives the advantage of an increased modulation region, and thereby a larger control-region. Because of the elimination of 3rd harmonic multiples, this does not affect the voltage output.

Figure 3.14 shows the injection of a third harmonic with an amplitude of one sixth of the control signal. From the figure it can be observed that an increase of 15% is possible.

The space vector modulation results in the same utilization improvement as the third harmonic injection in CBPWM. In [31], it is shown that the modulation index in SVPWM can be increased by $\frac{2}{\sqrt{3}}$ compared with the CBPWM, thus increasing the DC-link utilization by 15%.

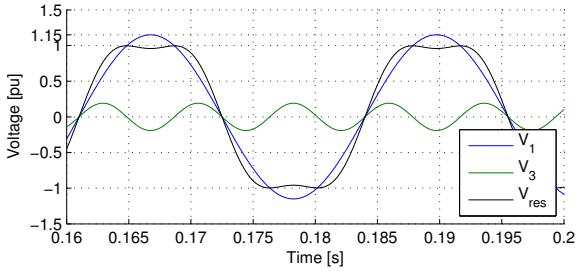

Figure 3.14: An example of 3rd harmonic injection

3.5 Multilevel topologies

A literature review was performed to find actual multilevel alternatives to the two-level converter. This chapter describes today's most popular topologies. A choise is made for which converter topology to include in the more thorough studies and simulations.

3.5.1 Neutral Point Clamped VSC

The diode clamped converter was derived as a manipulation of a cascaded multilevel converter by Nabae et. al. in 1981 [34].

The topology is shown in figure 3.15, and has been called Neutral-Point Clamped (NPC) converter because of the diodes connecting the point between each IGBT to the DC-link neutral point.

In comparison to the two-level VSC, this three-level topology mainly adds one component: the clamping diode. The DC-link voltage is then divided between the switches, thus doubling the obtainable voltage level with the same type of IGBTs, compared to the two-level VSC. Because of this, the 3-level NPC prevailed in the 1980's and is today's state-of-the-art converter for medium voltage levels [29].

The switching combinations used to synthesise an AC phase is shown in table 3.1. From the topology in figure 3.1, it can be observed that if $\frac{1}{2}V_{dc}$ is imposed across the upper DC link capacitor, an activation of switch T_{r1+} and T_{r2+} will result in an AC output voltage on of $\frac{1}{2}V_{dc}$.

The NPC has been extended to a higher number of levels, as in [35] where a 5-level topology is described. In [36] a five level NPC is controlled and balanced for use in a STATCOM[1]. Because of the increase in complexity when going from three to five levels, this five-level topology has not been that popular. Both the

[1] A STATCOM is a VAr controller that provides instantaneous reactive compensation in utility grids [27].

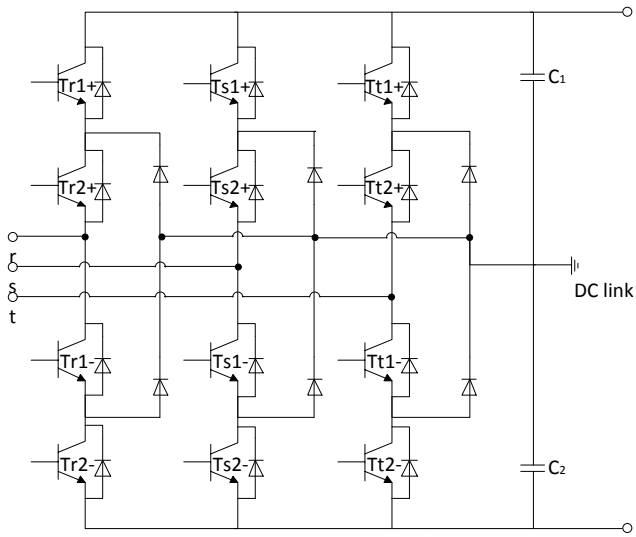

Figure 3.15: Converter topology - 3 level NPC

Table 3.1: NPC: Synthesis of 3-level AC phase voltage

Phase voltage	Switching Combinations			
V_{an}	T_{r1+}	T_{r2+}	T_{r1-}	T_{r2-}
$+\frac{1}{2}V_{dc}$	1	1	-	-
0	-	1	1	-
$-\frac{1}{2}V_{dc}$	-	-	1	1

increased number of components; switches, diodes and the structural size and a more advanced control system makes the topology more complex. In contrast to modular converters described later, the complexity is not linear to the number of levels added. Voltage balancing issues have also been mentioned as the main cause.

3.5.2 Active - Neutral Point Clamped

The Active-NPC converter was first described by T. Brückner and S. Bernet in 2001, as a way to balance the losses in a three level NPC [37]. It introduces a small change in the NPC topology described in 3.5.1; the clamping is done actively by using active components, in this case with IGBTs instead of diodes.

An ordinary NPC has unequally distributed switching losses. The rating of the

whole converter is then determined by the mostly stressed component. This gives an improvement potential in terms of power handling. The additional switches make it possible to further control the commutations in the converter, consequently increasing the rating. For larger converters the IGBTs and diodes are water-cooled. In case of large losses, the downside is bulky cooling systems and therefore a less compact system. The commutations in an A-NPC converter are controlled with feedback from temperature sensors in such a way that the resulting switching losses are equally distributed, and therefore minimized.

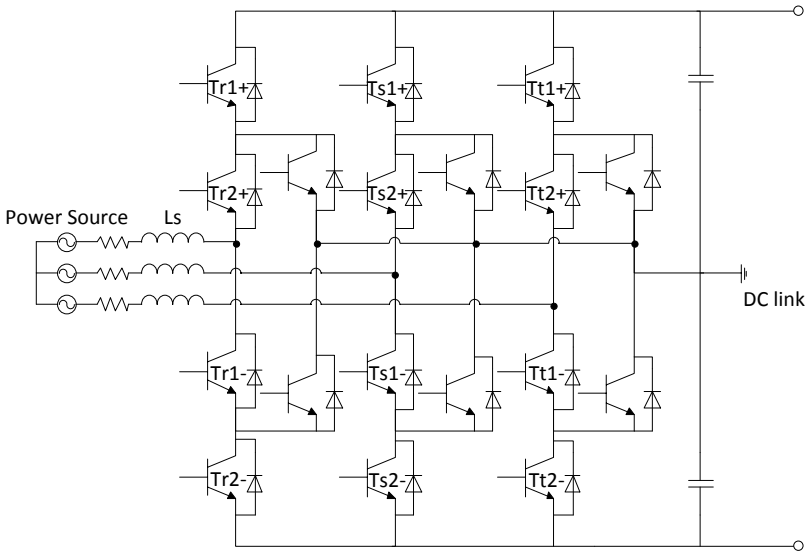

Figure 3.16: Converter topology - 3 level A-NPC

Simulations done in [37] show that implementing the active-loss balancing system improve the total power handling by 20%. This does not reduce the total losses in the converter, but equally distributes the losses. Alternatively, the switching frequency could be increased from 1050Hz to 1950Hz, an increase of 85%. The trade-off is a more complex topology, i.e. an increased component cost.

3.5.3 Flying Capacitor Converter

The flying capacitor converter (FCC) was introduced in 1992 [38]. Clamping capacitors instead of diodes gives a more flexible topology where multiple switching combinations result in the same voltage levels [1].

Figure 3.17 shows the Flying Capacitor topology for a 5-level structure. If each capacitor handles the same voltage level, an n-level converter consists of $2(n-1)$

switches, $(n-1)(n-2)/2$ clamping capacitors and $(n-1)$ main DC capacitors [1]. The number of clamping capacitors in series illustrate the charged voltage on each clamping leg [29]. This means that if the total DC link voltage is V_{dc}, the capacitors C_4 are charged with a voltage $\frac{1}{4}V_{dc}$. Since all the capacitors have the same voltage rating, the voltage in all the other capacitors in the figure is: $V_{C_1,C_2,C_3} = \frac{1}{4}V_{dc}$.

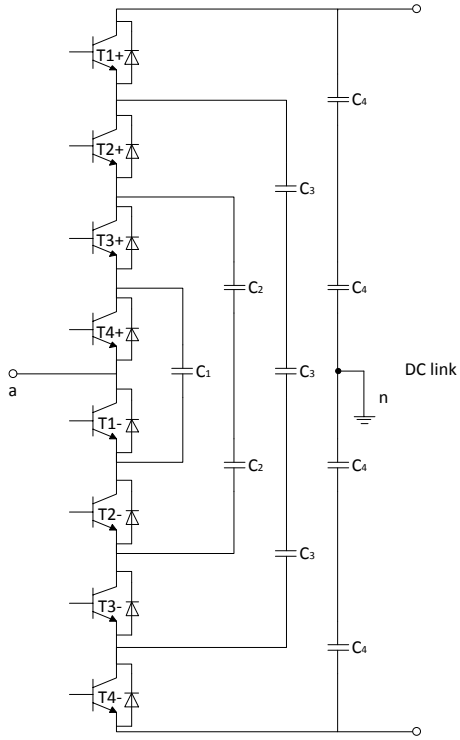

Figure 3.17: Converter topology - 5 level Flying Capacitor Converter

To illuminate the flexibility in terms of switching combinations compared with the NPC, all switching combinations of a 5-level phase leg are shown in table 3.2 below[2]. The switches are not complementary pairs in the FCC topology, so T_{1+} and T_{1-} can be switched *on* simultaneously. The table shows that three combinations exists for $\frac{1}{4}V_{dc}$ and $-\frac{1}{4}V_{dc}$, six for 0 V and one combination for both $\frac{1}{2}V_{dc}$ and $-\frac{1}{2}V_{dc}$.

For clarification, some voltage combinations are explained in detail.

[2]A similar table is presented in [1], but the structure presented does not include a grounded neutral point as shown in figure 3.17. The switching combinations are therefore different, and the combinations presented in table 3.2 have been derived from the structure in figure 3.17.

$\frac{1}{2}V_{dc}$: If all four of the upper switches are turned *on*, the path from the neutral point n to a, includes the voltage $\frac{1}{2}V_{dc}$ from the upper two C_4-capacitors. The C_4-capacitors are now in discharging mode.

$\frac{1}{4}V_{dc}$(c): If switches T_{1+}, T_{3+}, T_{4+} and T_{3-} are turned *on*, the phase output V_{an} will be the sum of; $\frac{1}{2}V_{dc}$ (from the upper two C_4-capacitors) - $\frac{3}{4}V_{dc}$ (from capacitors C_3), + $\frac{1}{2}V_{dc}$ (from capacitors C_2). In this case the capacitors C_4 and C_2 are in discharging mode, and the capacitors C_3 are in charging mode.

$-\frac{1}{4}V_{dc}$(b): If the switches T_{4+}, T_{2-}, T_{3-}, T_{4-} are turned *on*, the phase output V_{an} will be the sum of; $\frac{1}{4}V_{dc}$ (from C_1) - $\frac{1}{2}V_{dc}$ (from lower C_4's). In this case the C_4's are in charging mode, and C_1 is in discharging mode.

0(c): V_{an} = $\frac{1}{2}V_{dc}$ (from upper C_4's) - $\frac{3}{4}V_{dc}$ (from C_3's) + $\frac{1}{2}V_{dc}$ (from C_2's) - $\frac{1}{4}V_{dc}$ (from C_1). In this case the C_4's and C_2's are in discharging mode, while the C_2's and C_1 are in charging mode.

Table 3.2: FCC: Synthesis of 5-level AC phase voltage

Phase voltage	Switching Combinations							
V_{an}	T_{1+}	T_{2+}	T_{3+}	T_{4+}	T_{1-}	T_{2-}	T_{3-}	T_{4-}
$\frac{1}{2}V_{dc}$	1	1	1	1	-	-	-	-
$\frac{1}{4}V_{dc}$	1	1	1	-	1	-	-	-
	-	1	1	1	-	-	-	1
	1		1	1	-	-	1	-
0	1	1	-	-	1	1	-	-
	-	-	1	1	-	-	1	1
	1	-	1	-	1	-	1	-
	1	-	-	1	-	1	1	-
	-	1	-	1	-	1	-	1
	-	1	1	-	1	-	-	1
$-\frac{1}{4}V_{dc}$	1	-	-	-	1	1	1	-
	-	-	-	1	-	1	1	1
	-	-	1	-	1	-	1	1
$-\frac{1}{2}V_{dc}$	-	-	-	-	1	1	1	1

The clamping capacitor voltages must be maintained at a specified level if the converter is to operate as intended. This means that the charging and discharging of the capacitors have to monitored and controlled to maintain a constant capacitor voltage. This is however quite complicated, and many FCC configurations have challenges with floating capacitor voltages [1]. In [38], a control strategy that regulates the capacitor voltages for a multilevel flying capacitor

converter is presented. The method has been demonstrated to work in simulations with inverters up to nine-levels.

In [39], a new flying capacitor topology is presented, where a modular multilevel mixture is introduced. Advantages in the modular multilevel converter (MMC) are utilized, solving some of the problems with the flying capacitor converter. The modification allows the FCC to be extended to any practical number of levels without any capacitor voltage balancing problems. A disadvantage compared to the MMC, presented in section 3.5.6, is increased conversion losses.

3.5.4 Cascaded H-Bridge Converter

The Cascaded H-Bridge converter (CHB) is a modular converter, and consists of several blocks of H-bridge cells in series. Each H-bridge block is constructed with two pairs of switches with diodes in anti-parallel. In figure 3.18, two of these cells are connected, showing the phase structure in a CHB converter. By using n H-bridge cells, V_{an} is synthesised using $2n - 1$ voltage levels [2].

Each module in this configuration needs a separate DC-power output, or for the inverter operation; separate DC sources. The converter's applications are therefore somewhat limited. This topology with separate DC sources is instead well suited for renewable energy sources such as photovoltaic banks, where many separate sources are available. It has also been applied to wind energy conversion, where concentrated generator windings supply rectifier units to get separated DC sources.

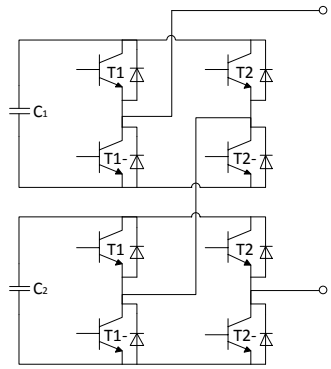

Figure 3.18: Two modules of a Cascaded H-Bridge converter topology

For the proposed structure however, this topology does not fit very well because of the need for separate DC outputs. One separated DC output is generated for each H-bridge cell. In order to achieve a combined DC link these outputs must be series connected. As shown in figure 3.19, this is not that straight forward.

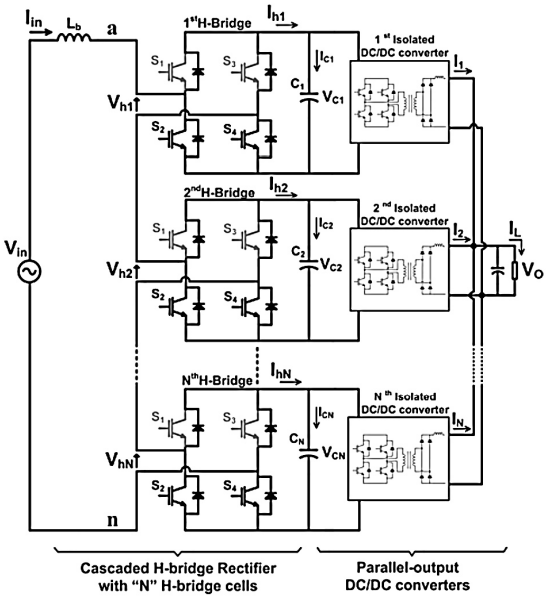

Figure 3.19: CHB-converter used for AC/DC conversion. From [2]

One solution is to use isolated DC/DC converters for each H-bridge cell. This topology is shown in figure 3.19. The component count increases considerably, reducing the reliability. There is however a possibility of adding redundancy to the structure. If a fault occurs in one of the H-bridge cells, it can be included in the control that the faulty cell is short-circuited and the structure continues with $n - 1$ cells.

3.5.5 Hexagram Converter

Figure 3.20 shows the basic topology of the Hexagram converter, described by K. Smedley in 2008 [3]. The converter utilizes six full bridge converter modules, similar to the CHB described in the previous chapter. The hexagram converter is used in STATCOMs for reactive compensation, and in medium voltage motor drives.

Advantages from the Hexagram converter are a modular structure, no voltage unbalance problems, straight forward control and low-voltage stress compared to the 2-level VSC [3].

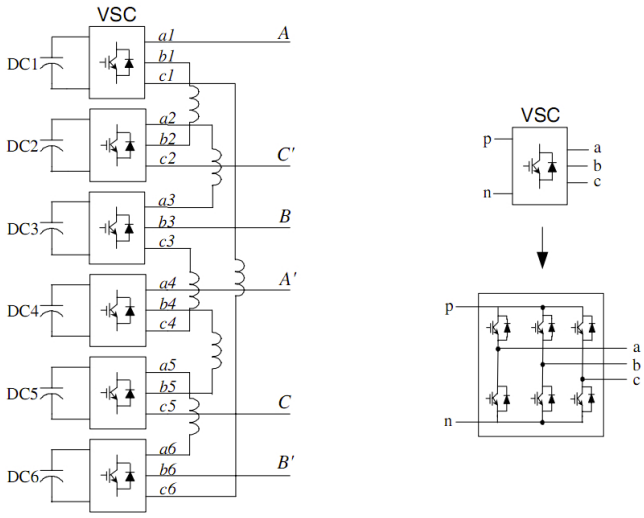

Figure 3.20: Topology - Hexagram converter - from [3]

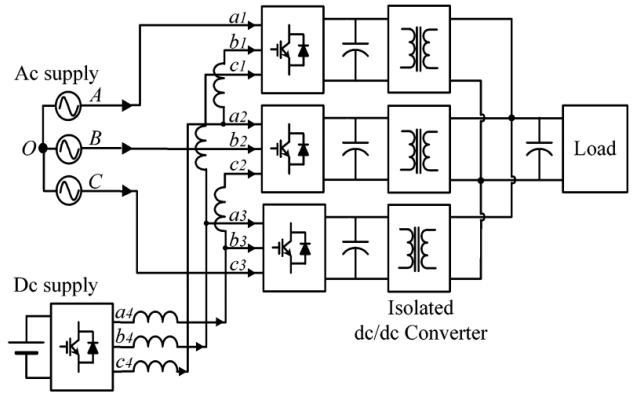

Figure 3.21: Example of a Hexagram rectifier, with isolated DC/DC converters - from [4]

In [4] the Hexagram converter is compared to the cascaded H-bridge, and presented as a *competitive candidate* because of lower component count and lowered energy storage.

A disadvantage with the hexagram converter is the need for many inductors to suppress circulating currents [4]. To apply the hexagram converter as a rectifier unit supplying a high voltage DC link, each VSC block has to be series connected. This is done in figure 3.21, with isolated DC/DC converters for each block, showing the same impractical or complex principle as for the CHB.

3.5.6 Modular Multilevel Converter

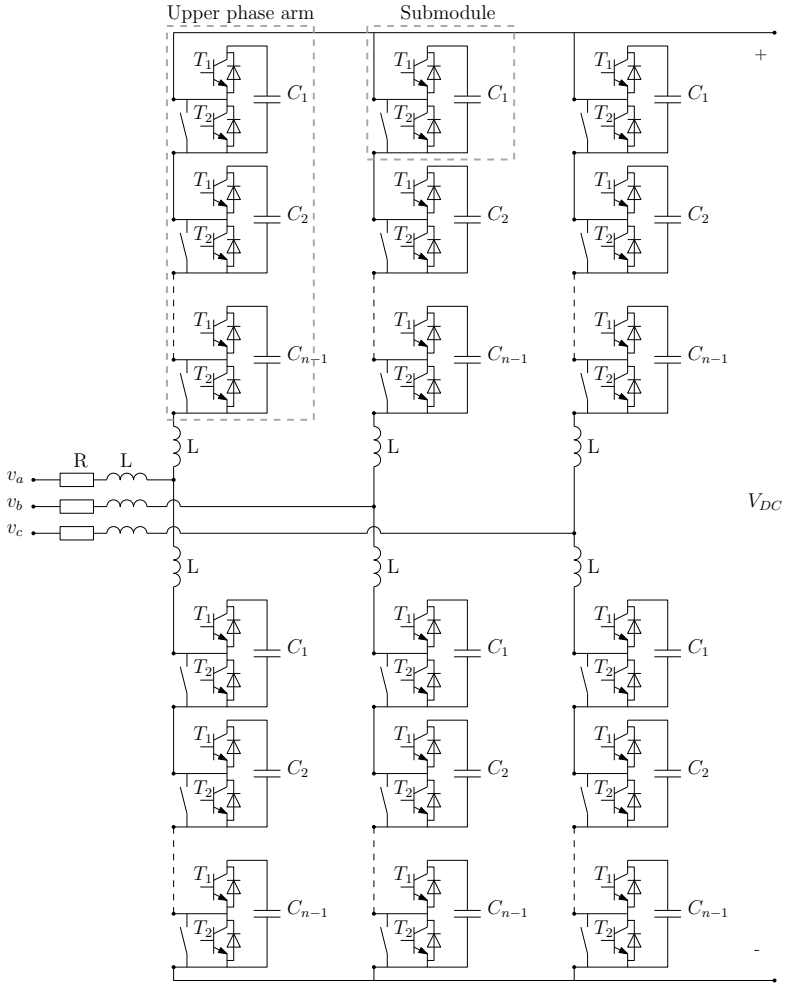

Figure 3.22: The MMC: General n-level structure

Rainer Marquardt invented the Modular Multilevel Converter (MMC) as a development from the Cascaded H-Bridge Converter.[40].

The MMC has received great attention because of its modular structure, which gives many benefits as a multilevel converter. Lately, The MMC technology have been used in large HVDC transmissions, and hence well suited for high voltage structures. It is therefore natural to include the MMC in studies regarding high voltage installations. Mentionable projects are the new cable connection between Norway and Denmark (Skagerrak 4[41]), Trans Bay Cable in San Fransisco[42], German offshore wind projects (HelWin, BorWin, DolWin),

and the cable connection between Sweden and Lithuania [43]. Table 3.3 shows some of the latest projects that include MMC technology. Both Siemens and ABB have developed HVDC concepts which uses some sort of modular multilevel converter topologies. The two concepts are called HVDC Plus (Siemens) and HVDC Light (ABB).

Table 3.3: Some of today's MMC projects

Site	Contractor	Power (MW)
Trans-Bay San Francisco (2010)	Siemens	400
Skagerrak 4 (2014)	ABB	700
DolWin1 Germany (2013)	ABB	800
DolWin2 Germany (2015)	ABB	900
BorWin2 Germany (2013)	Siemens	800
NordBalt Swe-Lit (2013)	ABB	700

The MMC has also been discussed for an inverter for medium voltage drives. This is described in [44].

Design

In an MMC, the basic building block, figure 3.23, consists of three simple units; two IGBT switches and one capacitor. The idea is to connect multiple blocks in stacks to form a phase module, shown in figure 3.22. The total DC voltage V_{dc} is added up from the sum of power submodules[3]. It is thereby possible to determine the strain on each submodule. A higher DC-link voltage is obtained by adding more modules to the stack [45].

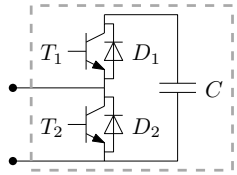

Figure 3.23: A basic MMC block: The submodule

In addition to the version shown in figure 3.23, an MMC version with full-bridge modules exists. This configuration is capable of supplying an additional voltage level, and gives better fault handling than the half-bridge module because of the possibility to block the fault current. The freewheeling diode makes fault current blocking impossible in the half-bridge module.

[3]Throughout the thesis, whenever a submodule is mentioned, it points to the submodule of the MMC. The nomenclature *submodule* is easy confused with one of the nine *converter modules* of the proposed system.

Operation principle

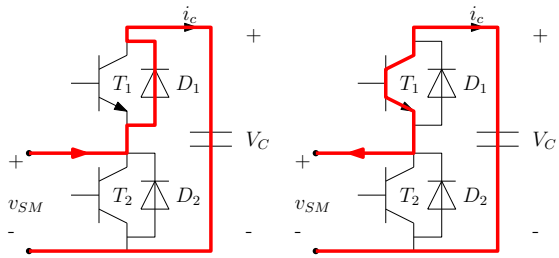

Figure 3.24: MMC submodule operating state ON. T_1 is on while T_2 is off

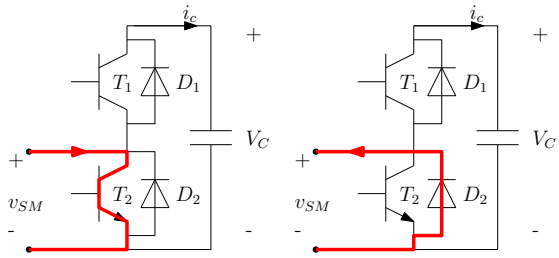

Figure 3.25: MMC submodule operating state OFF. T_1 is off while T_2 is on

The submodule of an MMC has four operating states, depending on the current direction and the switching states. For switching state *ON*, the upper IGBT (T_1) is leading, while the lower IGBT (T_2) is blocking. As shown in figure 3.24 the current is then passed trough the capacitor in both directions. The capacitor is charging when the current i_C is positive, and discharging when the current i_C is negative. The voltage across the sub-module is in both current directions equal to the capacitor voltage V_C.

In switching state *OFF*, the upper IGBT (T_1) is blocking, while the lower IGBT (T_2) is leading. The positive current is then passed trough (T_2), while a negative arm current is passed through the freewheeling diode, (D_2), shown in figure 3.25. The capacitor voltage is kept at V_C, and the voltage at the sub-module terminals, v_{SM} is zero.

Mathematical model

Figure 3.26 shows the per phase equivalent circuit of the MMC. The submodules in each phase arm are substituted by variable capacitors, with the voltages V_{CU} and V_{CL} for the Upper and Lower arm, respectively. R is the arm resistance and L the arm inductance. R is often neglected as the inductance is dominating at higher frequencies [46]. V_V is the per phase voltage from line to ground, and i_V is the phase current.

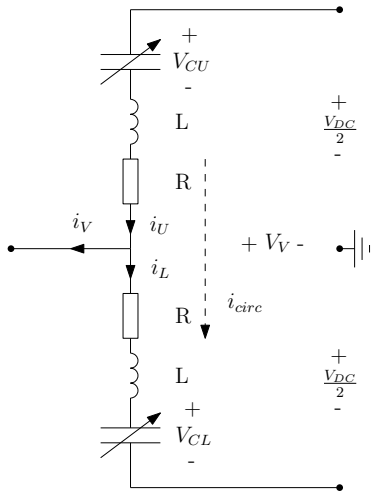

Figure 3.26: Single phase equivalent circuit of the MMC

The arm voltages are dependent on the number of ON-state submodules, and their voltages. Let N_{on} be the number of ON-state submodules in the arm. The arm voltage is then given by:

$$V_C = N_{on} \sum_{i=1}^{n} V_{Ci} \tag{3.7}$$

Because the capacitor voltages in the different submodules will be charged unequally, a circulating current will flow between the upper and lower arm, i_{circ}. As seen in figure 3.26, the arm currents for the upper and lower arm, i_U and i_L can be expressed as:

$$\begin{aligned} i_U &= i_{circ} + \frac{i_V}{2} \\ i_L &= i_{circ} - \frac{i_V}{2} \end{aligned} \tag{3.8}$$

Consequently,

$$\begin{aligned} i_U - i_L &= i_V \\ i_U + i_L &= 2i_{circ} \end{aligned} \tag{3.9}$$

From the equivalent circuit, using Kirchoff's voltage law on the upper and lower arm, the phase voltage can be expressed as:

$$V_V = \frac{V_{DC}}{2} - V_{CU} - L\frac{di_U}{dt} - Ri_U \tag{3.10}$$

$$V_V = -\frac{V_{DC}}{2} + V_{CL} + L\frac{di_L}{dt} + Ri_L \tag{3.11}$$

By combining equations 3.10 and 3.11, and using the relation in equations 3.9, the following two equations explain the outer and inner relationships for the MMC [46][47]:

$$V_V = \frac{V_{CL} - V_{CU}}{2} - \frac{L}{2}\frac{di_V}{dt} - \frac{R}{2}i_V \tag{3.12}$$

$$L\frac{di_{circ}}{dt} + Ri_{circ} = \frac{V_{DC}}{2} + \frac{V_{CU} + V_{CL}}{2} \tag{3.13}$$

Short circuit protection

The MMC topology makes the DC link capacitor dispensable [40]. A benefit from this is the protection against component damage in case of a short circuit in the DC link. If a DC link short circuit should occur, this topology is safer because of the distributed capacitors. In addition, an inductor is included in every phase arm, to suppress the circulating current. This inductor will also limit the short-circuit current.

Easy expandable

Compared to other topologies where there are constraints on how many levels that are realistic in terms of complexity, the MMC topology is easily expandable to hundreds of levels [45]. This gives a near perfect sinusoidal AC waveform, and because of this the demand for filtering is reduced [45]. Filtering of AC harmonics is space consuming, so the MMC provides therefore the possibility to build a compact unit.

With mass-produceable submodules, the MMC topology makes it possible to build cheaper VSCs that have high voltage ratings and low harmonic distortion, in addition to lower switching losses [45]. Because of the modularity, it is easier to build a customized unit.

Redundancy

Because of the large number of power submodules, reliability is an important issue. If a converter consists of one hundred levels, there are two hundred power submodules in a phase module, and 600 power submodules in total. Each submodule consists of two IGBTs, diodes and one capacitor, as shown in figure 3.23. This means that the failure rate for 1200 IGBTs, diodes and capacitors should be included when calculating the reliability for the whole converter. A shut-down of the whole converter because of failure in one of the IGBTs, is not satisfactory. The MMC uses the modularity in the structure to its advantage, making the

converter operational with faulty power submodules. If a fault occurs in one of the submodules, the faulty unit is bypassed. The rest of the converter can still operate, with a smaller increase in the submodule voltage. Controlling the switching could even disconnect some faults, without mechanical switches [40]. A mechanical bypass switch is included in each submodule, to ensure correct disconnection in case of a fault.

Simplified black start

Another favourable benefit with the MMC topology, is the possibility to run a *simplified* black start, i.e. to start the converter without feed from the power grid. By using a smaller auxiliary voltage source with voltage output equal to a power submodules capacitor voltage, the whole converter can be energized [40]. This is an advantage in island operation scenarios.

3.6 Comparison

The five multilevel topologies represent a small amount of all existing topologies. There are many special-breeds and configurations, but not all of them are mentioned here. The ones mentioned are believed to represent the main topologies.

For different reasons, not all of the converter topologies are equally suitable for the proposed structure. This chapter gives a quantitative comparison based on the description of the converters.

3.6.1 Unsuitable topologies

The **cascaded H-bridge** converter does not fit the proposed structure, as it requires separate DC loads. There exists sub-versions which uses special DC/DC converter modules to connect the different dc-outputs in series, but this makes the structure extremely complex. The **Hexagram converter** is similar to the cascaded H-bridge converter in structure and application. An isolated DC/DC converter is needed to build a high voltage DC link. Because of the complexity needed for the converter to work with the proposed structure, these two topologies are therefore excluded from further studies.

3.6.2 Reliability

Reliability is one of the key elements in offshore projects. The cost of maintenance is larger than on shore, much because of the sparse availability. A

certain reliability in the structure is therefore important, and also a benefit of the proposed structure [18].

Some of the converters have reliability benefits because of a modular structure, like the MMC. As mentioned in section 3.5.6, it is possible to control an $n-1$ (or even better) operation of the converter.

The capacitors are often the critical components in converter systems. Electrolytic capacitors are ageing components that derate over time depending on the stress. Electrolytic DC-filter capacitors are frequently the reason for converter breakdown, so a fault prediction system is often the solution [48]. An alternative is to use dry film capacitors. Dry film capacitors have higher energy density, smaller size and are lighter. There is no risk for leakage, as in the traditional oil-impregnated capacitors, so the fire-hazard is reduced [49]. In addition, dry film capacitors offer a self-healing ability. A key downside is the price.

Choosing a topology that creates less strain on the capacitors, or reduces the need for filtering capacitors, will increase the total reliability of the converter. This argument favours the MMC, as filtering is less required. Furthermore, if a capacitor in one of the submodules should fail, that module can be bypassed. This increases the reliability, for extended continuous operation of the wind turbine.

3.6.3 Complexity and series connections of IGBTs

IGBTs are today max rated for voltages 1700 V - 6500 V [50]. With a converter DC voltage of 11.1 kV, the number of IGBTs sharing this voltage, becomes a design criterion.

The baseline converter, the two-level VSC described in 3.2 switches between $\frac{1}{2}V_{dc}$ and $-\frac{1}{2}V_{dc}$, hence stressing each phase leg with the whole DC-link voltage. This means that even if 6.5 kV IBGTs are used, the IGBTs are strained for more than their rating. A series connection of IGBTs is therefore necessary.

In the three level NPC, the switching is between $\pm\frac{1}{2}V_{dc}$ and 0. Compared to the two-level converter, this halves the switching voltage for each IGBT. This results in a strain on each IGBT set of 5.55 kV, i.e 85% of the maximal IGBT voltage rating. Because of the characteristics of an IGBT, a high voltage rating gives larger switching losses. In many cases it is therefore beneficial to reduce the size of the IGBTs, and in stead build a converter with more IGBTs in series. This compromises the reliability of the converter, and an evaluation that considers the combination of reliability and losses has to be done. To avoid the series connection of IGBT modules, a level increase is necessary. This requires a fully functioning voltage balancing control system for a ≥ 5 level topology.

The flying capacitor converter has a disadvantage with regards to the total capacitor volume, see figure 3.17. In a five level converter, each phase leg needs

three clamping capacitors resulting in nine clamping capacitors for the whole converter, plus two capacitors for the separation of the DC link.

Expanding a modular multilevel converter to a great number of levels is stated as unproblematic [45]. The complexity increases in both structure and control, but voltage balancing is not mentioned as a problem. Each submodule contains one capacitor, so the total capacitor volume is high in configurations with many levels. The hazard by short circuit is however lower, since the capacitors are distributed in several submodules and controlled separately by switching. By expanding the MMC topology to a desired number of levels, the IGBT rating is selected with respect to optimal performance. Series connection of IGBTs is not necessary in a MMC, since the MMC has this feature "built-in".

3.6.4 THD

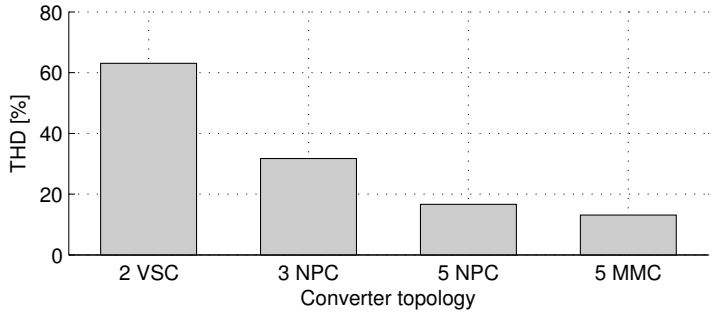

Figure 3.27: Measured THD in the line-to-line voltage V_{ab} in four converter topologies

Calculations of the Total Harmonic Distortion (THD) are performed in PSCAD to quantify the harmonic content in the line voltage. The results are shown in figure 3.27. Because the simplified models do not include any form for filtering, the values are high. However, the trend is evident and in agreement with [31]: The largest THD-reduction is between a 2-level and 3-level structure. This indicates that the gain in choosing a 5-level structure over a 3-level is not that high in terms of harmonic content, i.e. it might not be worth the increase in complexity.

3.6.5 Power losses

The efficiencies of state-of-the-art converters are very high. In [51], the converter station loss in a two level converter solution and a multilevel converter solution is compared. The results show significantly reduced switching losses in the multilevel converter station. The multilevel topology is a cascaded two-level

(CTL)[4]. Converter station losses include filter, reactor, transformer and valve (switching) losses, and is as low as 1 % for the multilevel converter. For the two level converter station the total losses are 1.7 %. The main reason for the lower losses in the multilevel converter is the reduced switching frequency.

3.6.6 Comparison summary and choice of converter topology

Table 3.4 below lists a summary of the focus points in the comparison between the present topologies.

Table 3.4: Summary of topology properties

Converter	Suitability	Cap. volume	Redundancy?	Voltage quality
2-l VSC	Series conn.	High	No	Low
NPC	Series conn.	High	No	Medium
FC	Good	Very high	No	Medium
Hexagram	Does not fit	-	-	-
CHB	Does not fit	Distributed	Yes	High
MMC	Good	Distributed	Yes	High

The two-level VSC and the NPC is marked as *Series connected* because of the necessary series connection of IGBTs. From the five multilevel topologies, the MMC and the NPC is the two best candidates, excluding the FC because of high capacitor volume. Of those two, the MMC is the most interesting because easy level expansion, low harmonics, redundancy possibilities and no voltage balancing issues. In addition, because the NPC is not practically expandable to more than three levels, series connection is required in the NPC as well.

The following simulations focuses therefore mainly on comparing the MMC to the 2-level VSC.

[4]CTL is ABBs approach to MMC, used in 4th generation HVDC Light [52]

Chapter 4

MMC: A closer look at the most promising candidate

4.1 Introduction

The MMC has, after the comparison in section 3.6, been chosen for further studies. This chapter describes the further studies conducted on the MMC. Challenges and benefits with the converter, which was experienced during the specialization project, are the basis for the further studies. This results in simulation models which include capacitor voltage balancing, and redundancy cases.

4.2 Redundancy

For a conventional two level converter, there is no built in redundancy. If one of the six IGBTs should fail, the whole converter breaks down. This applies for the other studied topologies as well.

A benefit with the MMC is the possibility to bypass a single module, and continue the operation of the converter with $n - 1$ modules. A failure in one of the submodules can either result in a short or an open circuit. A capacitor failure is undesired, so the submodule should be disconnected when a fault occurs. An external bypass switch is therefore required to prevent the problems with open circuit faults. This is illustrated in figure 4.1.

The bypass operation must be included in the control system. To obtain a symmetric three phase voltage, a bypass and level reduction should affect all three phases. To ensure the operation with for instance n-1 submodules, the

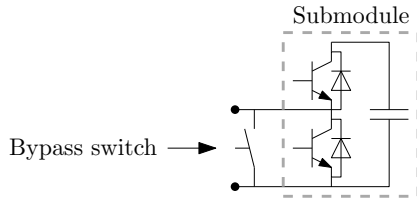

Figure 4.1: MMC submodule with external bypass switch

submodules have to be dimensioned with a safety factor in voltage ratings. If not, the remaining submodules will be highly stressed and might fail due to high voltages. See section 5.2.3 for simulations of the redundancy case.

4.3 Eliminating filters by reducing the harmonic content

The harmonic content is reduced when the number of voltage levels increases. The voltage is smoother, and less distorted. This is illustrated in figure 3.6 in section 3.3, where a level increase results in a more sinusoidal voltage.

Increasing the number of levels results in reduced $\frac{dv}{dt}$, as the switching voltages are divided into more "steps", as illustrated in figure 3.6 in section 3.3. A reduced $\frac{dv}{dt}$ is favourable because it regulates the demand for filtering. An advantage with the multilevel approach is therefore the possibility of eliminating the demand for filters.

Both size and weight are important issues in the proposed system, so bulky AC filters are undesired. A consequential question is then: *How many levels will be required to completely avoid the filtering?*

This section presents the standards for voltage quality, to get an idea of how low harmonic content that is desired.

4.3.1 Voltage quality standards

IEEE standard 519 [6] describes recommendations, practices and requirements regarding harmonic control in electric power systems. The requirements defined in the standard applies for the point of common coupling (PCC), and gives a pointer to what goals converter designers should aim for. The voltage distortion limits in IEEE standard 519 is given in table 4.1.

The point of common coupling is the point where a local Electrical Power System (EPS) is connected to the area EPS [6]. Because the proposed system terminates

Table 4.1: IEEE Standard 519: Voltage distortion limits [6]

Bus voltage at PCC	Individual voltage distortion (%)	Total voltage distortion THD (%)
69 kV and below	3.0	5.0
69.001 kV - 161 kV	1.5	2.5
161.001 and above	1.0	1.5

at a common DC link, instead of a PCC, the typical standards are just used as an indication to what level of THD the converter should produce.

4.3.2 The number of levels to avoid filtering

The goal in THD is selected with respect to standards for requirements for electrical power systems, shown in table 4.1. For 100 kV systems, the THD requirement is maximum 2.5 %. If one converter is studied alone, the voltage falls under a more moderate recommendation in table 4.1, and the THD requirement is 5 %.

Converters for standard machine sizes have typical standard specifications, and are well-tested, supplied right off the shelf. The corresponding machines are designed to cope with most types of standard converters, and their harmonic content. Standards like the IEEE 519 are made to protect the many consumers that are connected to the grid behind the PCC. Because of this, grid recommendations are relatively strict. In the proposed system described in chapter 2, the PMSG is the only "consumer" affected by the AC harmonics from the converter. In such special generator/converter arrangements, good communication between the converter producer and generator producer is very important. Both parties must cooperate for the custom-made solution to function adequately. This means that the generator can be specially constructed to withstand a high harmonic content. For the generator side converter in such a system, it is therefore not necessary to satisfy the strict recommendations in for instance IEEE 519.

Simulations in PSCAD are performed to see how the THD develops with an increasing number of levels. See section 5.2.4.

4.4 The amount of transistors

The number of series connected IGBTs in a conventional two-level VSC is dependent on the voltage level, V_{dc}, and the desired over-rating of the transistors. The over-rating of transistors can be quite high to reduce losses [1], and to protect the devices against over-voltages.

Three factors are mentioned in [53], when calculating the achievable output voltage rating:

1. The DC-voltage which determines the cosmic radiation failure rate, and long term leakage current stability.

2. The repetitive overshoot voltage spikes during turn-off.

3. The maximum voltage against which the device is supposed to switch a specified current to guarantee its Safe Operating Area.

A quick calculation for comparing the number of switching devices in the MMC against the two-level VSC is done. This is interesting in a reliability survey, as an increase in the number of switching devices, increases the possibility for fault. Basis for the comparison is the same DC voltage output of 11.1 kV. The devices should also be equally rated.

In the two-level VSC structure, the DC-link voltage will be shared by the series connected IGBTs in each arm. With a safety margin of 60% [53], this means at least three IGBTs in series, if using the highest available IGBT with a blocking voltage of 6.5 kV. Thus, if N_s is the number of series connected IGBTs in one arm, the total number in a two level converter is $6 \cdot N_s$.

The MMC is similar to the two level converter with series connected switches. All the submodules in one phase arm divides the DC voltage, as all the series connected switches do in the two level converter. A submodule consists of two IGBTs, which both needs to be rated for the same blocking voltage. The number of IGBTs in the MMC exceeds therefore the number of IGBTs in a two level converter by a factor of two, i.e. $12 \cdot N_s$ IGBTs in total.

As the neutral clamped converter imposes each arm with half the DC-link voltage, the total IGBT count for a NPC is $3 \cdot N_s$. The different topologies are summarized in table 4.2.

Table 4.2: Number of switching devices in different converter topologies

	2-level VSC	NPC	MMC
Number of devices:	$6 \cdot N_s$	$3 \cdot N_s$	$12 \cdot N_s$

As the MMC has the largest number of switching devices, it has also the highest component cost. Even though the cost of IGBTs is relatively small in a complete wind turbine system, the MMC has to offer other benefits to be a viable solution, from an economical point of view.

4.5 MMC voltage balancing control strategy

4.5.1 The challenge

The MMC converter has been stated as unproblematic when expanding to several levels [45]. Nevertheless, a voltage balancing issue is known in the MMC model as well as the five level NPC. As seen is previous studies during the specialization project, voltage balancing control is required for the MMC to function as expected. Without a good balancing strategy, the mid-capacitor voltages drifts towards zero, and the top- and bottom submodules in one arm are stressed with the whole DC-voltage. This is shown i figure 4.2.

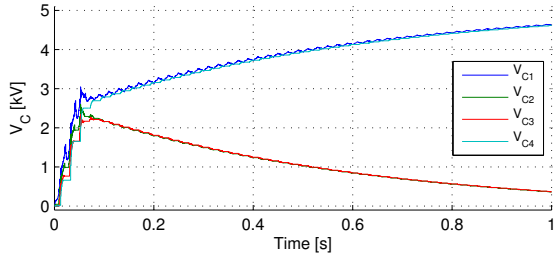

Figure 4.2: 5-level MMC without capacitor voltage balancing - drifting capacitor voltages

The capacitor voltages in the four submodules in the upper leg of phase a is shown in figure 4.2. The voltage in the two middle capacitors approaches zero after some time. This means that the DC-link voltage is shared by the two other capacitors, and that the whole converter eventually acts as a three level converter - increasing the stress on each switch. The effect on the phase voltages is indicated in figure 4.3 below, where the increasing imbalance creates a pattern similar to the three level converter.

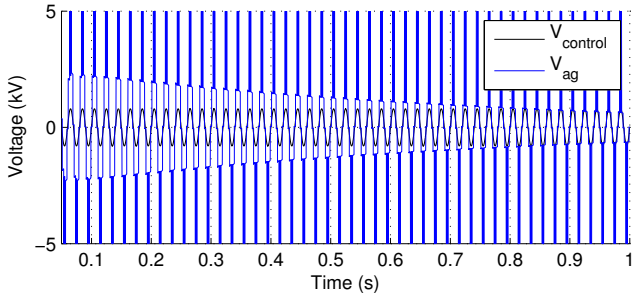

Figure 4.3: 5-level MMC without capacitor voltage balancing: The phase voltage gradually transforms to a three-level voltage.

4.5.2 Balancing strategies

Some capacitor voltage balancing strategies have been briefly explained in litterature. Hagiwara and Akagi mention in [54] the use of *averaging control* and *balancing control* to give separate voltage references to each submodule in the MMC. A sorting algorithm is introduced in [55]. The voltage sorting strategy gives a direct feedback from the capacitor voltages, and controls the gate signals accordingly.

A detailed description of the capacitor voltage balancing strategies is usually left out in literature, so this chapter will give a thorough description of one balancing strategy with voltage sorting. A model is built in PSCAD to study and verify the idea of voltage balancing strategy by sorting algorithm. See section 5.1.2 and 5.2.2.

Voltage sorting strategy

In [55], a balancing strategy that implements a voltage sorting algorithm to select the switching pattern for the gate signals to the MMC is presented. The intention is to charge those submodules with the lowest capacitor voltages, and discharge the submodules with highest capacitor voltages.

A problem with using conventional PWM control without capacitor balancing is that the switching of each submodule does not take into account the voltage in each capacitor, thus charging and discharging the capacitors randomly with regards to the capacitor voltages. There is no connection between capacitor voltage and the generation of gate-signals. This leads to an unbalance in capacitor voltages as seen in the figures 4.2 and 4.3.

The idea with the sorting strategy is therefore to charge or discharge the correct submodule. This is possible because the voltage level generated in the MMC converter depends upon the *number* of ON-state switches in the upper arm and the lower arm, and not by the specific *order* these are turned on. The following table describes one of many possible switching states of the 5 level MMC.

Table 4.3: One of the many switching states for each voltage level in a MMC

V_{ph}	SM_1	SM_2	SM_3	SM_4	SM_5	SM_6	SM_7	SM_8
$-\frac{V_{dc}}{2}$	1	1	1	1	0	0	0	0
$-\frac{V_{dc}}{4}$	0	1	1	1	1	0	0	0
0	0	0	1	1	1	1	0	0
$\frac{V_{dc}}{4}$	0	0	0	1	1	1	1	0
$\frac{V_{dc}}{2}$	0	0	0	0	1	1	1	1

As shown in table 4.3, the phase voltage is zero when submodule number 3, 4, 5 and 6 is in ON-state. The number of ON-state submodules in the positive arm is equal to the number of ON-state submodules in the negative arm, i.e. two in positive and two in negative for a five-level MMC. But for a five-level MMC, many switch combinations leads to this voltage level. The following equation is known from combination theory [56]:

$$\text{nCr} = \frac{n!}{(n-r)!r!} \tag{4.1}$$

nCr is the number of combinations when placing r elements into n slots. There are six ways of turning on two of the four submodules in one arm, and the five-level MMC has therefore 36 switching combinations for a phase voltage of zero, and 16 combinations for $\pm\frac{V_{dc}}{2}$. The number of combinations increase rapidly when expanding the number of levels, and therefore also the amount of calculations.

The capacitor voltage balancing strategy can be summed up as follows. For each switching instant,

1. The capacitor voltages of all capacitors are measured and indexed
2. The arm current direction is identified
3. The necessary number of submodules in ON state is calculated
4. A selection of the submodules is done
5. Gate pulses based on the selection of submodules are generated

Elimination of harmonic components depends upon the modulation. Multiple carrier based modulation strategies are presented in [33], which shows that the harmonic distortion is varying between the PWM strategies. In this capacitor voltage balancing strategy, the multicarrier modulation is not used to directly control the IGBT switching, but to give a signal when a switching should occur. The voltage balancing is therefore independent on the PWM strategy.

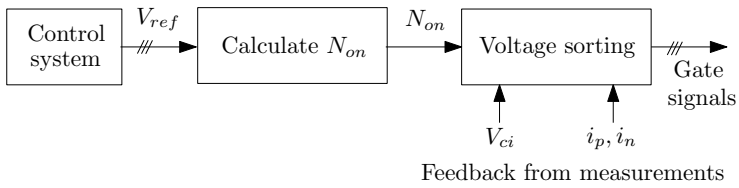

Figure 4.4: Block diagram of the balancing strategy

A schematic showing the voltage sorting algorithm is shown in figure 4.5.

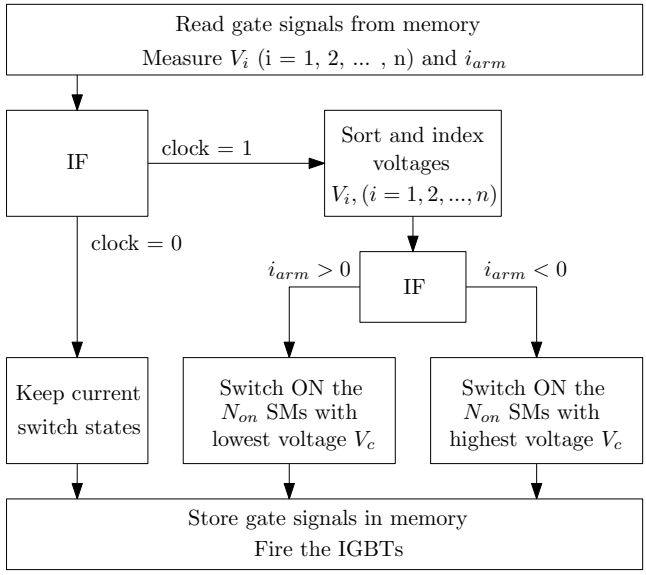

Figure 4.5: Algorithm: capacitor voltage sorting

4.5.3 Reduction of switching losses

The recalculation of gate signals for each control cycle results in a very high switching frequency, and consequently a higher switching loss. The algorithm updates the IGBT gate signals with respect to the capacitor voltages and the desired number of submodules i.e. the desired AC voltage amplitude. This means that even if there is no change in the number of submodules that need to be switched on, the capacitor voltages would have changed during the control cycle, resulting in a new priority of submodules.

Methods for reducing the number of switch operations should be implemented for a better utilization of the MMC. This section presents three ways of achieving a reduced switching frequency.

By using controlled switch time

The PSCAD model used in simulations, and presented in 5.1.1, has been built with a PWM block to produce a signal that decides when the gate signals should change. The gate signals are still updated once every control cycle, but no calculations or changes are made during the control cycles between each switching signal.

When applying a conventional PWM block that controls the time of switching, the voltage balancing strategy does not increase the switching frequency, com-

pared to a conventional PWM control. However, other strategies can reduce the switching frequency additionally and improve the efficiency of the MMC.

By introducing threshold voltages

By implementing capacitor voltage variation limits, and maintaining the switching state for the submodules that does not exceed these voltage limits, the number of switching operations are reduced [57]. A challenge with this method is to find an optimal limit [47].

By using selective switching

To additionally reduce the switching losses, a method that maintains the switch states for a longer period is proposed in [47]. The so-called *Reduced Switching Frequency (RSF)* voltage balanging algorithm is summarized as follows [47]:

- If extra submodules (SMs) need to be switched on during the following control cycle (i.e. ΔN_{on} is positive), no switching is applied to those SMs currently in the ON-state. The conventional balancing algorithm mentioned before will only be applied to those SMs currently in the off-state.
- If some SMs that are currently in the on.state need to be switched off during the following control cycle (i.e. ΔN_{on} is negative), no additional SMs that are currently in the off-state vill be switched on. The conventional balancing algorithm mentioned before will only be applied to the SMs currently in the on-state.

An idea would be to combine this method with the one described in 4.5.3. This is however not implemented in this work, as switching losses is only briefly discussed in this thesis.

Chapter 5

Simulations

5.1 Description

Simulation models for the MMC have been built in PSCAD[1] A three level converter was first utilized, but eventually expanded to five levels to illustrate a clearer example of multilevel operation. In addition, models with up to 23 levels have been built to study the influence on harmonics. The five level models have been used in different studies, to study the operation of the converter, and to implement voltage balancing control and redundancy.

Since the study was focused on one converter module instead of the whole system with nine converter modules in series, the first simulations where performed on a single three phase converter model.

After thorough simulations performed on the single operated MMC model, the MMC model has been implemented in full-system models including turbine model, wind gust, voltage and current controllers. The full-system models have been provided by Ph.D. candidate Sverre S. Gjerde [16]. The purpose of using full system models, was to evaluate the operation of the MMC in comparison with the conventional two-level model, in a more realistic system.

5.1.1 MMC PSCAD model

The single operated converter block is a modified version of the model built during the specialization project in the fall of 2011. The modifications include:

- Submodule voltage balancing, described in section 5.1.2

[1] PSCAD is a general-purpose time domain simulation tool for studying transient behaviour of electrical networks. NTNU have provided an educational licence version. (4.4.0.0) For additional info; http://www.pqsoft.com/pscad.

- Submodule fault redundancy, described in section 5.1.3

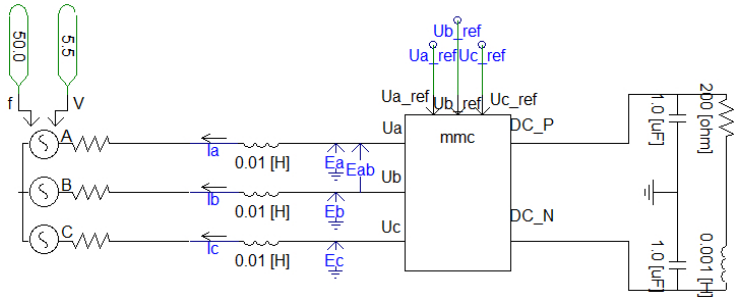

Figure 5.1: Overview of the MMC simulation model connected as a rectifier

Figure 5.1 shows the system with an ideal AC source with the voltage of $V_a = 5.5$ kV, and the converter connected in rectifier mode.

5.1.2 MMC capacitor voltage balancing block

The following section describes the implementation of the balancing strategy as it is done in PSCAD. A voltage balancing block has been programmed, and this block replaces the ordinary PWM gate-control. Programming in PSCAD is done in Fortran 77 [58], and the code is supplied in appendix C.

To select the correct submodules, a feedback measurement from each of the capacitor voltages is needed. In addition, the arm current is measured. The measurements are done continuously, and fed to the calculation block shown in figure 5.2. The output consists of the eight gate signals, which are inverted for the second IGBT in each submodule.

A conventional carrier based PWM is used to calculate when a switching should occur. A reference voltage is then compared with four triangular carriers. This PSCAD block is described in figure 5.4, and the output is shown in figure 5.6. The comparison scheme is shown in figure 5.3. This is the normal operation of the five level MMC.

An edge detector block is used to produce a pulse just at one switching instance shown in figure 5.6. This pulse is controlling the calculation block, feeding a signal for each time the calculations will be executed and the IGBT gate signals updated.

The calculation block does the following.

a) As long as the clock signal is *false*, i.e. no switching should occur, the block reads the old gate signals from memory, and sends the same signals to the output.

b) If the clock signal is *true*,

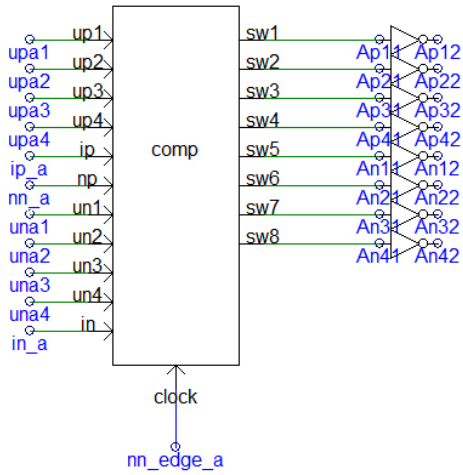

Figure 5.2: Fortran-programmed balancing calculation block in PSCAD

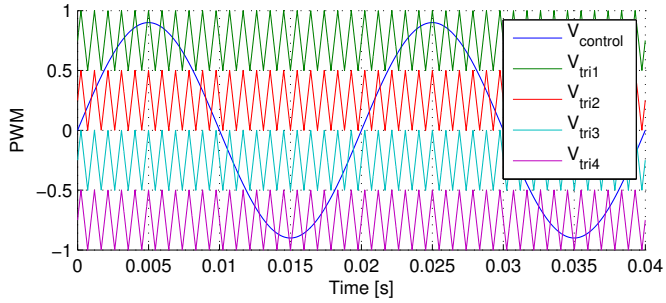

Figure 5.3: PWM comparator scheme for four submodules

1) The capacitor voltages are stored in arrays, and indexed after value.

$$v_{cp} = [v_{cp1}, v_{cp2}, ..., v_{cpn}] \qquad v_{cn} = [v_{cn1}, v_{cn2}, ..., v_{cnn}] \tag{5.1}$$

$$index_{vp} = [i_{vp1}, i_{vp2}, ..., i_{vpn}] \qquad index_{vn} = [i_{vn1}, i_{vn2}, ..., i_{vnn}] \tag{5.2}$$

   By indexing the voltages from high to low, the n submodules with highest or lowest voltage are easily identified for switching.

2) Based on the current direction in upper and lower arm, and the desired number of ON-state submodules, the correct submodules are selected:

   - If the arm current is positive, all ON-state submodules are charging. The n_p and n_n *last* submodules in the indexed array are turned ON, while the other submodules are turned OFF. This increases the voltage in those submodules with the lowest capacitor voltage.

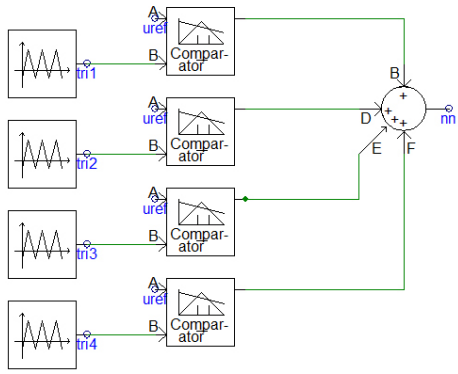

Figure 5.4: PSCAD: Calculation of the desired number of ON-state submodules, n_n

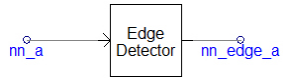

Figure 5.5: Edge detector block used to set a switching instant

- If the arm current is negative, all ON-state submodules are discharging. The n_p and n_n *first* submodules in the indexed array are turned ON, while the other submodules are turned OFF. This decreases the voltage in those submodules with highest capacitor voltage.

3) The gate signals are updated, and stored in memory.

The amount of calculations and switch operations are limited by the frequency of the clock signal.

5.1.3 Redundancy in the MMC: An n-1 scenario

The simulations were preformed in order to describe the possibility of redundancy in the MMC. The converter should be able to withstand a fault in one of the submodules, and operate while the faulty unit is bypassed. This is described as a beneficial feature of the MMC, and therefore included in the simulations.

Some changes are made to the model. Breakers are added to one of the submodules, in order to disconnect and bypass the submodule at a given instant. The breakers are standard modules from the PSCAD library, with a current chopping limit of 0 A, i.e. not ideal. In this case the first submodule in the positive arm of phase a is disconnected. This is shown in figure 5.7.

- BRK1 is used to bypass the submodule. It is set as *closed* to simulate a fault in the submodule.

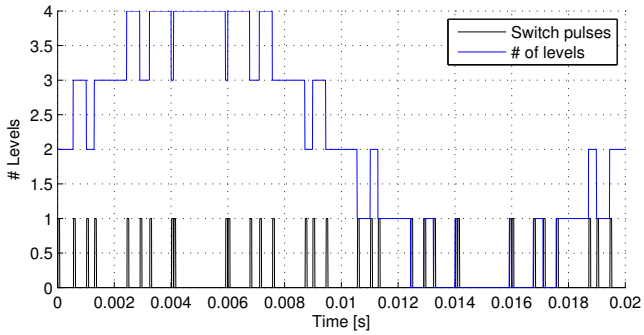

Figure 5.6: Output n_n from the comparison block in figure 5.4

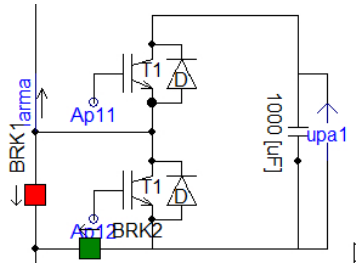

Figure 5.7: Submodule with breakers for disconnection and bypass

- BRK2 is used to completely disconnect the submodule from the system. This is set to *open* at the time of fault.

The control system is also affected in this scenario. The voltage balancing is originally built around four submodules, and will not work properly if one submodule is bypassed. This is avoided by changing the desired number of submodules in the positive arm to max three modules. An input selector is used to select a new PWM-comparison signal at the instant of fault. This comparison signal is simply produced from a reduced version of the original comparator stack with four triangle signals and four comparators. Figure 5.8 shows the new comparator stack, and the selector switch.

The PWM comparators utilize a new triangle scheme, shown in figure 5.9. The difference from the normal operation is observable by comparing the scheme with figure 5.3. The three triangle signals $V_{1,2,3}$ are compared with the reference voltage signal, $V_{control}$, and the maximum output from the addition of the three outputs are thus three.

At the instant of bypassing the first submodule, the number of available submodules are reduced from four to three. The desired number of submodules in ON-state should therefore be max three. The transition from four to three can be observed in figure 5.10. As shown, the desired number of submodules in

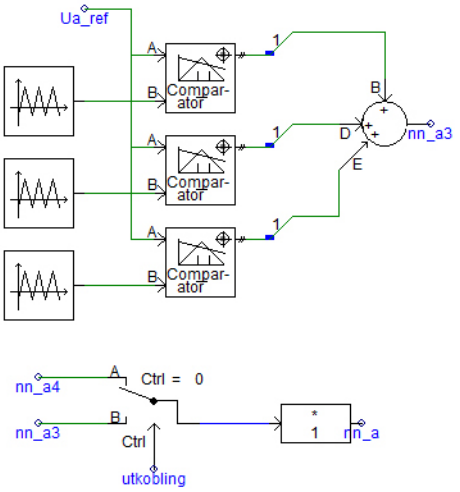

Figure 5.8: Reduced PWM comparator with three triangle-signals

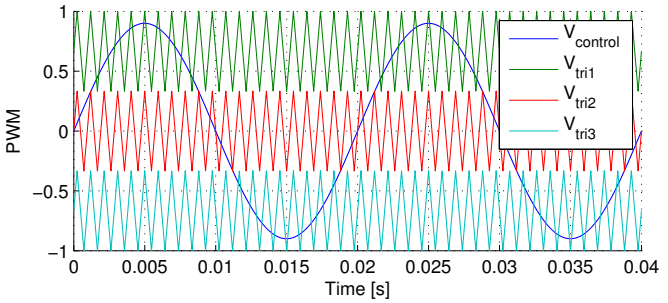

Figure 5.9: PWM comparator scheme for the bypassed system with three sub-modules

ON-state (n_n) is following the referance signal to a max number of three instead of four. In this case, the fault occurs at t = 0.4 s. This should lead to a level reduction to four levels for phase a. See section 5.2.3 for results.

5.1.4 The full system

Simulations were preformed on the full system, to document how the chosen converter operates in comparison to the conventional 2-level VSC. One part of the setup is shown in figure 5.11. The figure shows one of the machine models, and one of the converter modules. All the converter modules are series connected with the two terminals `dcPlus` and `dcMin`.

The idea is that the system should operate with any voltage controlled converter

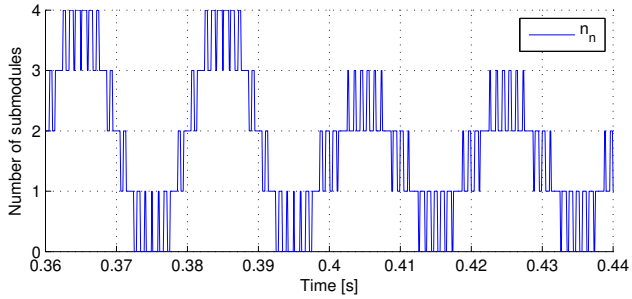

Figure 5.10: Signal from comparator at the bypassing of submodule 1

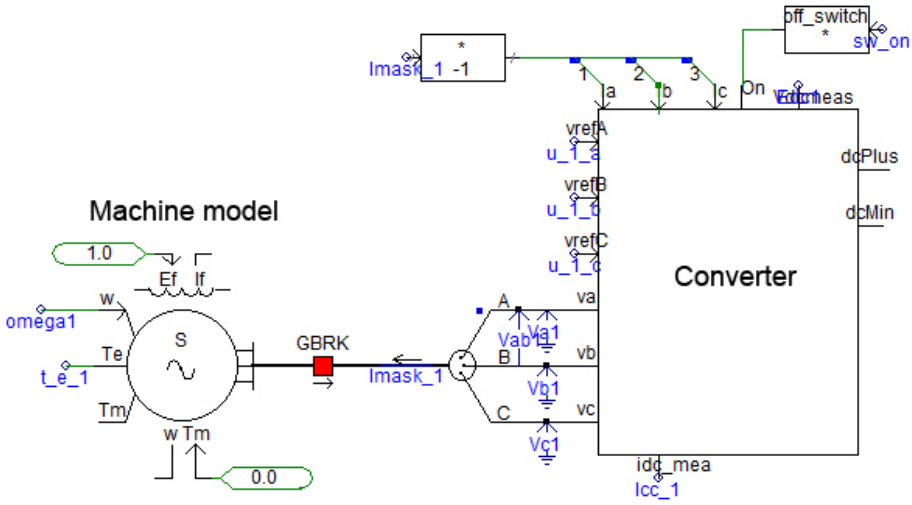

Figure 5.11: PSCAD model of one machine model and one converter from the full system

topologies. Two detailed converter modules have been used in the full-system simulations. Both models have been built by the author.

1. A Conventional 2-level VSC, described in section 3.2.
2. A 5-level Modular Multilevel Converter, described in section 3.5.6.

Description of the complete model can be found in [16].

Reduced to three converter modules

In the educational licence of PSCAD, the system is limited to have maximum 200 nodes. This limits the size of the simulation model, and therefore the full system which originally was built with averaging models in nine converters.

These nine modules had to be reduced to three converter modules when the full converter modules was implemented.

To obtain the functionality and specifications of one converter, the DC-link voltage was because of this reduced to 33.3 kV, from 100 kV. Although the simulation models are reduced, the computation time is very long which leads to limitations in the model resolution.

Generator model

As a simplification, the full system model of the proposed wind turbine uses separate synchronous machine models, instead of one large custom-built PMSG model.

Specifications for the generator models are given in table 5.1:

Table 5.1: Full system - simulation model specifications

Generator parameters	Value
Generator rating	1.1 MW
Stator resistance, r_s	0.015 pu
Stator reactance, x_s	0.33 pu
Nominal frequency f_n	30 Hz
Nominal line voltage (rms) v_n	3.93 kV
Nominal generator current (rms) i_n	94 A
DC-link parameters	
Total DC-link voltage V_{dc}	33.3 kV
DC-link inductance L_{dc}	25 mH
DC-link resistance R_{dc}	1.49 Ω
Converter parameters	
Submodule capacitance V_{dc}	1000 μF
Phase leg inductance L_{dc}	0.1 μH

Simulation sequence

Some of the following simulations show the first seconds of operation of the full system, like the DC output voltages shown in section 5.2.5. Important events in the start-up sequence are summarized below.

0 s Initializing, DC link voltage source on (ramp up time = 0.005 s) and connected to converters, speed reference = 0.25 pu, windspeed = 4 $^{m}/_{s}$.

5.0 s Wind speed = 10.0 $^{m}/_{s}$.

6.2 s Speed reaches 0.25 pu, and generator breaker GBRK closes.

7.0 s Speed reference = 0.8 pu.

12 s Turbine reaches speed reference of 0.8 pu.

5.2 Simulation results and analysis

This section describes and analyses the simulation results.

5.2.1 Single operated MMC converter

This section describes the simulation results from the operation of one separate MMC, as described in section 5.1.1.

The three phase voltages are shown in figure 5.12. The voltages have the classical five-level staircase shape with the following voltage steps;

$$V_{abc,5} \in \{5.5, 2.75, 0, -2.75, -5.5\} \text{ kV} \tag{5.3}$$

The line-to-line voltage THD is about 13 %, which is much lower than in the two level converter, operated in the same model. The line-to-line THD in the two-level model was 63 % as seen in the comparison of section 3.6.4.

Figure 5.13 shows the corresponding phase currents. The current is filtered to some extent by the not purely resistive load and the line impedances. The current THD is about 5 %, in contrast to 12 % in the two-level converter model.

In each submodule, the capacitor voltages are captured. Figure 5.14 shows a detailed print of the four upper capacitor voltages in phase a. The voltage balancing ensures that the voltages is kept balanced around 2.75 kV. As shown in the figure, the oscillations follow the system frequency of 50 Hz.

The MMC operates as expected in the single rectifier mode.

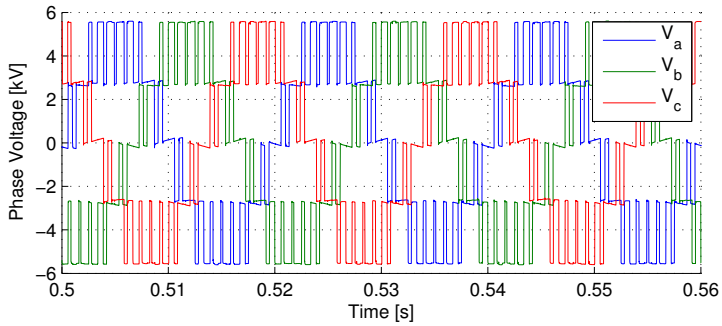

Figure 5.12: Phase voltages V_a, V_b and V_c in the separated operation of an MMC in rectifier mode.

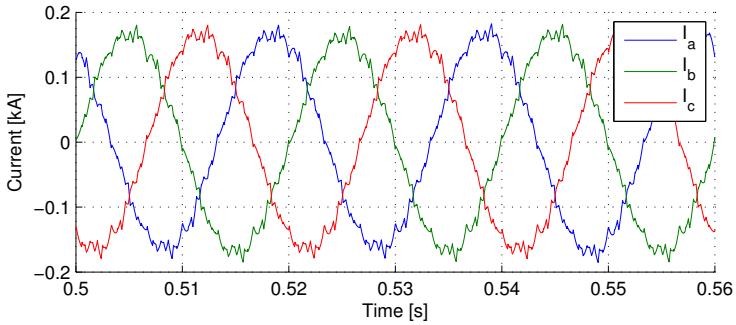

Figure 5.13: Line currents I_a, I_b and I_c in the separated operation of an MMC converter in rectifier mode.

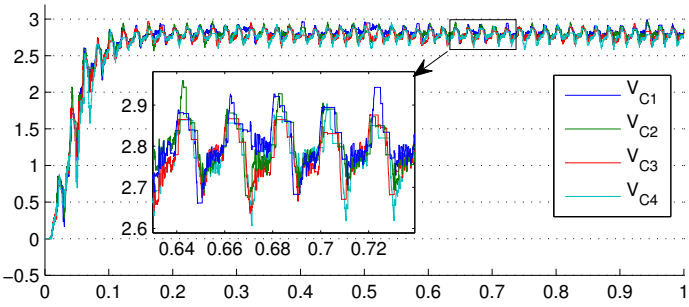

Figure 5.14: Submodule capacitor voltages V_{C1} - V_{C4}, phase a, upper arm. Separated operation of an MMC converter in rectifier mode.

5.2.2 MMC voltage balancing control algorithm

Simulations in PSCAD confirms the basic idea of voltage balancing by the sorting algorithm. As shown in figure 5.15, the capacitor voltages in the upper arm of phase a is balanced around 2.75 kV, which is one fourth of the DC-link voltage. At t = 0.5 s, the capacitor voltage sorting is disabled in the calculation block, and as expected the voltages drift towards zero and $\frac{V_{dc}}{2}$ = 5.5 kV.

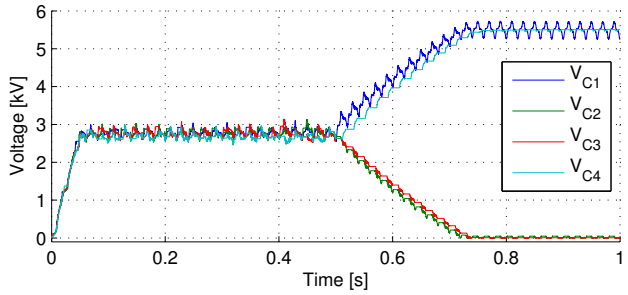

Figure 5.15: Submodule capacitor voltages in upper arm, phase a: The voltage balancing control is disabled at t = 0.5 s, resulting in drifting capacitor voltages.

The phase voltage is a stable five level voltage until the balancing is disabled. At t=0.7s the voltages are totally imbalanced, and the converter acts as a three level converter. The voltage waveform is shown in figure 5.16.

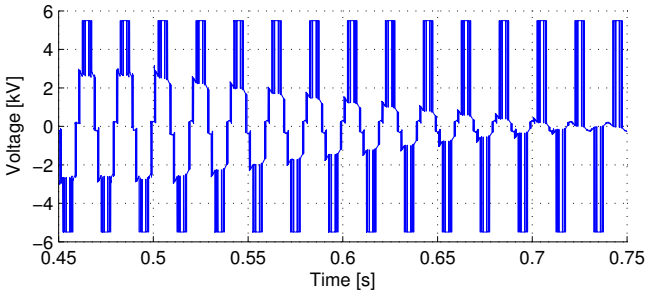

Figure 5.16: Phase voltage V_a, capacitor voltage balancing control disabled at t = 0.5 s, resulting in a three-level functionality.

Figure 5.17 shows the phase current i_a before disabling the balancing. As observed from figure 5.18, the phase current is seriously distorted after disabling the voltage balancing.

The measured total harmonic distortion (THD) in the line to line voltage V_{ab} increases from 14% (before disabling balancing) to 35% (after t = 0.7s).

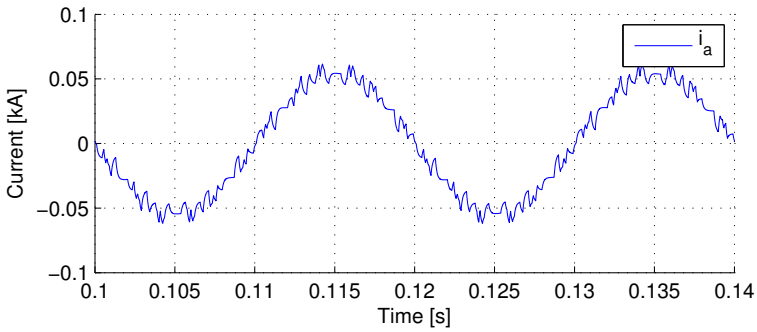

Figure 5.17: Phase current i_a: Before capacitor voltage balancing control is disabled at 0.4 s.

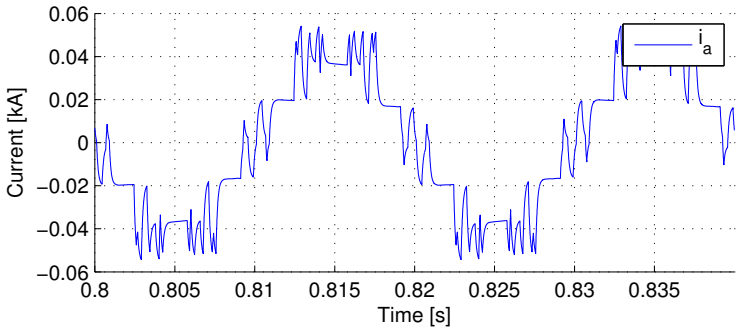

Figure 5.18: Phase current i_a: After capacitor voltage balancing control is disabled, and the phase voltage has developed a three-level form.

5.2.3 Redundancy, n-1 scenario

When bypassing one submodule in phase a, upper arm, the following observations can be made:

- The number of submodules in the upper arm are reduced to three. This is previously shown in figure 5.10.
- The voltages in each of the remaining submodules are increased.
- The phase voltage in the converter is reduced to four levels.
- The harmonic content in voltages and currents is increased.

Submodule capacitor voltages

Figure 5.19 shows the capacitor voltages in the four submodules in the upper arm of phase a. The bypassing is executed at t = 0.4 s. At this instant, the DC-link voltage is divided among three submodules instead of four. This means that the voltages should balance around:

$$V_{Ci,4} = \frac{11 \text{ kV}}{4} = 2.75 \text{ kV} \qquad V_{Ci,3} = \frac{11 \text{ kV}}{3} = 3.67 \text{ kV} \tag{5.4}$$

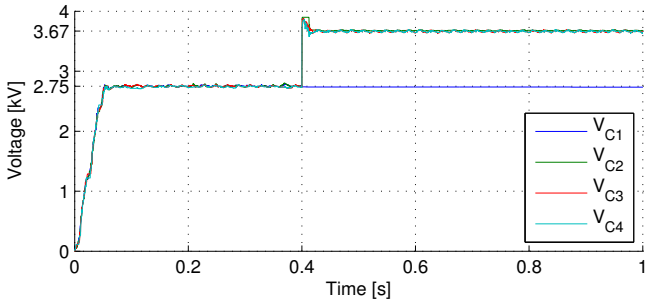

Figure 5.19: Capacitor voltages, upper arm, phase a: Redundancy test at t = 0.4 s. The first submodule of phase a is bypassed.

The result from the simulation scenario shows the same behaviour as expected. The voltage in submodule 1, V_{C1}, remains at 2.75 kV after the disconnection. The voltage in the three other submodules increases to be balanced at 3.67 kV after the disconnection and bypass at t = 0.4 s.

The capacitors have to be over-rated to withstand the operation with bypassed units. In the current scenario, the over-rating should therefore exceed a factor of:

$$K_{red} = \frac{3.67}{2.75} = 1.33 \tag{5.5}$$

I.e. the the voltage rating should be at least 3.67 kV, an over-rating of 33 % from the normal operation voltage. With an increasing number of levels, this factor is reduced. Depending on the redundancy factor, a converter with more levels is generally possible to operate with a higher amount of bypassed submodules.

A small overshoot is experienced before new balancing is obtained. This will also affect the dimensioning of the capacitors, and should therefore be included in a more thorough system design.

Phase voltages

The phase voltages are captured to see the influence from the submodule bypass. A detailed view of the phase voltages are included in figure 5.20.

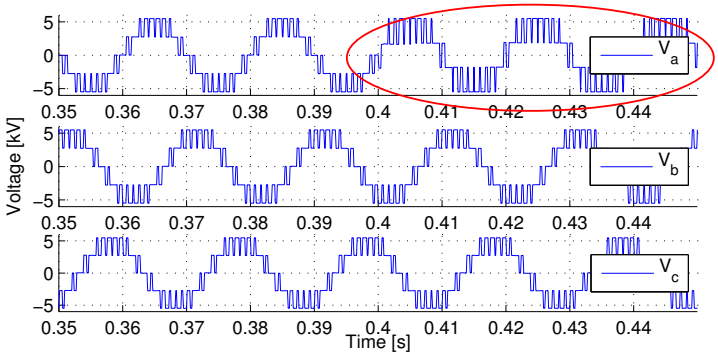

Figure 5.20: Phase voltages V_a, V_b, V_c: Redundancy test: The first submodule of phase a is bypassed at t = 0.4 s.

As illustrated in figure 5.20, only phase a is influenced by the short circuit of submodule 1. The voltage shape in phase a is as expected reduced from five levels to four levels. Phase voltages b and c are not affected, and maintains the same shape after the bypass of submodule 1 in phase a.

Line-to-line voltages

The line-to-line voltages V_{ab} and V_{ac} are affected, as described in figure 5.21. This corresponds with the phase voltages in figure 5.20, where only phase a is affected by the submodule bypass. Since neither of the two phase voltages V_b and V_c are affected, the line-to-line voltage between these two phases, V_{bc} remains unchanged after the bypass at t = 0.4 s.

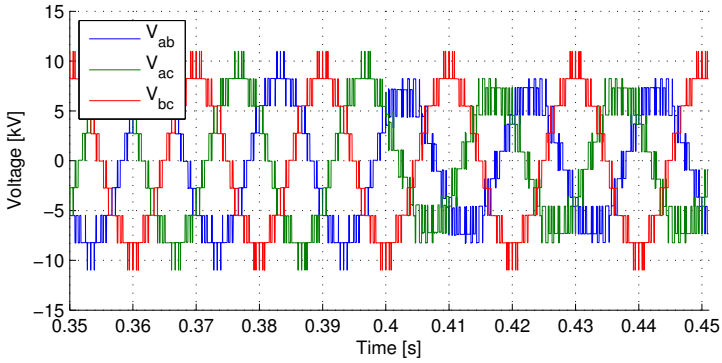

Figure 5.21: Line-to-line voltages V_{ab}, V_{bc} and V_{ac}: Redundancy test: The first submodule of phase a is bypassed at t = 0.4 s.

Phase currents

The phase currents are also investigated to see the influence from the altered phase voltage after a submodule bypass. The measurements are done per phase in PSCAD, and shown in figure 5.22.

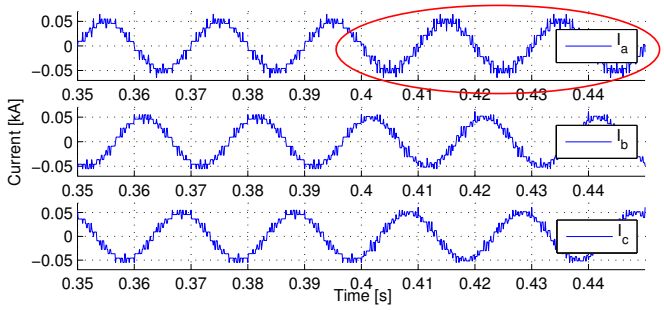

Figure 5.22: Phase currents I_a, I_b, I_c. Redundancy test: The first submodule of phase a is bypassed at t = 0.4 s.

As for the phase voltages, there is no significant change in the phase currents for the two phases c and c. Phase a is slightly affected, as seen in figure 5.22.

THD

To quantify the distortion in the voltage, the Total Harmonic Distortion is measured in the line-line voltage, V_{ab}. The bypass results in an increase in THD of 65%. This is illustrated in figure 5.23.

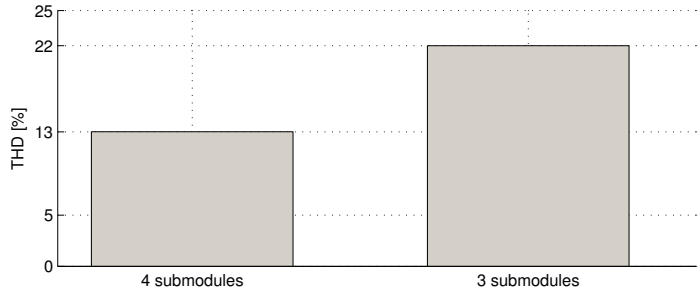

Figure 5.23: THD in V_{ab} before and after bypass of submodule 1 in phase a.

The increase in THD is substantial. This is however expected, as the phase voltage is greatly distorted from four to three levels, seen in figure 5.20, and the distorted line-to-line voltages of figure 5.21.

5.2.4 MMC Multilevel arrangement - reducing filtering

An argument for the MMC has been the reduced demand for filtering because of the high level count. There is however difficult to see from literature exactly how many levels that are needed to avoid filtering in the proposed wind turbine system. Therefore, nine additional MMC models have been built in PSCAD to measure the reduction in harmonic content when increasing the number of levels.

To reduce the time-consuming work of modelling, these MMC models were built without control systems and voltage balancing algorithms. Instead, the current is reduced to avoid capacitor voltage drifting while the THD is measured.

Figure 5.24 shows how the THD in the line-to-line voltage V_{ab} is reduced from 13% to 2%, when the number of levels in the MMC model is increased from 5 to 23 levels.

Corresponding phase voltages and currents, as well as harmonic spectra for the ten models are attached in appendix B.

5.2.5 MMC model in the full system

The following section presents the results from operating the MMC in the full wind turbine system. It is expected to see a similar behaviour as in the separate operation of one converter, described in section 5.2.1.

When implementing the 5-level MMC and comparing it with a 2-level VSC, the following features are desired:

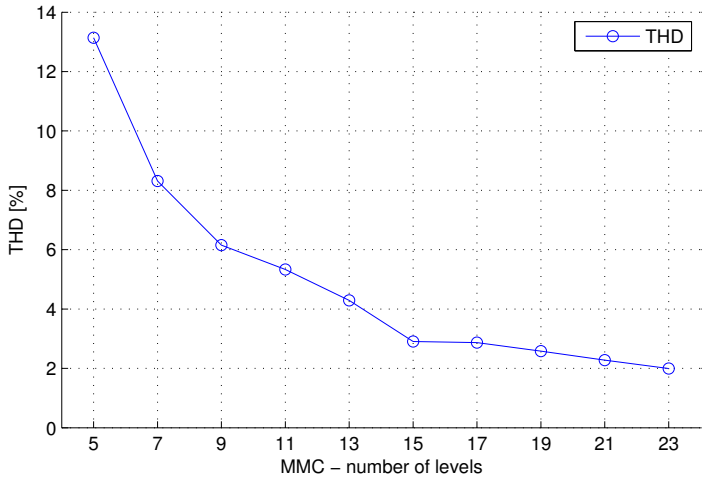

Figure 5.24: The reduction in THD in line-line voltage V_{ab} when the number of levels is increased in MMC models from 5 to 23 levels.

- All MMC features should function as expected. This means especially functions like submodule voltage balancing.
- The voltage shapes should have the expected 5-level shape as shown in simulations of the separate MMC model, i.e. with less harmonic content than the two-level converter model.
- The line currents should be less distorted than in the two-level model.
- In addition to balanced submodule voltages, the output DC voltages from each converter module should balance.
- The system itself should function in the same way, and not be negatively affected by the introduction of the MMC.

The turbine is started up with the sequence described in 5.1.4. Figure 5.25 shows the rotational speed in the turbine. This figure is included to explain the events observed in simulations that show the first seconds of operation, like the DC-link voltages in section 5.2.5. Some speed is built up before the generator is connected, and a very hard ramp up is set to get the system up to operational speed. This is not realistic, but implemented to shorten the simulation time.

Voltage waveforms

Both phase-to-ground and line-to-line voltages are recorded at the input of one converter block in the full system. The full system with conventional three phase, 2-level converters is used as baseline for the comparison.

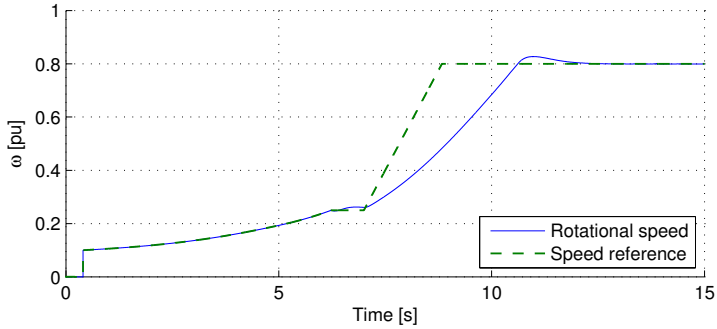

Figure 5.25: Startup sequence of the full system: The rotational speed of generator 1 and its reference.

The three graphs in figure 5.26 show the phase-to-ground voltage V_a when a 2-level converter is used. Because of the grounding reference and the series connection of the converter modules, there is a DC offset of ± 11.1 kV in converter 1 and 3. The inductance in the DC-link (L_{dc}) is set to zero to illustrate the typical two level switching pattern. When the DC-link inductance is included, the phase voltage is similar but with a sinusoidal component following the system frequency. The DC-link voltages seems to be balanced, since all three phase voltage shapes have the same amplitude.

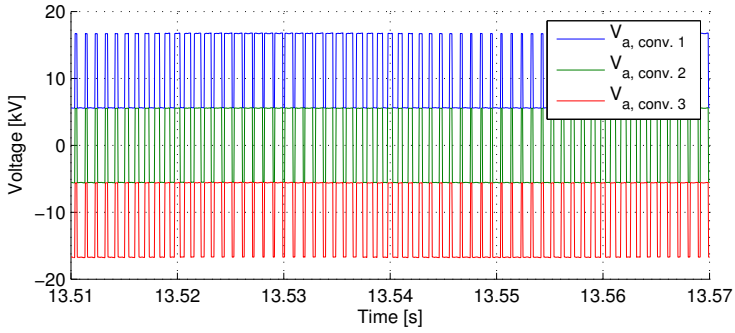

Figure 5.26: Full system model with 2-level converters. Phase-to-ground voltage V_a in all three converters. $L_{dc} = 0$

A more detailed view of all the three phase voltages in converter 1 is shown in figure 5.27.

The line-to-line voltage V_{ab} in the upper two-level converter is shown in figure 5.28. The voltage show a typical shape of a two level line-to-line voltage.

When implementing the five-level MMC instead of the two-level converter, the

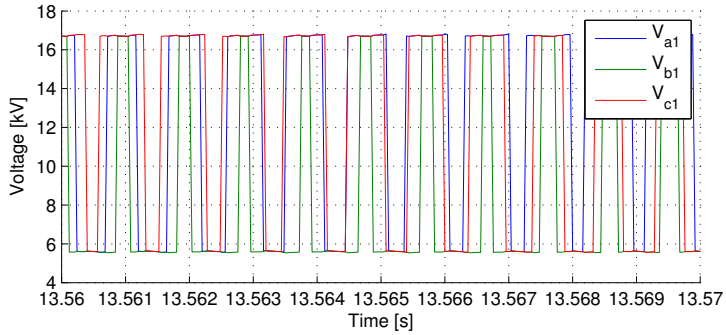

Figure 5.27: Full system model with 2-level converters. Phase-to-ground voltages V_a, V_b and V_c in converter 1. $L_{dc} = 0$

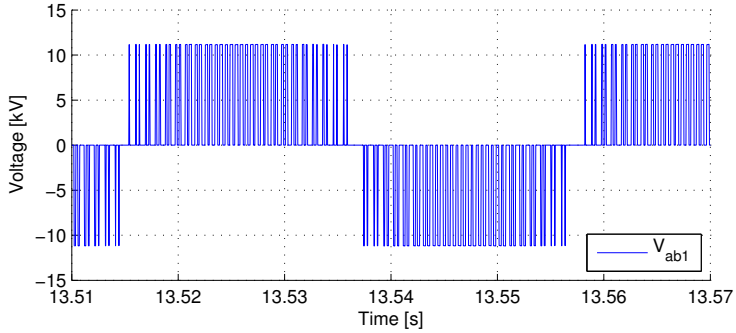

Figure 5.28: Full system model with 2-level converters. Line-to-line voltage V_{ab} in converter 1. $L_{dc} = 0$

voltages become as expected more sinusoidal[2]. Figure 5.29 shows the phase voltages measured at the AC side of the three MMC converter modules. For illustration purposes, the DC-link inductance is set to zero. The classical staircase voltage shape is clearly visible, and the DC-outputs seem to have the same value, as the voltages have the same DC offset. This is, as for the two-level setup ± 11.1 kV for converter 1 and 3.

Figure 5.30 show a more detailed view of the symmetrical three phase voltages of converter 1.

As for the two-level setup, the line-to-line voltage V_{ab} for converter 1 is included, and shown in figure 5.31. The voltage has a 7-level shape, because the generator does not run at nominal speed, resulting in a lower peak voltage. At nominal voltage, the line-to-line voltage would show a 9-level shape, as in figure 5.21

[2]The resolution in the plots for the MMC is lower than for the two-level setup. This is because of memory limitations in PSCAD. The switching patterns in the voltage shapes are therefore not as clean as the ones in section 5.2.1 and Appendix B.

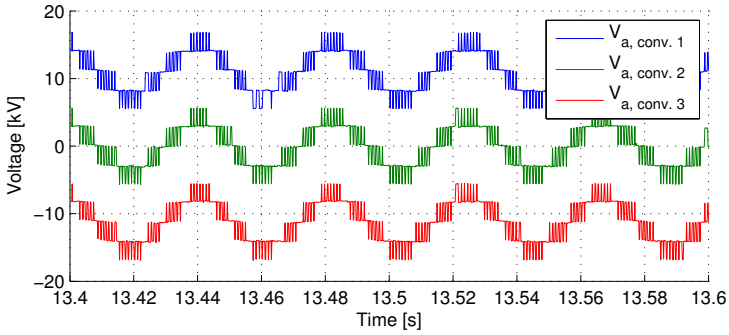

Figure 5.29: Full system model with MMC converters. Phase voltages V_a in all three converter modules. $L_{dc} = 0$

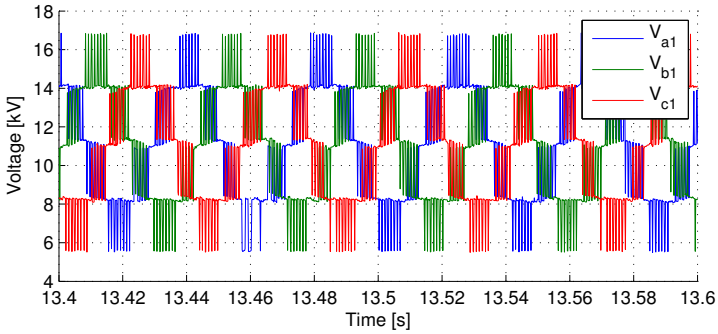

Figure 5.30: Full system model with MMC converters. Phase voltages V_a, V_b and V_c in converter 1. $L_{dc} = 0$

where the modulation index is $m_a = 0.9$.

The voltage shapes indicate that the MMC functions as expected in the full system as well.

Phase currents

All phase currents in the first converter module are examined. As with the voltages, an improvement was expected with the five level MMC. Figure 5.32 shows the line currents I_a, I_b and I_c in the first converter module.

As seen from the figure, the system frequency is about 25 Hz, and the smaller oscillations follow the switch frequency of 1050 Hz. The system frequency is dependent of the wind speed, and the switching frequency is set equal for all simulations. The quality is acceptable, seen from low fuzziness in the phase currents in figure 5.32.

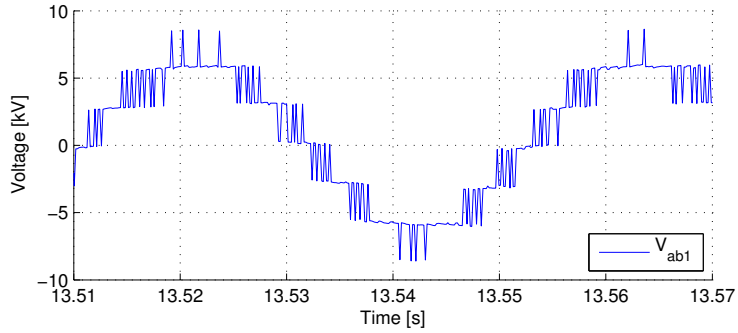

Figure 5.31: Full system model with MMC converters. Line-to-line voltage V_{ab} in converter 1. $L_{dc} = 0$

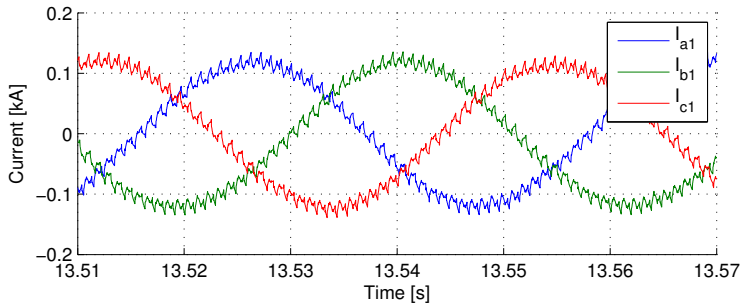

Figure 5.32: Full system model with standard 2-level VSC. Line current I_a, I_b and I_c in the first converter module.

The same plot is done in the model with a five-level MMC, and the results are very good. Figure 5.33 shows the corresponding line currents I_a, I_b and I_c in the first converter module.

The expansion from two to five levels makes a substantial difference also in the current. As in figure 5.32, figure 5.33 shows a system frequency of about 25 Hz, and although almost not visible, a switching frequency of 1050 Hz. The distortion is very low.

When compared to figure 5.17 in section 5.2.3, which shows the line current for a nearly unfiltered five-level MMC, it is observed that the line current is smoother in the full system. This is because the machine model, described in 5.1.4, contains larger reluctances than the single operated MMC model, which filters the current.

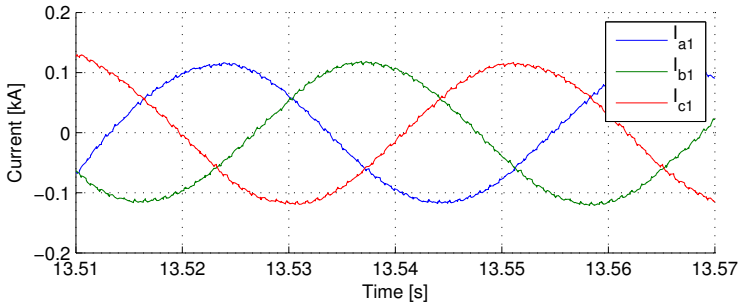

Figure 5.33: Full system model with 5-level MMC as converter. Line current I_a, I_b and I_c in first converter module.

DC voltages

Since the MMC system includes a voltage balancing control, the DC voltages are compared. In the MMC model, the voltages in each submodule capacitor are measured. In addition, the DC output from each converter module, and the total DC link voltage is captured.

The MMC is expected to operate with submodule voltage balancing in the full system, and be comparable to the isolated model simulations, shown in section 5.2.2.

Figure 5.34 shows the DC voltage for each converter module in the full system, V_{dc1}, V_{dc2} and V_{dc3}, and the full DC link voltage, $V_{dc,tot}$. The submodule voltages for phase a, upper arm are shown in figure 5.36.

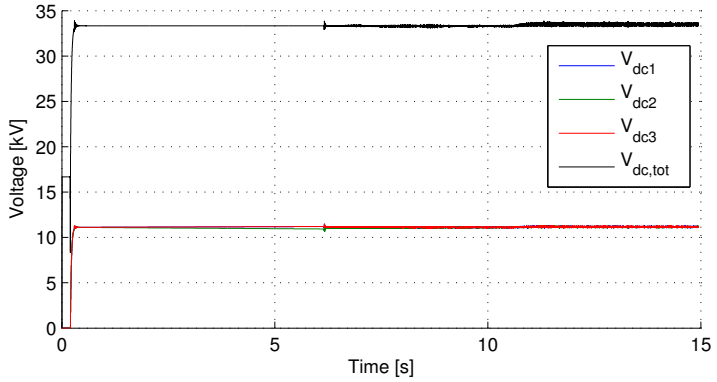

Figure 5.34: Converter module voltages and total DC-link voltage in the full system with two-level converters.

Figure 5.35 shows the same voltages for the system with the MMC.

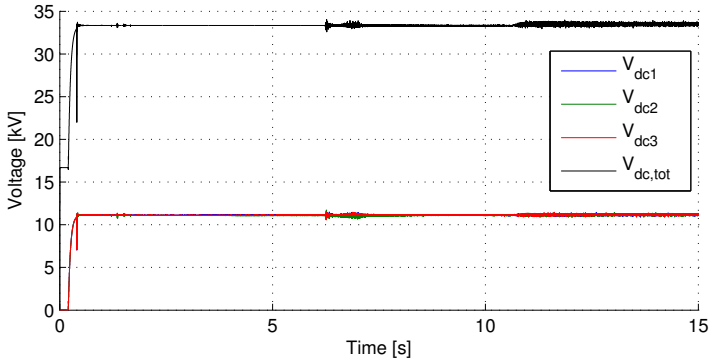

Figure 5.35: Converter module voltages and total DC-link voltage in the full system with five-level MMC.

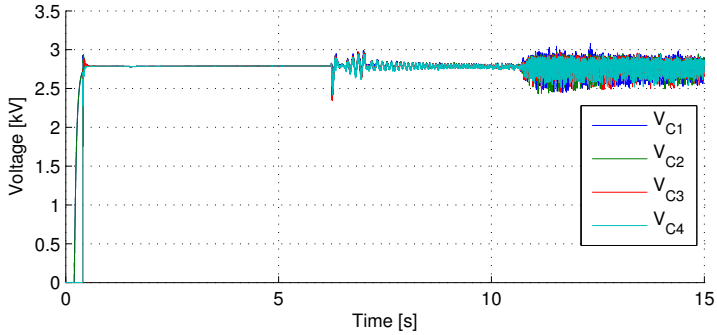

Figure 5.36: Submodule capacitor voltages V_{C1-4} in phase a of the MMC, upper arm, for the full system.

As shown in the two figures 5.34 and 5.35, the DC voltage ripple is quite similar in both models. There are some increased oscillations around 6-7 s. At these instants, the speed crosses its reference, and the generator is connected to the system. There is a increased torque to balance the speed overshoot, and therefore an increased current. The ripple in the DC voltage is larger when the current is increased. The same oscillations are visible in submodule voltages in figure 5.36. This is in accordance with observations from the simpler models as well. The balancing of submodules is more oscillating when the current is high.

A minor drift in converter DC output voltages might be observed in figure 5.34, for the two-level setup, at the time before the generator is connected at t = 6.2 s. This however a numerical PSCAD error only, as there is no current in the converter.

Both systems give a small peak when the generator is connected, and at arround 11 seconds the torque is again higher than the reference. In addition, the

setpoint changes to increase production. The current is higher, and therefore both models have increased DC voltage oscillations at the end of the simulation.

5.3 Discussion

5.3.1 Performance

The MMC performs well in the proposed system. The simulation results have shown that the MMC outperforms the two-level converter in terms of voltage and current quality, at least at the generator side. A minor increase in ripple is experienced at the grid side, which is believed to be a result from the submodule voltage balancing. Balancing of capacitor voltages is harder in transient periods, and the model uses a very steep ramp-up. In addition, the voltage balancing algorithm and parameters in the MMC are not fine-tuned.

Moreover, the system behaves very well to the implementation of a new converter model as well. This is an indication of that the system can tolerate any voltage source converter with a three phase input and a DC-link output.

5.3.2 Number of levels

This thesis has pointed out many reasons for increasing the number of levels. Low amount of harmonics, increased redundancy and decreased losses are examples. On the other hand, increasing the number of levels will increase the complexity, with the consequence of a more advanced control system. From a practical point of view, it is often best to keep a system as simple as possible. Reasons are that a simpler design is more reliable, and cheaper to install, maintain and supervise. But if one of the goals is to avoid series connection of IGBTs, the multilevel approach is necessary.

Besides, simulations have shown that a five level converter results in submodule voltages for the full system of about 3 kV, when ripple and balancing is included. With a certain overrating to protect the transistors against transients and over voltages, this is ok if the largest IGBTs available are used. As mentioned in section 4.4, if minimizing losses is important, the amount of levels could be increased in order to use IGBTs with lower ratings. In addition, the results in section 5.1.3 have shown that an increased level count is beneficial to make the system more able to operate with faulty, bypassed modules.

Section 4.3 introduced the question of how many levels that are needed to avoid filtering. Results in section 5.2.4 have shown that the harmonic distortion in both voltage and current is quickly reduced when the amount of levels increase. The AC current is, to some degree, filtered by inductances in the machine, and requirements to harmonic content is mainly restricted to the PCC. A high

increase in levels should therefore not be motivated only by the reduction in harmonics. The generator can be built to withstand a relative high amount of harmonic distortion, especially compared to customer appliances in larger grids. It will instead be a question of price and losses, and the complexity involved in a final mass production of the turbine.

An optimization is in the end required, to come up with the best number of levels, with regards to the desired combination of IGBT rating, redundancy, total harmonics, $\frac{dv}{dt}s$, generator insulation and oscillating torque.

Chapter 6

Conclusions

In this thesis the five most popular multilevel converter topologies have been presented, and compared with focus on suitability for a special weight reducing wind turbine generator concept. The modular multilevel converter (MMC) has several benefits which made it the most interesting topology for further studies: The MMC makes direct series connection of IGBTs unnecessary. In addition, it offers high voltage quality, redundancy possibilities, lower demand for filtering and is easier expandable to a larger amount of levels than the other topologies.

Preliminary studies showed that the MMC requires balancing control to avoid capacitor voltage drifting. The simulations of a single operated MMC have therefore focused on the balancing strategy. A voltage balancing strategy was implemented and analysed to ensure correct operation of the converter. The feature of redundancy with module failure has also been simulated in PSCAD.

Because of today's limitations in voltage handling of IGBTs, the MMC should have at least five levels to prevent damage to IGBTs because of over voltages in transient periods. An optimal amount of levels depend upon the desired level of losses, specifications of the generator, voltage quality and a weighting of reliability versus complexity. This optimization has yet to be performed in a complete generator design, with cooperation between generator and converter producers.

The converter has been compared to a conventional two-level converter in a full wind turbine simulation of the proposed generator system. The MMC functioned well in the system, and outperformed the two-level in terms of voltage quality, as was expected. By implementing the features of a multilevel converter into the proposed system, the system can improve in terms of reliability. This is very beneficial in offshore installations where accessibility is limited.

Chapter 7

Further work

Additional work is required for a verification of the proposed combination of converter and generator system.

The work of this thesis has not included laboratory models. A natural continuation of the work would therefore be to build a model of the MMC, and include the model in a prototype of the special generator. A laboratory model would probably highlight additional challenges with the combination, and give a better background for more detailed reliability calculations.

To optimize the number of levels in the special system, many factors have to be considered. Among these factors are the calculation of losses, which is not thoroughly covered in this thesis. In addition, a cooperation with the producer of the generator is needed to find a satisfactory amount of harmonic components.

A benefit of multilevel converters is the possible reduction of the switching frequency to reduce the switching losses. Simulations in this work have had a constant switching frequency of 1050 Hz. An interesting study would be the question of how low the switching frequency can be in a multilevel converter.

In addition more practical aspects of the MMC converter should be included in a more thorough study. This includes structural issues, and detailed weight estimates.

Finally, it it worth to mention the optimization of the whole generator-converter system. This master's thesis has used the proposed system with 100 kV DC link and nine converter modules as a basis, and with a desire to avoid series connection of IGBTs. The choice of converter topology is very dependent of this configuration, especially because of the voltage level and number of converter modules. Another full system configuration could in total be more economical.

Bibliography

[1] R. Lund. *Multilevel Power Electronic Converters for Electrical Motor Drives*. PhD thesis, NTNU, 2005.

[2] H. Iman Eini, Sh. Farhangi, and J.L. Schanen. A modular AC/DC rectifier based on cascaded H-bridge rectifier. In *Power Electronics and Motion Control Conference, 2008. EPE-PEMC 2008. 13th*, pages 173 –180, sept. 2008.

[3] J. Wen and K. Smedley. Hexagram Rectifier x2014; Active Front End of Hexagram Inverter for Medium-Voltage Variable-Speed Drives. *Power Electronics, IEEE Transactions on*, 23(6):3014 –3024, nov. 2008.

[4] J. Wen and K. Smedley. Synthesis of Multilevel Converters Based on Single- and/or Three-phase Converter Building Blocks. In *Industrial Electronics Society, 2007. IECON 2007. 33rd Annual Conference of the IEEE*, pages 1780 –1786, nov. 2007.

[5] World Wind Energy Association. World Market for Wind Turbines recovers and sets a new record, accessed may 28th, 2012. `http://wwindea.org/home/index.php`.

[6] IEEE. IEEE Recommended Practices and Requirements for Harmonic Control in Electrical Power Systems. *IEEE Std 519-1992*, 1993.

[7] ABB. Success factors for Electrification on the NCS, accessed april 11th, 2012. `http://www.zero10.no/innleggene/Asmund_Maland.pdf`.

[8] Statoil. Annual Report 2010, Electrification of offshore installations, accessed april 11th, 2012. `http://www.statoil.com/AnnualReport2010/`.

[9] World Wind Energy Association. World Wind Energy Report 2010, accessed sept. 13, 2011. `http://www.wwindea.org/home/images/stories/pdfs/worldwindenergyreport2010_s.pdf`.

[10] J.F. Manwell, J.G. McGowan, and A.L. Rogers. *Wind Energy Explained: Theory, Design and Application*. John Wiley and Sons, Ltd, 2002.

[11] Stortingets informasjonstjeneste. Samtykke til inngåelse av avtale med Sverige om et felles marked for elsertifikater, accessed June 4rd, 2012. `http://www.stortinget.no/no/Saker-og-publikasjoner/Saker/Sak/?p=51456`.

[12] Technoport RERC. Book of Abstracts, accessed June 3rd, 2012. `http://2012.technoport.no/upload/Technoport_RERC_2012_abstract_book.pdf`.

[13] Zhaoqiang Z., A. Matveev, S. Ovrebo, R. Nilssen, and A. Nysveen. State of the art in generator technology for offshore wind energy conversion systems. In *Electric Machines Drives Conference (IEMDC), 2011 IEEE International*, pages 1131 –1136, 2011.

[14] J. Ribrant and L. Bertling. Survey of failures in wind power systems with focus on Swedish wind power plants during 1997-2005. In *Power Engineering Society General Meeting, 2007. IEEE*, pages 1 –8, june 2007.

[15] S. Gjerde and T. Undeland. Power conversion system for transformerless offshore wind turbine. In *Power Electronics and Applications (EPE 2011), Proceedings of the 2011-14th European Conference on*, pages 1 –10, 30 2011-sept. 1 2011.

[16] S.Gjerde and T. Undeland. A Modular Series Connected Converter for a 10 MW, 36 kV, Transformer-Less Offshore Wind Power Generator Drive. In *Energy Procedia: DeepWind, 19-20 January 2012, Trondheim, Norway, Elsevier Ltd*, 2011.

[17] E. Spooner, P. Gordon, and C.D. French. Lightweight, ironless-stator, PM generators for direct-drive wind turbines. In *Power Electronics, Machines and Drives, 2004. (PEMD 2004). Second International Conference on (Conf. Publ. No. 498)*, volume 1, pages 29 – 33 Vol.1, march-2 april 2004.

[18] S. Gjerde and T. Undeland. Fault Tolerance of a 10 MW, 100 kV Transformerless Offshore Wind Turbine Concept with a Modular Converter System. In *15th International Power Electronics and Motion Control Conference, EPE-PEMC 2012 ECCE Europe, Novi Sad, Serbia*, 2012.

[19] E. Koutroulis and K Kalaitzakis. Design of a maximum power tracking system for wind-energy- conversion applications. In *Industrial Electronics, IEEE Transactions*, pages 486 – 494, 2006.

[20] M. Chinchilla, S. Arnaltes, and J.C. Burgos. Control of permanent-magnet generators applied to variable-speed wind-energy systems connected to the grid. *Energy Conversion, IEEE Transactions on*, 21(1):130 – 135, march 2006.

[21] V. Blasko and V. Kaura. A new mathematical model and control of a three-phase AC-DC voltage source converter. *Power Electronics, IEEE Transactions on*, 12(1):116 –123, jan 1997.

[22] Chandra Bajracharya, Marta Molinas, Jon Are Suul, and Tore M Undeland. Understanding of tuning techniques of converter controllers for VSC-HVDC. *IEEE Control Systems*, 2008.

[23] N. Jelani and M. Molinas. Stability investigation of control system for power electronic converter acting as load interface in AC distribution system. In *Industrial Electronics (ISIE), 2011 IEEE International Symposium on*, pages 408 –413, june 2011.

[24] Thomas Ackermann. Transmission Systems for Offshore Wind Farms. *Power Engineering Review, IEEE*, 22(12):23 –27, december 2002.

[25] Jürgen Häfner and ABB AB HVDC Sweeden Björn Jacobson. Proactive Hybrid HVDC Breakers - A key innovation for reliable HVDC grids. In *Cigré: The electric power system of the future - Integrating supergrids and microgrids International Symposium*, 2011.

[26] R.M. Nilssen J. Holto P.K. Olsen, S. Gjerde and S. Hvidsten. A Transformerless Generator-Converter Concept making feasible a 100 kV Low Weight Offshore Wind Turbine Part I - The Generator. In *Accepted for IEEE Energy Conversion Congress & Exposition (ECCE), Raleigh, NC, USA, 2012*, 2012.

[27] W. Robbins N. Mohan, T. Undeland. *The Power Electronics: Converter, Applications and Design*. Ed. Wiley, 2003.

[28] Mitsubishi Electric. Mitsubishi Electric HVIGBT Module Data Sheets, accessed June 4rd, 2012. `http://www.mitsubishielectric.com/semiconductors/php/eSearch.php?FOLDER=/product/powermod/powmod/hvigbtmod`.

[29] J. Rodriguez, Jih-Sheng Lai, and Fang Zheng Peng. Multilevel inverters: a survey of topologies, controls, and applications. *Industrial Electronics, IEEE Transactions on*, 49(4):724 – 738, 2002.

[30] L. Yang, C. Zhao, and X. Yang. Loss calculation method of modular multilevel HVDC converters. In *Electrical Power and Energy Conference (EPEC), 2011 IEEE*, pages 97 –101, oct. 2011.

[31] D Holmes and Thomas A Lipo. *Pulse Width Modulation for Power Converters; Principles and Practice*. Wiley, 2003.

[32] Hasmukh S. Patel and Richard G. Hoft. Generalized Techniques of Harmonic Elimination and Voltage Control in Thyristor Inverters: Part I–Harmonic Elimination. *Industry Applications, IEEE Transactions on*, IA-9(3):310 –317, may 1973.

[33] G.S. Konstantinou and V.G. Agelidis. Performance evaluation of half-bridge cascaded multilevel converters operated with multicarrier sinusoidal PWM techniques. In *Industrial Electronics and Applications, 2009. ICIEA 2009. 4th IEEE Conference on*, pages 3399 –3404, 2009.

[34] A. Nabae, I. Takahashi, and H. Akagi. A New Neutral-Point-Clamped PWM Inverter. *Industry Applications, IEEE Transactions*, IA-17(5):518 –523, sept. 1981.

[35] N.S. Choi, J.G. Cho, and G.H. Cho. A general circuit topology of multilevel inverter. In *Power Electronics Specialists Conference, 1991. PESC '91 Record., 22nd Annual IEEE*, pages 96 –103, 1991.

[36] D. Dupuis and F. Okou. Modeling and control of a five-level Diode-Clamped Converter based StatCom. In *Industrial Technology, 2009. ICIT 2009. IEEE International Conference on*, pages 1 –6, feb. 2009.

[37] T. Bruckner and S. Bemet. Loss balancing in three-level voltage source inverters applying active NPC switches. In *Power Electronics Specialists Conference, 2001. PESC. 2001 IEEE 32nd Annual*, pages 1135 –1140 vol.2, 2001.

[38] M. Khazraei, H. Sepahvand, K. Corzine, and M. Ferdowsi. A generalized capacitor voltage balancing scheme for flying capacitor multilevel converters. In *Applied Power Electronics Conference and Exposition (APEC), 2010 Twenty-Fifth Annual IEEE*, pages 58 –62, 2010.

[39] G.P. Adam, B. Alajmi, K.H. Ahmed, S.J. Finney, and B.W. Williams. New flying capacitor multilevel converter. In *Industrial Electronics (ISIE), 2011 IEEE International Symposium on*, pages 335 –339, june 2011.

[40] A. Lesnicar and R. Marquardt. An innovative modular multilevel converter topology suitable for a wide power range. In *Power Tech Conference Proceedings, 2003 IEEE Bologna*, volume 3, page 6 pp. Vol.3, june 2003.

[41] ABB. Skagerrak HVDC Interconnections, accessed may 24th, 2012. `http://www.abb.com/industries/ap/db0003db004333/448a5eca0d6e15d3c12578310031e3a7.aspx`.

[42] Siemens Energy. Living Energy - Siemens Debuts HVDC Plus with San Fransisco's Trans Bay Cable, accessed oct. 27, 2011. `http://www.energy.siemens.com/hq/pool/hq/energy-topics/living-energy/issue-5/LivingEnergy_05_hvdc.pdf`.

[43] ABB. ABB HVDC Reference projects, accessed oct. 27, 2011. `http://www.abb.com/industries/no/9AAF400191.aspx?country=00`.

[44] H. Akagi. New trends in medium-voltage power converters and motor drives. In *Industrial Electronics (ISIE), 2011 IEEE International Symposium on*, pages 5 –14, june 2011.

[45] U.N. Gnanarathna, S.K. Chaudhary, A.M. Gole, and R. Teodorescu. Modular multi-level converter based HVDC system for grid connection of offshore wind power plant. In *AC and DC Power Transmission, 2010. ACDC. 9th IET International Conference on*, 2010.

[46] A. Antonopoulos, L. Angquist, and H.-P. Nee. On dynamics and voltage control of the Modular Multilevel Converter. In *Power Electronics and Applications, 2009. EPE '09. 13th European Conference on*, pages 1 –10, sept. 2009.

[47] Qingrui Tu, Zheng Xu, and Lie Xu. Reduced Switching-Frequency Modulation and Circulating Current Suppression for Modular Multilevel Converters. *Power Delivery, IEEE Transactions on*, 26(3):2009 –2017, july 2011.

[48] A. Lahyani, P. Venet, G. Grellet, and P.-J. Viverge. Failure prediction of electrolytic capacitors during operation of a switchmode power supply. *Power Electronics, IEEE Transactions on*, 13(6):1199 –1207, nov 1998.

[49] Y. Chen, H. Li, F. Lin, F. Lv, Z. Li, and M. Zhang. Effect of interlayer air on performance of dry-type metalized film capacitor in DC, AC and pulsed applications. *Dielectrics and Electrical Insulation, IEEE Transactions on*, 18(4):1301 –1306, august 2011.

[50] B. Backlund, M. Rahimo, S. Klaka, and J. Siefken. Topologies, voltage ratings and state of the art high power semiconductor devices for medium voltage wind energy conversion. In *Power Electronics and Machines in Wind Applications, 2009. PEMWA 2009. IEEE*, pages 1 –6, june 2009.

[51] B. Jacobson et. al. ABB Sweden. VSC-HVC Transmission with Cascaded Two-Level Converters. *Cigre 2010*, 2010.

[52] ABB. HVDC and HVDC Light, accessed may 24th, 2012. `http://www.abb.co.uk/industries/us/9AAC30100013.aspx`.

[53] B. Backlund, M. Rahimo, S. Klaka, and J. Siefken. Topologies, voltage ratings and state of the art high power semiconductor devices for medium voltage wind energy conversion. In *Power Electronics and Machines in Wind Applications, 2009. PEMWA 2009. IEEE*, pages 1 –6, june 2009.

[54] M. Hagiwara and H. Akagi. PWM control and experiment of modular multilevel converters. In *Power Electronics Specialists Conference, 2008. PESC 2008. IEEE*, pages 154 –161, june 2008.

[55] P. M. Meshram and V. B. Borghate. A novel voltage balancing method of Modular Multilevel Converter (MMC). In *Energy, Automation, and Signal (ICEAS), 2011 International Conference on*, pages 1 –5, 2011.

[56] R. Walpole, R. Myers, S. Myers, and K. Ye. Probability and Statistics for Engineers and Scientists (8th ed.). Prentice-Hall, 2006.

[57] Minyuan Guan, Zheng Xu, and Hairong Chen. Control and modulation strategies for modular multilevel converter based HVDC system. In *IECON 2011 - 37th Annual Conference on IEEE Industrial Electronics Society*, pages 849 –854, nov. 2011.

[58] Stephen J. Chapman. *Fortran 90/95, For Scientists and Engineers.* McGraw-Hill, 2004.

[59] Ned Mohan. *Advanced Electric Drives: Analysis, Control and Modeling using Simulink.* MNPERE, 2001.

Appendix

Appendix A

DQ-transformation

For a simplified analysis, vector control employs the technique of DQ-transformation and rotating reference axis. And as seen in the block diagram for the complete control system, figure 2.4, the output from the current controller is referred to direct and quadrature axis. Hence, a transformation block is needed.

In rotating machines, an analytic analysis is somewhat limited by the fact that the calculations can become quite complicated when introducing time-dependent angles. The DQ-transformation is used to simplify the analysis by introducing a rotating reference plane, called the d-q frame. By definition, the direct axis is aligned with the rotor flux, while the rotor quadrature axis is always perpendicular to the direct axis.

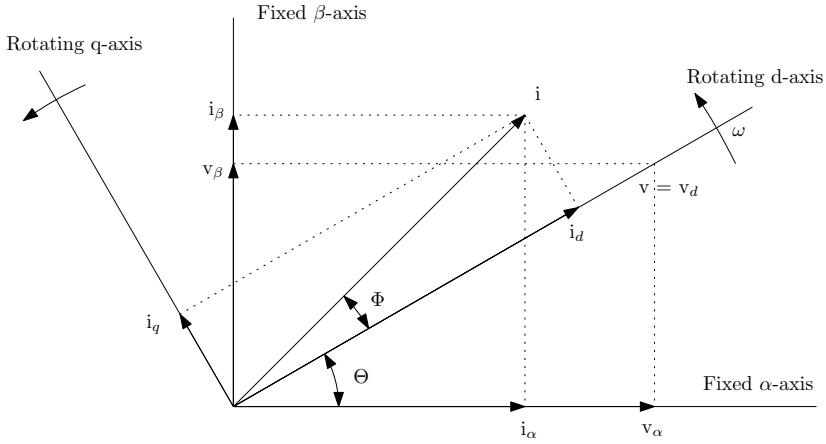

Figure A.1: General principle of vector control DQ-transformation

By transforming time-dependent components like voltage, current or flux into equivalent quantities that rotate in synchronism with the machine rotor, the

quantities are described by a constant and a constant angle. The angle is constant because of the rotating reference, the d-q frame [59].

The transformation can be split into two parts. First, using the Clark-transformation from the *abc*-frame to the α-β frame, and then using the Park transformation from the α-β frame to the d-q frame. This gives the following transformation matrices [59]:

$$\mathbf{T}_{abc-\alpha\beta} = \frac{2}{3}\begin{bmatrix} 1 & -\frac{1}{2} & -\frac{1}{2} \\ 0 & \frac{\sqrt{3}}{2} & -\frac{\sqrt{3}}{2} \end{bmatrix} \tag{A.1}$$

and,

$$\mathbf{T}_{\alpha\beta-dq} = \begin{bmatrix} \cos\theta & \sin\theta \\ -\sin\theta & \cos\theta \end{bmatrix} \tag{A.2}$$

The transformation from *abc* to α-β is:

$$\mathbf{S}_{\alpha\beta} = \mathbf{T}_{abc-\alpha\beta} \cdot \mathbf{S}_{abc} \tag{A.3}$$

Here $\mathbf{S}$ represents the voltage, current or flux to be transformed.

The inverse transformation matrices are:

$$\mathbf{T}_{dq-\alpha\beta} = \begin{bmatrix} \cos\theta & -\sin\theta \\ \sin\theta & \cos\theta \end{bmatrix} \tag{A.4}$$

and,

$$\mathbf{T}_{\alpha\beta-abc} = \begin{bmatrix} 1 & 0 \\ -\frac{1}{2} & \frac{\sqrt{3}}{2} \\ -\frac{1}{2} & -\frac{\sqrt{3}}{2} \end{bmatrix} \tag{A.5}$$

A combination of these equations give the complete transformation from the measured abc-frame to the rotating dq-frame [59]. These matrices assume a balanced stationary system, neglecting the zero-sequence component.

$$\mathbf{T}_{abc-dq} = \sqrt{\frac{2}{3}}\begin{bmatrix} \cos\theta & \cos(\theta - \frac{2\pi}{3}) & \cos(\theta + \frac{2\pi}{3}) \\ -\sin\theta & -\sin(\theta - \frac{2\pi}{3}) & -\sin(\theta + \frac{2\pi}{3}) \end{bmatrix} \tag{A.6}$$

With the following inverse transformation matrix:

$$\mathbf{T}_{abc-dq} = \sqrt{\frac{2}{3}} \begin{bmatrix} \cos\theta & -\sin\theta \\ \cos(\theta - \frac{2\pi}{3}) & -\sin(\theta - \frac{2\pi}{3}) \\ \cos(\theta + \frac{2\pi}{3}) & -\sin(\theta + \frac{2\pi}{3}) \end{bmatrix} \tag{A.7}$$

Example

An example of dq-transformation. The voltages are defined in an abc-frame as:

$$\mathbf{V}_{abc} = \begin{bmatrix} V_a \\ V_b \\ V_c \end{bmatrix} = \begin{bmatrix} V\cos\theta \\ V\cos(\theta - \frac{2\pi}{3}) \\ V\cos(\theta + \frac{2\pi}{3}) \end{bmatrix} \tag{A.8}$$

First a transformation to the α-β frame (Clark-transformation):

$$\mathbf{V}_{\alpha\beta} = \begin{bmatrix} V_\alpha \\ V_\beta \end{bmatrix} = \begin{bmatrix} 1 & -\frac{1}{2} & -\frac{1}{2} \\ 0 & \frac{\sqrt{3}}{2} & -\frac{\sqrt{3}}{2} \end{bmatrix} \cdot \begin{bmatrix} V\cos\theta \\ V\cos(\theta - \frac{2\pi}{3}) \\ V\cos(\theta + \frac{2\pi}{3}) \end{bmatrix} = \begin{bmatrix} V\cos\theta \\ V\sin\theta \end{bmatrix} \tag{A.9}$$

Then a transformation to the d-q frame, using the Park-transformation to get the equivalent voltage in direct and quadrature axis reference:

$$\mathbf{V}_{dq} = \begin{bmatrix} V_d \\ V_q \end{bmatrix} = \begin{bmatrix} \cos\theta & \sin\theta \\ -\sin\theta & \cos\theta \end{bmatrix} \cdot \begin{bmatrix} V\cos\theta \\ V\sin\theta \end{bmatrix} = \begin{bmatrix} V \\ 0 \end{bmatrix} \tag{A.10}$$

It can be observed that the voltage is in the direct axis only.

Appendix B

Multilevel simulations: MMC 5-23 levels

This appendix includes the results from simulation models built for the MMC with 5, 7, 9, 11, 13, 15, 17, 19, 21 and 23 levels. The intention of building all these models have been to see the reduced demand for filtering because of reduced THD when increasing the number of levels. A graph describing the reduced THD is shown in figure 5.23.

For each model, the phase voltage, phase current and the THD in the line-to-line voltage is measured. It is worth to notice that the voltage axis of the THD figures are, for illustration purposes, limited to 0.1, while the fundamental harmonic stretches to 1.0.

B.1 5 levels

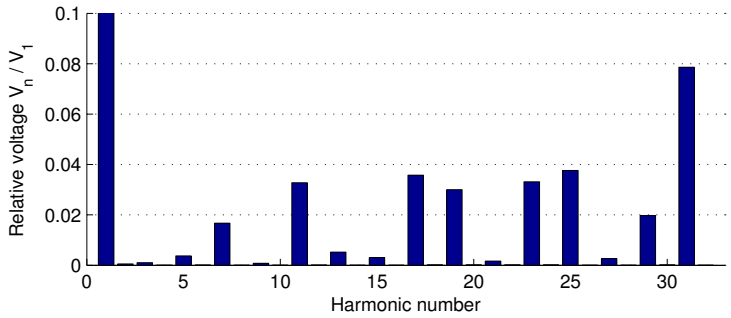

Figure B.1: Harmonic content in line-line voltage V_{ab} in MMC model with 5 levels

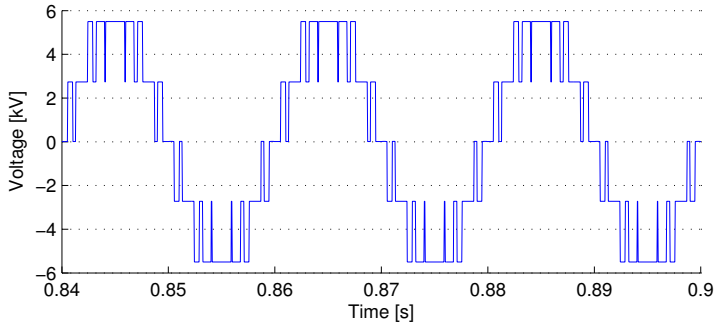

(a)

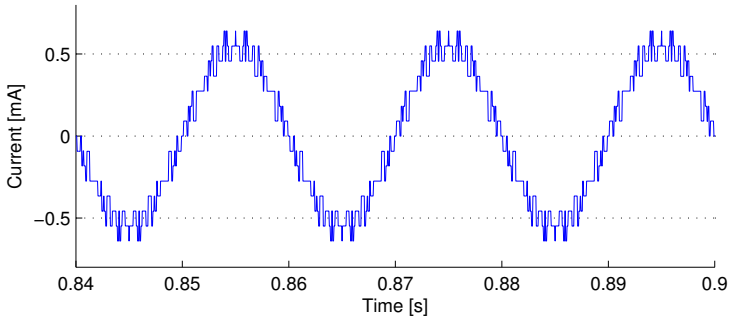

(b)

Figure B.2: MMC 5-level a) Phase voltage V_a b) Phase current I_a

B.2 7 levels

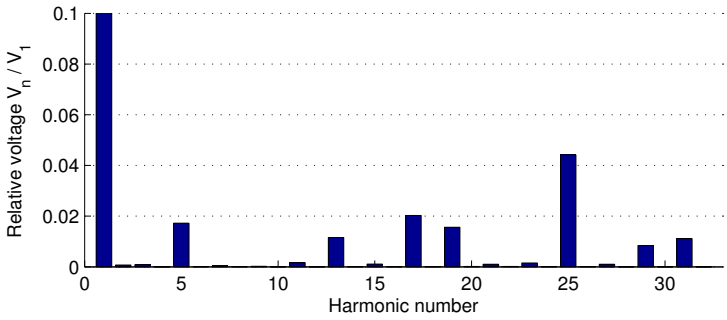

Figure B.3: Harmonic content in line-line voltage V_{ab} in MMC model with 7 levels

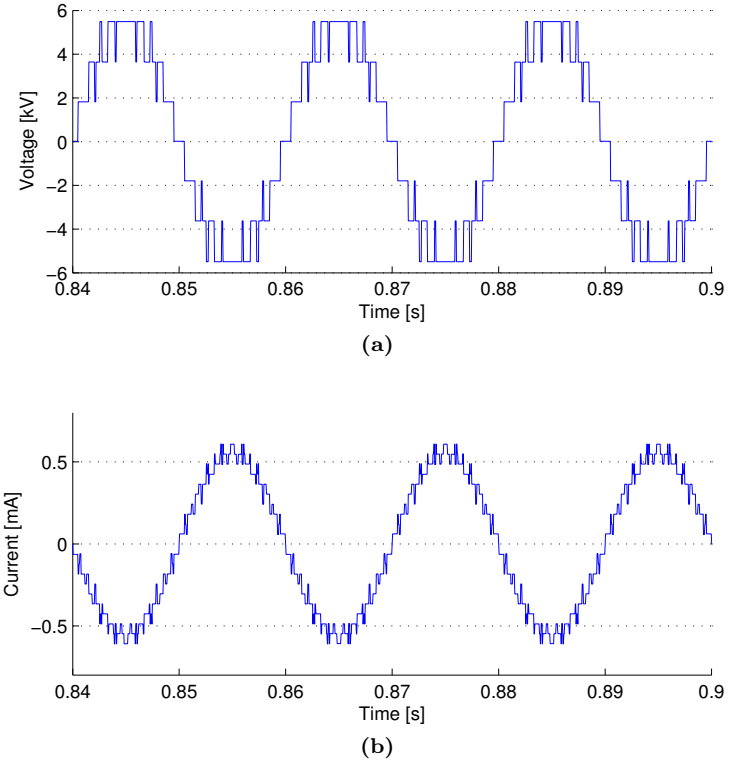

Figure B.4: MMC 7-level a) Phase voltage V_a b) Phase current I_a

B.3 9 levels

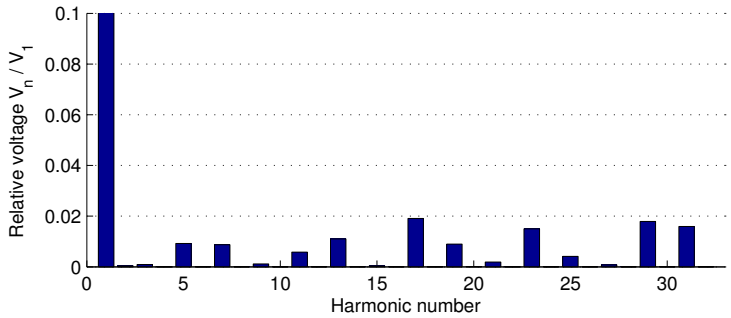

Figure B.5: Harmonic content in line-line voltage V_{ab} in MMC model with 9 levels

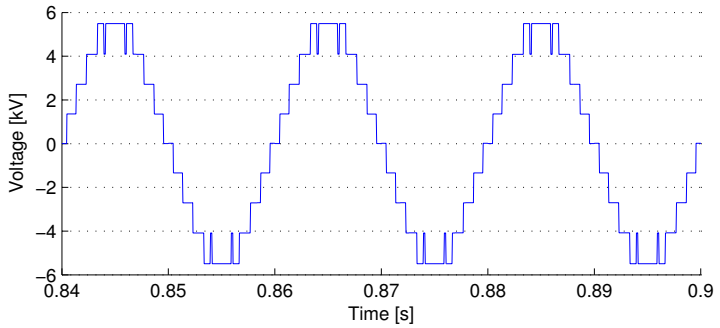

(a)

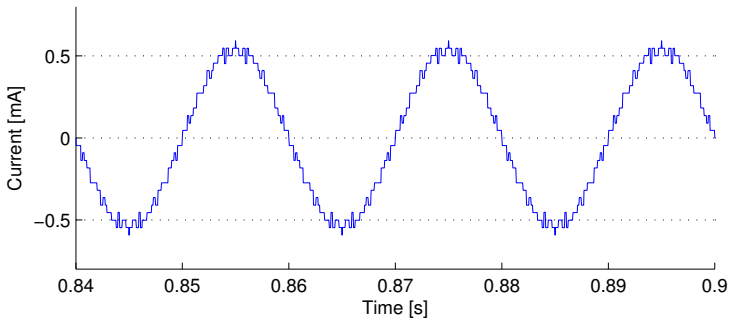

(b)

Figure B.6: MMC 9-level a) Phase voltage V_a b) Phase current I_a

B.4 11 levels

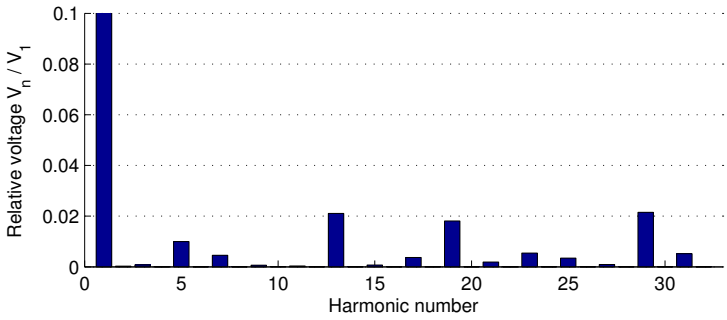

Figure B.7: Harmonic content in line-line voltage V_{ab} in MMC model with 11 levels

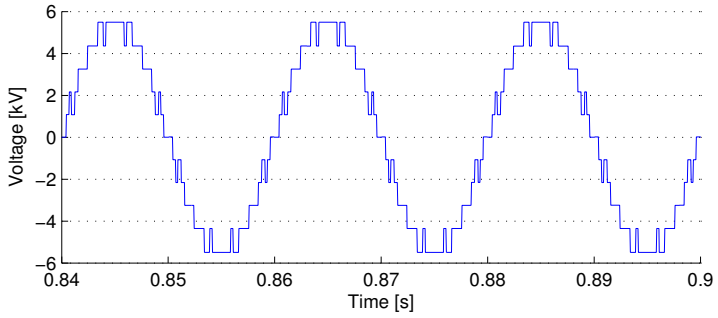

(a)

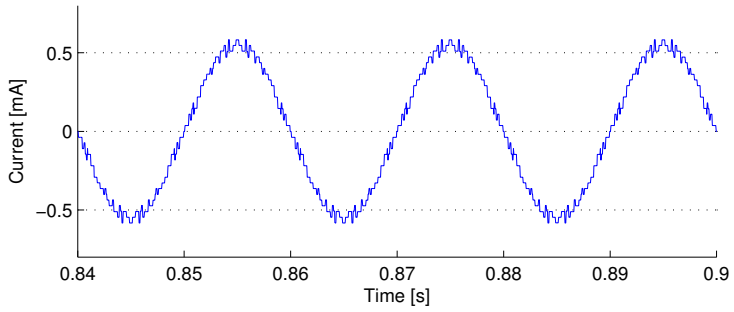

(b)

Figure B.8: MMC 11-level a) Phase voltage V_a b) Phase current I_a

B.5 13 levels

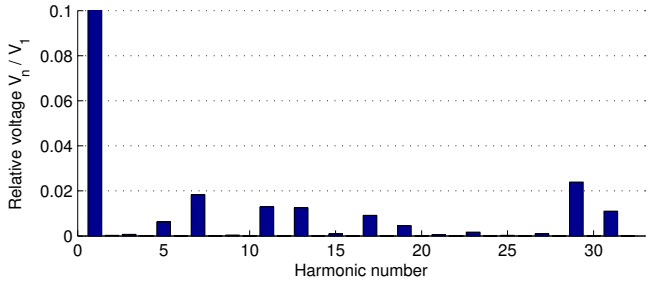

Figure B.9: Harmonic content in line-line voltage V_{ab} in MMC model with 13 levels

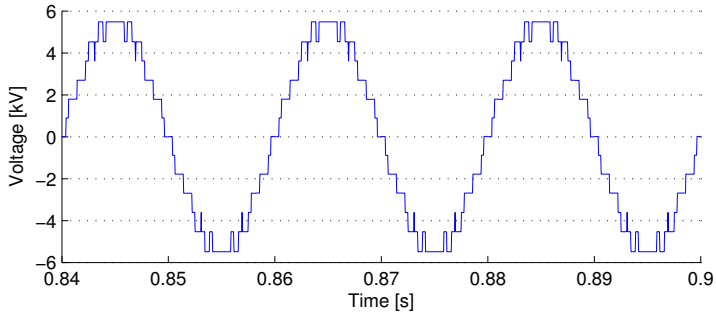

(a)

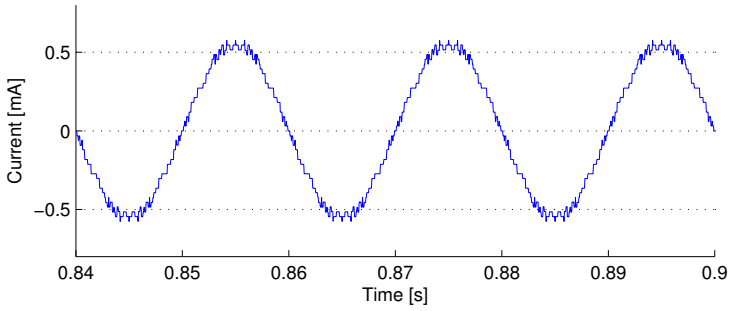

(b)

Figure B.10: MMC 13-level a) Phase voltage V_a b) Phase current I_a

B.6 15 levels

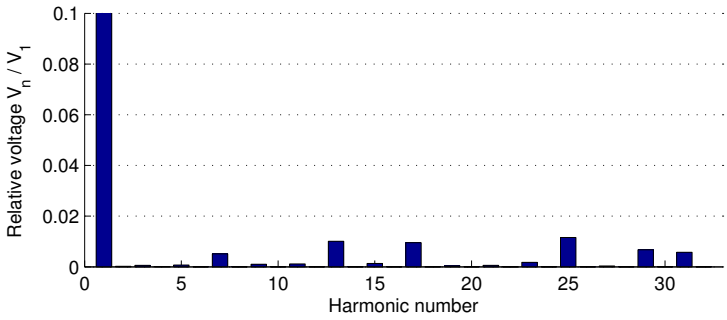

Figure B.11: Harmonic content in line-line voltage V_{ab} in MMC model with 15 levels

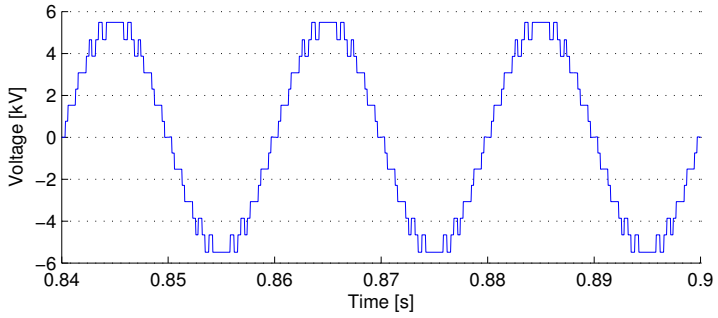

(a)

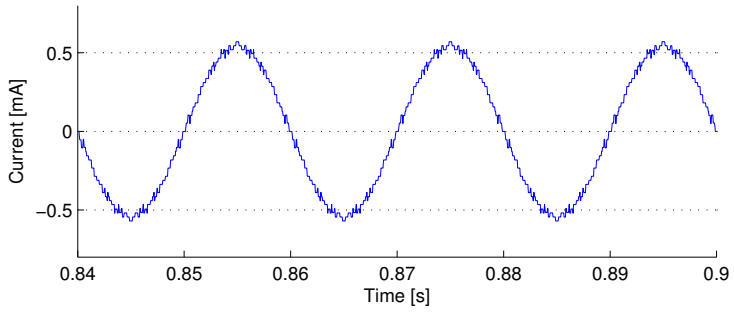

(b)

Figure B.12: MMC 15-level a) Phase voltage V_a b) Phase current I_a

B.7 17 levels

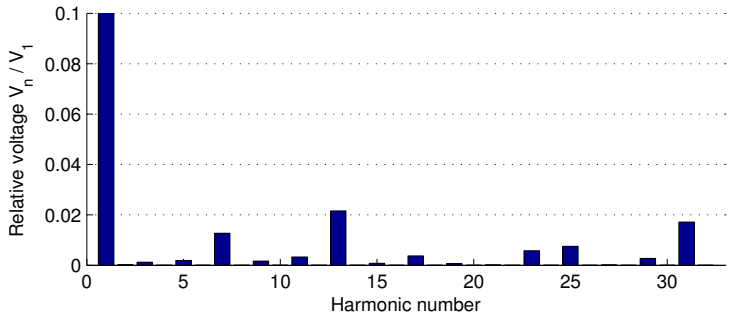

Figure B.13: Harmonic content in line-line voltage V_{ab} in MMC model with 17 levels

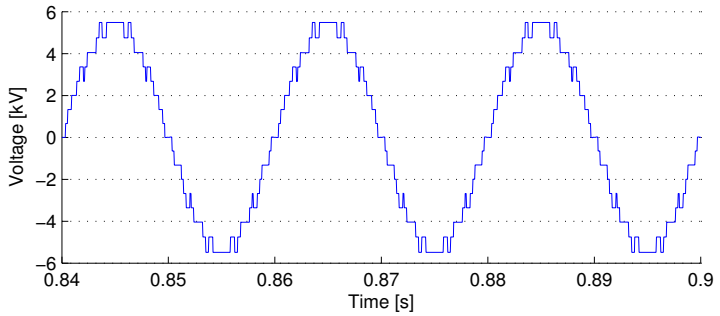

(a)

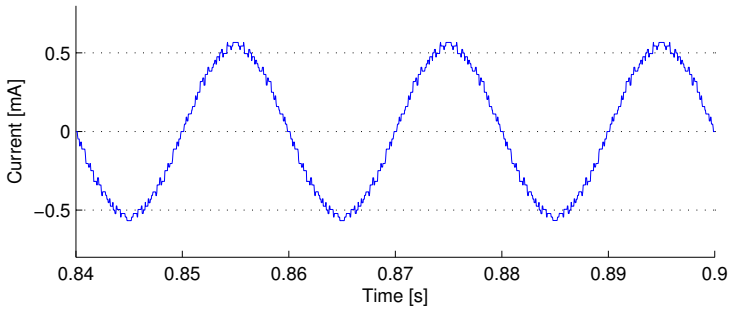

(b)

Figure B.14: MMC 17-level a) Phase voltage V_a b) Phase current I_a

B.8 19 levels

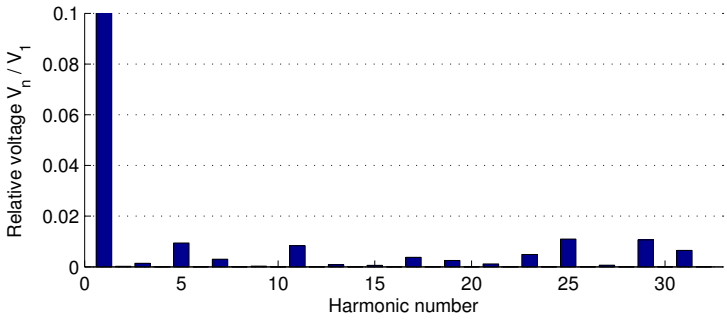

Figure B.15: Harmonic content in line-line voltage V_{ab} in MMC model with 19 levels

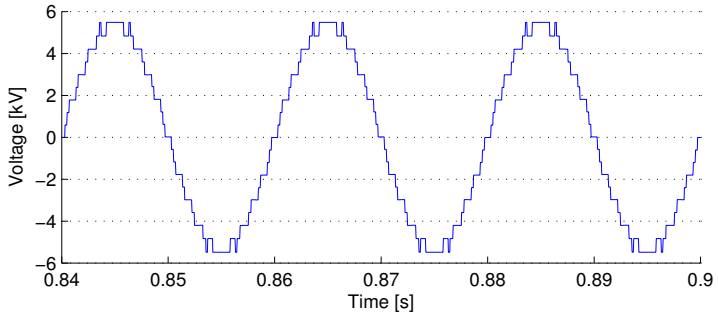

(a)

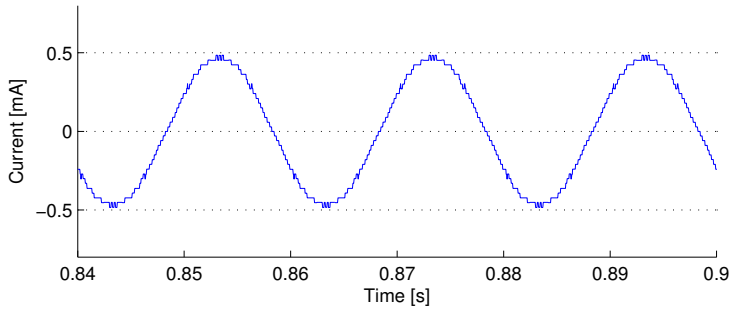

(b)

Figure B.16: MMC 19-level a) Phase voltage V_a b) Phase current I_a

B.9 21 levels

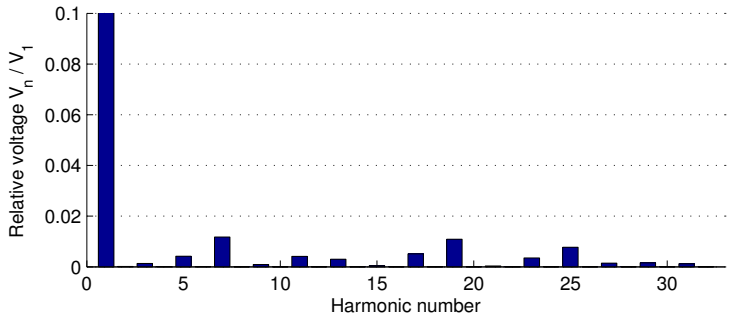

Figure B.17: Harmonic content in line-line voltage V_{ab} in MMC model with 21 levels

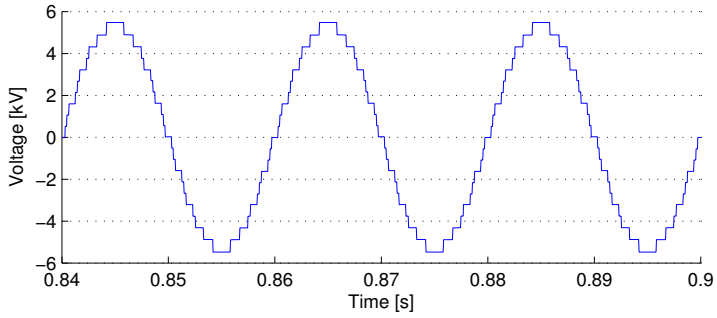

(a)

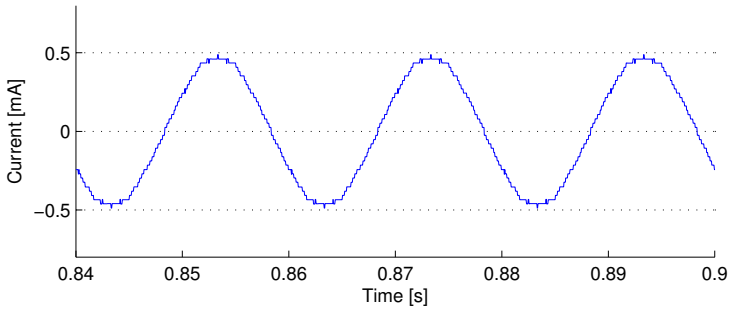

(b)

Figure B.18: MMC 21-level a) Phase voltage V_a b) Phase current I_a

B.10 23 levels

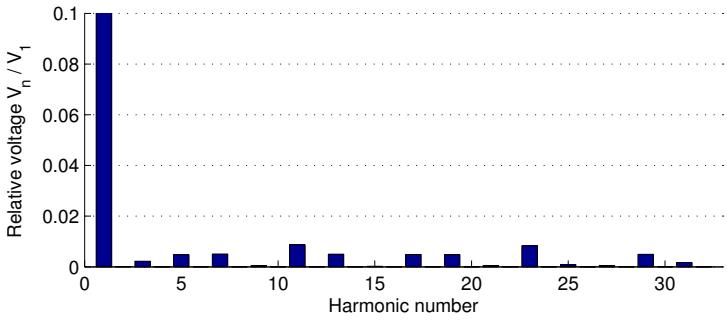

Figure B.19: Harmonic content in line-line voltage V_{ab} in MMC model with 23 levels

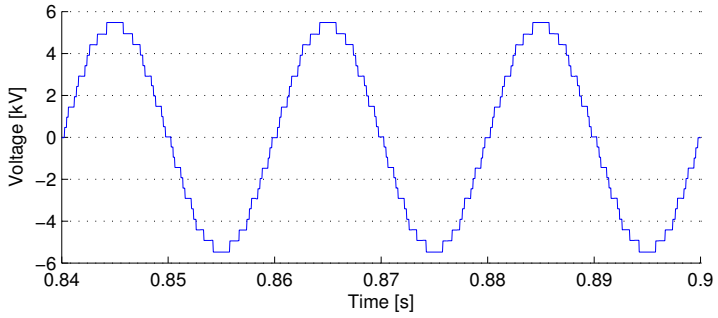

(a)

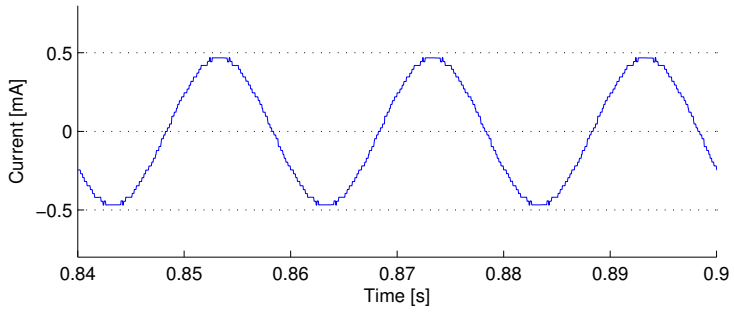

(b)

Figure B.20: MMC 23-level a) Phase voltage V_a b) Phase current I_a

Appendix C

Fortran code: Balancing block

This appendix describes the Fortran code implemented in the capacitor voltage balancing block. The operation of the block is described in section 4.5. A block diagram is also given in figure 4.5.

The variables are defined, using the `#STORAGE` to set the number of memory allocations used for storage.

```
!Define variables
  #STORAGE REAL:8
  #LOCAL REAL vcp 4
  #LOCAL REAL vcn 4
  #LOCAL REAL gatep 4
  #LOCAL REAL gaten 4
  #LOCAL REAL indexp 4
  #LOCAL REAL indexn 4
  #LOCAL REAL n, np, nn
```

The constant n is the available number of submodules in each phase arm.

```
!Set constants:
  n = 4
```

Previous gate signals are fetched from memory. `gatep` and `gaten` are vectors for the positive-arm and the negative-arm gate signals, respectively.

```
!Get the previous switchstates:
  gatep(1) = STORF(NSTORF)
  gatep(2) = STORF(NSTORF+1)
  gatep(3) = STORF(NSTORF+2)
  gatep(4) = STORF(NSTORF+3)
  gaten(1) = STORF(NSTORF+4)
  gaten(2) = STORF(NSTORF+5)
```

```
19    gaten(3) = STORF(NSTORF+6)
20    gaten(4) = STORF(NSTORF+7)
```

To reduce the number of calculations by the block, a trigger signal is used to activate the sorting. This signal is generated by a edge-detector, and the following if-statement ensures that the calculations only happen when a switching should occur. Figures 5.4 and 5.5 show the edge-detector block:

```
21    IF ($clock .EQ. 1 ) THEN
```

The voltages in each submodule capacitor is continously (for each time-step) measured and fed to the block. The voltages are stored in two vectors; `vcp` and `vcn`, for positive and negative arm, respectively.

```
22  !Read the capacitor voltages into a vector vc:
23    vcp(1) = $up1
24    vcp(2) = $up2
25    vcp(3) = $up3
26    vcp(4) = $up4
27    vcn(1) = $un1
28    vcn(2) = $un2
29    vcn(3) = $un3
30    vcn(4) = $un4
```

The following part index the voltages in two vectors, `indexp` and `indexn`. `indexp` and `indexn` are sorted in descending order, i.e. the position of the largest voltage first.

```
31  !Find the order of the voltages:
32  !Upper arm:
33    indexp = (/1,1,1,1/)
34    DO j = 1,4
35      largest = 0
36      pos = 1
37      DO i = 1,4
38        if (largest < vcp(i)) THEN
39          largest = vcp(i)
40          pos = i
41        ENDIF
42        END DO
43    vcp(pos) = -2
44    indexp(j) = pos
45    END DO
46  !Lower arm:
47    indexn = (/1,1,1,1/)
48    DO j = 1,4
49      largest = 0
50      pos = 1
51      DO i = 1,4
52        if (largest < vcn(i)) THEN
```

```
53          largest = vcn(i)
54          pos = i
55        ENDIF
56        END DO
57    vcn(pos) = -2
58    indexn(j) = pos
59    END DO
```

Input from the block shown in figure 5.4 is the desired number of ON-state submodules in lower (negative) arm. `nn` and `np` is the two variables containing the desired number of ON-state submodules in lower and upper phase arm, respectively.

```
60 !Set the number of submodules in ON-state:
61    nn = $nn
62    np = n - nn
```

The following part is included to give the possibility to disable the balancing algorithm at a certain instant. If `disable` is *true*, the selection of the correct submodules is not used.

```
64    IF ($disable .EQ. 1) THEN
65 !Balancing turned off
66 !Upper arm:
67
68    DO i = 1,np
69    gatep(i) = 1
70    END DO
71    DO i = 1,n-np
72    gatep(np+i) = 0
73    END DO
74
75 !Lower arm:
76    DO i = 1,nn
77    gaten(i) = 1
78    END DO
79    DO i = 1,n-nn
80    gaten(nn+i) = 0
81    END DO
82
83    ELSE
```

As described in section 4.5, the correct submodules are chosen to turn ON or OFF:

```
84 !Choose the correct sub-modules
85 !Upper arm:
86    IF ($ip < 0) THEN
87      DO i = 1,np
88        gatep(indexp(i)) = 1
```

```
89      END DO
90      DO i = 1,n-np
91        gatep(indexp(np+i)) = 0
92      END DO
93    ELSE
94      DO i = 1,np
95        gatep(indexp(n+1-i)) = 1
96      END DO
97      DO i = np+1,n
98        gatep(indexp(n+1-i)) = 0
99      END DO
100   ENDIF
101 !$Lower arm:
102   IF ($in < 0) THEN
103     DO i = 1,nn
104     gaten(indexn(i)) = 1
105     END DO
106     DO i = 1,n-nn
107     gaten(indexn(nn+i)) = 0
108     END DO
109   ELSE
110     DO i = 1,nn
111     gaten(indexn(n+1-i)) = 1
112     END DO
113     DO i = nn+1,n
114     gaten(indexn(n+1-i)) = 0
115     END DO
116   ENDIF
117   ENDIF
118   ENDIF
```

The output gate signals (`sw1-sw8`) are updated with the correct value:

```
119   $sw1 = gatep(1)
120   $sw2 = gatep(2)
121   $sw3 = gatep(3)
122   $sw4 = gatep(4)
123
124   $sw5 = gaten(1)
125   $sw6 = gaten(2)
126   $sw7 = gaten(3)
127   $sw8 = gaten(4)
```

Finally, the gate signals are stored in memory:

```
128   STORF(NSTORF) = gatep(1)
129   STORF(NSTORF+1) = gatep(2)
130   STORF(NSTORF+2) = gatep(3)
131   STORF(NSTORF+3) = gatep(4)
132
133   STORF(NSTORF+4) = gaten(1)
134   STORF(NSTORF+5) = gaten(2)
135   STORF(NSTORF+6) = gaten(3)
136   STORF(NSTORF+7) = gaten(4)
```

```
137|   NSTORF = NSTORF+8
```

Appendix D

Technoport RERC Abstract

The following abstract was accepted for a lecture presentation at the Technoport RERC Conference in Trondheim 16-18th of April 2012.

Converter Topologies for Enhanced Performance of Wind Turbine Generators

Tor Martin Iversen (tormari@stud.ntnu.no),
Sverre S. Gjerde (sverre.gjerde@ntnu.no),
Tore Undeland (tore.undeland@elkraft.ntnu.no),

Norwegian University of Science and Technology

In the later years the demand for electricity has increased substantially and new technology has improved both efficiency and power handling of power producing devices. In the line-up of renewable energy generation options, wind power is a strong contestant, with total installed capacity of 200 GW worldwide[1]. When moving the wind power offshore, new challenges arise and the list includes mechanical strength, transport, assembly, electrical grid design, corrosion problems, maintenance and design and tuning of the best suitable electrical generation topology.

Reduction in the nacelle weight is a key aspect of offshore wind turbine design. A special generator concept[2] is under development, which uses a PMSG with several converter modules in series to obtain a high-voltage, high-power output to a DC grid. The figure shows a topology with five modules. The traditional 2-level VSC is utilized in the modules, but other topologies can be beneficial for optimizing losses, voltage quality and reliability of the system.

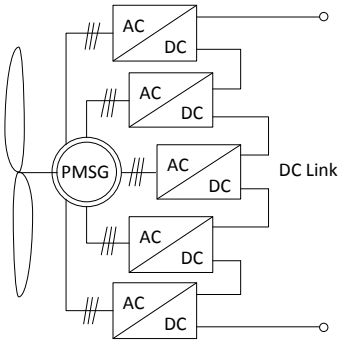

Structure with five modules

This paper presents a state-of-the-art study of multilevel converter topologies, and compares the topologies with regards to their suitability for the proposed concept. Modularity, harmonics and voltage quality is compared, also is the ability of redundancy for a high reliability. The size is often limited, so the bulkiness is important. PSCAD simulations will be performed to compare the most suitable converters.

The studies show that the MMC is a promising multilevel topology for this offshore wind concept. With its modular design, fault redundant structure and the large number of levels with less need for filtering it has clear advantages over a normal three-level NPC VSC. The backside is a more complex structure with advanced control systems.

Keywords: Multilevel converters, Offshore wind power

---

[1] World Wind Energy Association, *World Wind Energy Report 2010,* http://wwindea.org

[2] Gjerde, Sverre S; Undeland, Tore U., *Power Conversion System for Transformer-Less Offshor Wind Turbine*, 2011 NTNU Trondheim

Appendix E

EPE Wind Energy and T&D Chapters Seminar Paper

The following paper was accepted for an lecture presentation at the EPE Wind Energy and T&D Chapters Seminar in Aalborg, DK at the 28th and 29th of June 2012.

Because of the collision between the deadline of this master's thesis and the paper, this is not the final version. The final version will be made available at the IEEE Explore website.

Multilevel Converters for a 10 MW, 100 kV Transformer-less Offshore Wind Generator system

Tor Martin Iversen, Sverre S. Gjerde, Tore Undeland
Norwegian University of Science and Technology (NTNU)
Dep. Of Electric Power Engineering
Trondheim, Norway
Email: tormari@stud.ntnu.no, sverre.gjerde@elkraft.ntnu.no, tore.undeland@elkraft.ntnu.no
URL: http://www.ntnu.edu/elkraft

Keywords

<<Multilevel converters>>, <<Modular multilevel converter (MMC)>>, <<Wind energy>>, <<Transformer-less>>, <<HVDC>>

Abstract

The nacelle weight reduction is a key design criterion for offshore wind turbines, as these are reaching towards 10 MW. To overcome the weight challenge, a transformer-less concept is under development. This concept employs a special permanent magnet synchronous generator (PMSG) with an innovative system for high insulation level. The generator supplies nine series connected converter modules, which results in a high voltage DC output of 100 kV, reducing the total weight of the system.

The work presented here focuses on one of the 11.1 kV converter modules, and identifies the modular multilevel converter (MMC) as the best candidate for the proposed system. The compare criteria are no direct series connection of IGBTs, efficiency, voltage quality and redundancy for increased reliability. Simulations are performed in PSCAD/EMTDC, with focus on redundancy, submodule voltage balancing, and implementation of the MMC in full system models. The results show that the MMC performs well in the full system, and is therefore considered as a viable converter for the proposed system.

1 Introduction

1.1 Background and motivation

The increasing demand for electricity, combined with the necessity of reducing the CO_2-emissions is one of the greatest challenges of this century. There is a need for green energy, and the worldwide energy sector faces a huge public responsibility. A responsibility of not only providing the possibility for continuous growth in living standards, but also securing that the growth is sustainable. In addition to a greener utilization of fossil fuels like oil and gas, the use of renewable energy sources will be an important contribution to the energy mix.

Offshore wind is a relatively new approach to the generation of green electricity. Moving the electrical power generation offshore gives several benefits, but has a comprehensive list of challenges. This includes mechanical influence, fatigue, transport and assembly, electrical grid design and maintenance issues due to the scarce availability. However, the use of offshore wind has been increasing: 1.2 GW was installed in 2010, resulting in a worldwide total of 3.1 GW, and a share of 1.6 % of the total wind capacity [2].

There is high activity in the developing of offshore wind, as new technology is needed to overcome the technical and economical difficulties. As the average size in offshore wind turbines increases, from today's 3.8 MW [4], the overall nacelle weight becomes a key issue. A weight reducing strategy is therefore one of the motivations for this work. In addition, as a result of the scarce availability, an optimal solution should include redundancy for increased reliability [3].

1.2 Outline of the paper

The paper is organized as follows. Part 2 presents an overview of the concept. In part 3, the conventional converter is presented along with the multilevel idea and the following multilevel topologies. A converter is chosen for further studies, and part 4 describes the simulations. Conclusions and further work are summarized in part 5 and 6, respectively.

2 The proposed turbine concept

This chapter presents first the conventional wind turbine generator/converter solutions. The intention is to highlight some of the challenges with the conventional design in terms of weight and reliability. A new, weight-reducing concept is then presented, with possibilities of increased reliability.

2.1 The conventional solutions

The doubly-fed induction generator (DFIG) is today the most popular generator solution in offshore wind applications, and stands for almost 50 % of all operational generators [4]. A schematic of the solution is shown in figure 1a. The DFIG solution includes a gear box to step up the rotational speed, a proportionally rated AC/AC converter to control the exitation of the machine, and a step-up transformer.

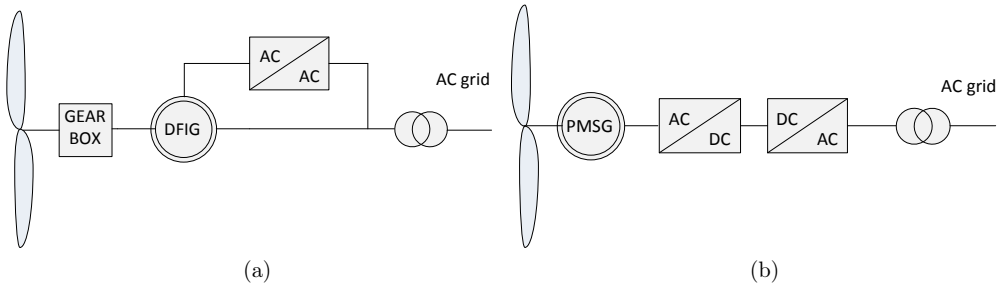

Figure 1: a) Standard DFIG solution, b) Standard PSMG solution

The gear box has a reputation of being a troublesome component, especially in offshore wind turbines where the reliability is very important. According to a Swedish survey, 20 % of the downtime for a typical turbine [5] is because of the gear box. The gear box is a large and heavy mechanical unit, which has to be mounted and replaced in one piece. This means that one of few existing crane vessels has to be brought to the site. Using solutions which omit the gear box will therefore increase the reliability and reduce the weight.

A directly driven PMSG is such a solution, and trends show an increase in the use of these [4]. The PMSG solution offers some advantages that are very useful compared to a DFIG-solution: The machine can be directly driven without the need for gearing. There is less maintenance; no brushes nor slip-rings. The PMSG has therefore increased reliability, and increased efficiency in a larger range of wind speeds [4].

However, the step-up transformer is still included in standard PMSG solutions, as illustrated in figure 1b. This is due to the large power handling of the generator, and the standard industrial voltage of 690 V. This results, in the MW-segment, in a very high current which needs to be transferred down the tower, and hence bulky cables. The cables have to be flexible enough to handle the yaw control of the turbine. The transformer for large offshore turbines is therefore placed in the nacelle.

The voltage output from the generator should therefore be increased in order to reduce the current, reduce the losses and to omit the transformer in the nacelle.

2.2 The low-weight high-voltage solution

To reduce the nacelle weight, a new generator concept is under development. The converter solution is presented in [6], [7], and the insulation solution in [1]. A schematic of the concept is

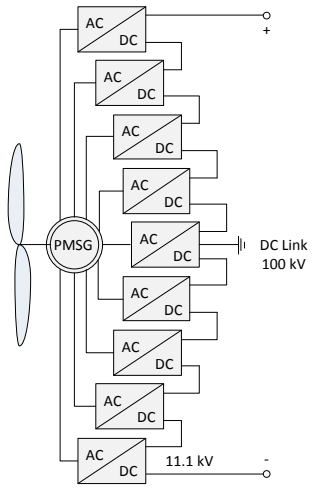

Figure 2: Schematic of the proposed low-weight, high voltage converter system

included in figure 2. The system consists of a special permanent magnet synchronous generator with nine sets of 3-phase windings. Each winding set is electrically separated from the others, and supplies a three phase converter module. Each converter module produces an output DC voltage of 11.1 kV, and the stack of modules are series connected to obtain a desired DC voltage of 100 kV.

As seen in figure 2, both the gear box and the step up transformer is now replaced by the special PMSG and converter structure. The weight reduction is believed to be significant, and is a direct result of the special solution. There are a few arguments for this:

- The generator is built by composite materials instead of cast steel, and is therefore lighter than a corresponding induction machine. The generator mass is typically 20-30 % of the equivalent iron-cored systems [8].
- The transformer and gear is omitted.

The schematic makes the converter part seem complex, but it is not that intricate - compared to the alternative. Because of component limitations at the desired power and voltage rating, a single two-level full-converter structure would also need both series and parallel connections to handle the power rating. An additional benefit is redundancy. This is indeed one of the intentions with the proposed system [9]. With a more complex system comes more complex support structures. A detailed study of weight and size is not included in this work.

2.3 Contribution of this work

This work focuses on one of the converter modules of the new light-weight, high voltage concept shown in figure 1b. The desired DC voltage is set to 100 kV, and the proposed 10 MW generator has nine separately isolated three phase windings. Each converter must therefore handle a DC voltage of 11.1 kV, and a power rating of 1.1 MW. The conventional two-level converter, used in initial concept studies, is because of this not necessarily the best choice for this system. Multi-level converters are believed to have several benefits in terms of voltage quality, efficiency, and redundancy for increased reliability. This work proposes the idea of using multilevel converters in the proposed sustem. Five converter topologies are therefore investigated for their suitability for the proposed concept, and one converter topology is chosen for studies through simulations.

3 Voltage source converters

3.1 Standard two-level

The standard two-level voltage source converter (VSC) [10] is the reference converter. It has the simplest structure of the evaluated, and consists of six IGBTs with diodes in anti-parallel. Figure 3 shows the basic structure of such a two-level VSC. The standard two-level VSC benefits from its simplicity, both in structure and control, and is a well-known technology. For low voltage and power ratings it is therefore very popular.

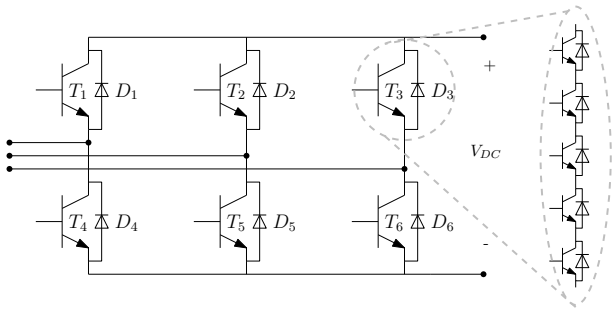

Figure 3: Topology of the conventional 2-level converter, with series connections in each switch because of 11.1 kV DC voltage.

However, with the higher voltage of the proposed system, each phase arm has to withstand a high voltage. Since each IGBT has limitations in voltage blocking capabilities, direct series connection of IGBTs is necessary to meet the increased voltage stress on each switch.

The two level converter has been used in high voltage transmissions, but then with series connection of switches as indicated in figure 3. In this figure, each switch really consists of five IGBTs in series. IGBTs are available with blocking voltages up to 6.5 kV [11]. A vital criteria with series connection of IGBTs is the switch control. The branch of IGBTs has to be able to switch simultaneously. This is however quite complicated, and the consequence of delayed switching in one part of the branch is severe. This is one of the reasons why multilevel converters have become popular. Another reason is the demand for filtering in two-level converters.

3.2 The Multilevel concept

Figure 4a shows a principle sketch of one leg in a three phase multilevel converter. The concept is to stack n-1 capacitors or voltage levels, and use controlled switching to obtain a desired n-level AC voltage. The amplitude of the voltage is then determined by the number of contributing levels [12].

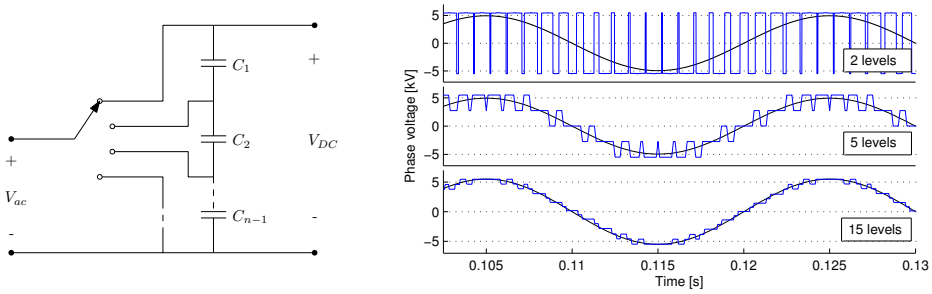

(a) (b)

Figure 4: a) Topology of an n-level converter phase leg, b) Phase voltages V_a and the voltage reference signal in a two level, five level and a 15 level converter

Figure 4b compares the typical unfiltered phase voltage shape of the two-level converter with multilevel converters. The upper graph shows the two-level phase voltage. This is an unfiltered voltage, switching between two levels. By introducing more levels, the phase voltage becomes more sinusoidal, and follows the voltage reference, normally a pure sinusoidal wave, more closely. The last graph of figure 4b illustrates this, with a 15 level phase voltage. The need for filtering is eventually removed, and the $\frac{dv}{dt}$ is much lower than for the two-level voltage. A low $\frac{dv}{dt}$ is beneficial for the generator design, and especially the turn insulation.

3.2.1 Advantages

Some of the advantages with multilevel converters are:

- The multilevel divides the total voltage into multiple levels, which results in a lower $\frac{dv}{dt}$.
- The losses in a converter include mainly conduction losses and switching losses [13]. Reduced switching frequency makes the reduction of switching losses possible.
- The harmonic distortion is reduced, resulting in lower loss due to harmonic components.
- Some multilevel topologies make redundancy possibilities easier to implement. This makes component failures less critical for the operation of the converter.
- The filtering demand in multilevel configurations is reduced, reducing the volume and cost, and the losses due to filtering.

3.2.2 Possible drawbacks

- The investment cost increases with more complex structures.
- An increase in complexity could jeopardize the reliability.
- Complex control strategies are needed. For instance, capacitor voltage balancing strategies are necessary for most multilevel converters.

3.3 Multilevel topologies

The five following multilevel voltage source converter topologies have been studied with regards to their suitability for the proposed concept: Neutral Point Clamped converter (NPC) [14], Flying Capacitor converter (FC) [15], Hexagram Converter [16], Cascaded H-Bridge converter (CHB) [17] and the Modular Multilevel Converter (MMC) [18]. Table I gives a summary of the converter properties:

Table I: Summary of topology properties

Converter	Suitability	Cap. volume	Redundancy?	Voltage quality
2-l VSC	Series conn.	High	No	Low
NPC	Series conn.	High	No	Medium
FC	Good	Very high	No	Medium
Hexagram	Does not fit	-	-	-
CHB	Does not fit	Distributed	Yes	High
MMC	Good	Distributed	Yes	High

Both the Hexagram Converter and the CHB does not fit the proposed concept, as they require separate DC loads. The FC has been excluded because of high capacitor volume and voltage balancing issues at higher levels [12].

Of the two remaining converter topologies, the MMC has been selected as the best alternative to the conventional two-level VSC. The NPC is the state-of-the-art converter for medium voltage applications, but is not practically expandable to more than three levels. Consequently, there is a need for direct series connection of IGBTs in the NPC as well as the two-level. The MMC offers the easiest expansion of levels for good voltage quality, avoids the direct series connection of IGBTs and has a modular structure with redundancy possibilities for increased reliability.

The following simulations focuses therefore mainly on the functionality of the MMC, comparing it to the 2-level VSC. An n-level MMC diagram is illustrated in figure 5.

4 Simulations

Simulations are performed to investigate the features in operation of the MMC, both in control and structure. Furthermore, the simulations compare the MMCs suitability for the proposed system, with a conventional two-level VSC. A five level MMC model is built in PSCAD. Features like redundancy and submodule voltage balancing are implemented. In addition, the converter model is implemented in a simulation of the complete system.

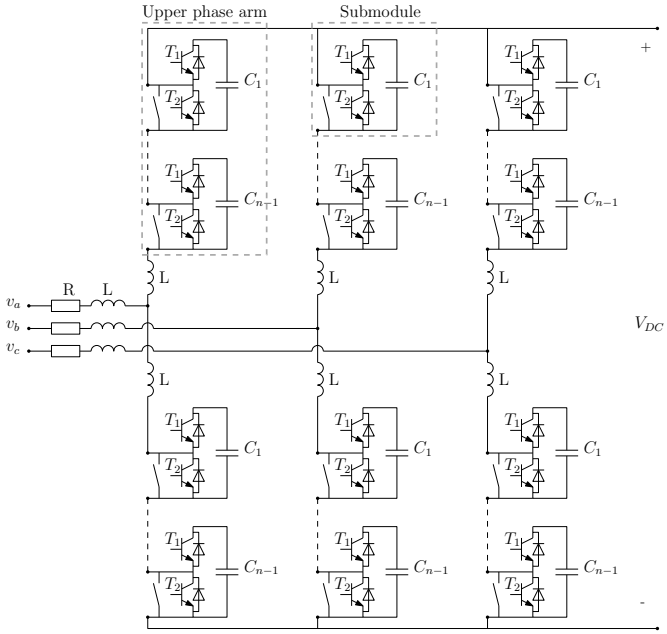

Figure 5: Principal drawing of an n-level MMC

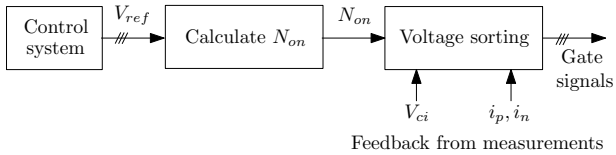

Figure 6: Balancing strategy

4.1 Capacitor voltage balancing strategy

A voltage balancing issue was in an initial study experienced in the MMC as well. Voltage balancing control is therefore needed for the multilevel modular converter to function as expected [19]. Without a good balancing strategy, the mid-capacitor voltages drifts towards zero, see figure 8a, and the top and bottom modules in one arm are stressed with the whole DC-voltage. This means that the DC-link voltage is shared by the two other capacitors, and that the whole converter eventually acts as a three level converter - increasing the stress on each switch. The effect on the phase voltages is indicated in figure 8b.

A balancing control is implemented in the simulation models. The strategy follows the one described in [20]. The strategy is to charge those sub-modules with the lowest capacitor voltages, and discharge the sub-modules with highest capacitor voltages. A sorting algorithm ensures the charge or discharge of the correct sub-modules. This is possible because the voltage level generated in the MMC converter depends upon the number of ON-state switches in the upper arm and the lower arm, and not by the specific order these are turned on.

The capacitor voltage balancing strategy can be summed up as follows. For each switching instant,

1. The capacitor voltages of all capacitors are measured and indexed
2. The arm current direction is identified
3. The necessary number of ON-state submodules is calculated
4. A selection of the sub-modules is done
5. Gate pulses based on the selection of sub-modules are generated

The overall control strategy is illustrated in figure 6. The outer control system is described in [7]. The calculation of the number of ON-state submodules is done using a conventional carrier

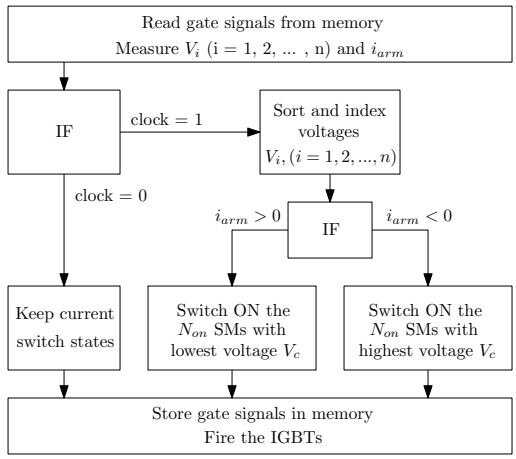

Figure 7: Schematic of the submodule voltage balancing algorithm implemented in simulations

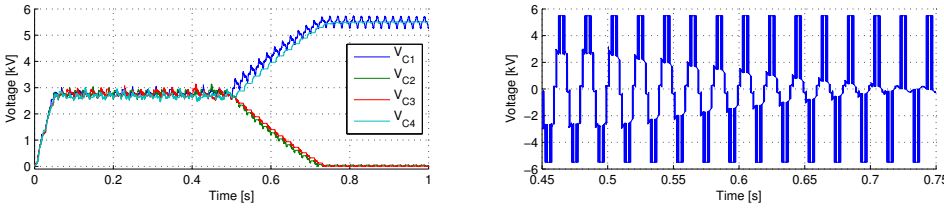

Figure 8: a) Capacitor voltages of phase a, upper leg. Capacitor voltage balancing disabled at t = 0.5 s, b) Phase voltage V_a from the instant of disabling the capacitor voltage balancing.

based pulse width modulation. A schematic showing the voltage sorting algorithm is shown in figure 7.

Simulations in PSCAD demonstrate that the sorting algorithm from [20] is required for the operation of the MMC, as expected. As shown in figure 8, the capacitor voltages in the upper arm of phase a is balanced around 2.75 kV, which is one fourth of the DC-link voltage. At t = 0.5 s, the capacitor voltage sorting is disabled in the calculation block, and as expected the voltages drift towards zero and V_{dc} = 5.5 kV, i.e. the extremities. The measured total harmonic distortion (THD) in the line to line voltage V_{ab} increases from 14 % (before disabling balancing) to 35 % (after t = 0.7s).

4.2 Redundancy

One benefit of the MMC, which is in line with ideas behind the proposed concept, is the possibility of redundancy [9]. A failure of one submodule in one phase arm is included in the simulations. The voltage balancing control algorithm is changed to adjust to this bypass.

The results of the bypass, described in figures 9a-d, demonstrate that the voltages in each of the remaining submodules are increased, the phase voltage in the converter is reduced to four levels, and the harmonic content in voltages and currents is increased. A fault in one of the submodules of phase a, does only affect the phase voltage of the same phase, and the corresponding phase current. This is indicated in figure 9b and 9c. The line-to-line voltages connected to phase a is also affected, as seen in figure 9d. On this basis, the converter performs as expected, and gives with this a redundancy to the system which increases the reliability and extends the continuous operation of the wind turbine.

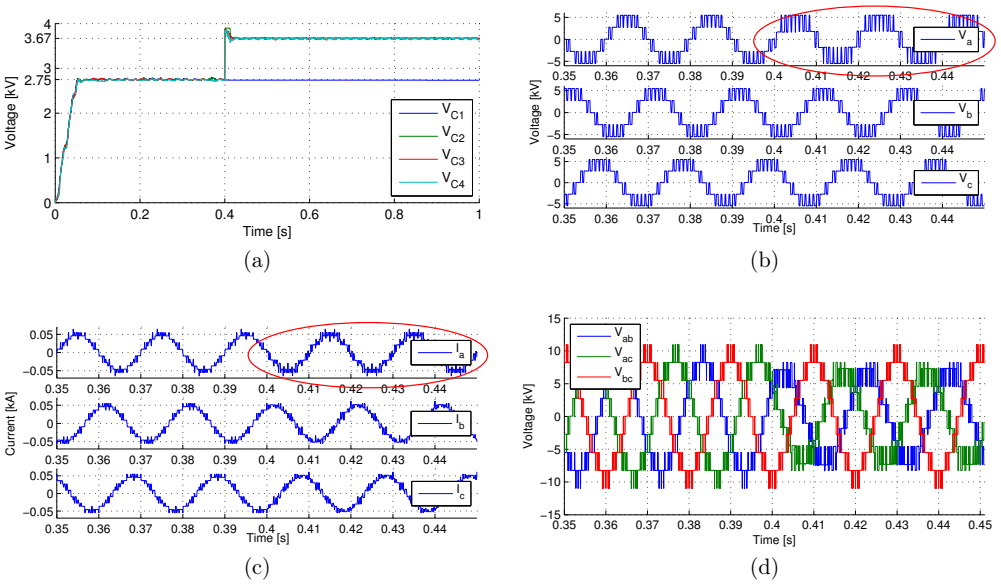

Figure 9: Redundant bypass of submodule 1 in phase a, upper leg at t = 0.4 s: a) Capacitor voltages, b) Phase voltages, c) Line currents, d) Line-to-line voltages

4.3 MMC in the proposed concept

Simulations were preformed on the full system, to document how the chosen converter operates in comparison to the conventional 2-level VSC. The idea is that the system should operate with any voltage controlled converter topologies. Description of the complete system model can be found in [6] and [7]. Due to limitations in the educational version of PSCAD, the system had to be reduced to three converter modules. The total DC link voltage is scaled with respect to the module rating, and reduced to one third of the original, to preserve the original voltage (of 11.1 kV) in each converter module DC output.

The results show that the MMC performs well in the full system, and is therefore considered as a viable candidate. It outperforms the conventional two-level in terms of voltage quality, as expected. Moreover, the system behaves very well to the implementation of a new converter model as well. This is an indication of that the system can tolerate any voltage source converter with a three phase input and a DC-link output.

As seen from figure 10a and b, the line current is less distorted in the MMC setup. The phase voltages have the typical five level staircase waveform with decreased $\frac{dv}{dt}$, and less harmonics than in the two-level setup, see figure 10c and d. Because of the series connection of the three converter modules, the phase currents in figure 10c and d have a offset of ± 11.1 kV. There is low ripple in the DC link voltages, as seen in figure 10e and f. There is however a minor increase in the oscillations of the DC voltage for the MMC, because of the submodule voltage balancing control.

5 Conclusions

In this paper the five most popular multilevel converter topologies have been compared with focus on suitability for a special weight-reducing wind turbine generator concept. The modular multilevel converter (MMC) has several benefits that made it the most interesting topology for further studies: The MMC makes direct series connection of IGBTs unnecessary. In addition, it offers high voltage quality, redundancy possibilities, lower demand for filtering and is easier expandable to a larger amount of levels than the other topologies.

The feature of redundancy is an important feature of the offshore installation, and a case of submodule failure has therefore been simulated in PSCAD. A fault and disconnection of one module is handled by the redundancy control system, and the reliability of the system is therefore increased. Preliminary studies showed that the MMC required balancing control to avoid

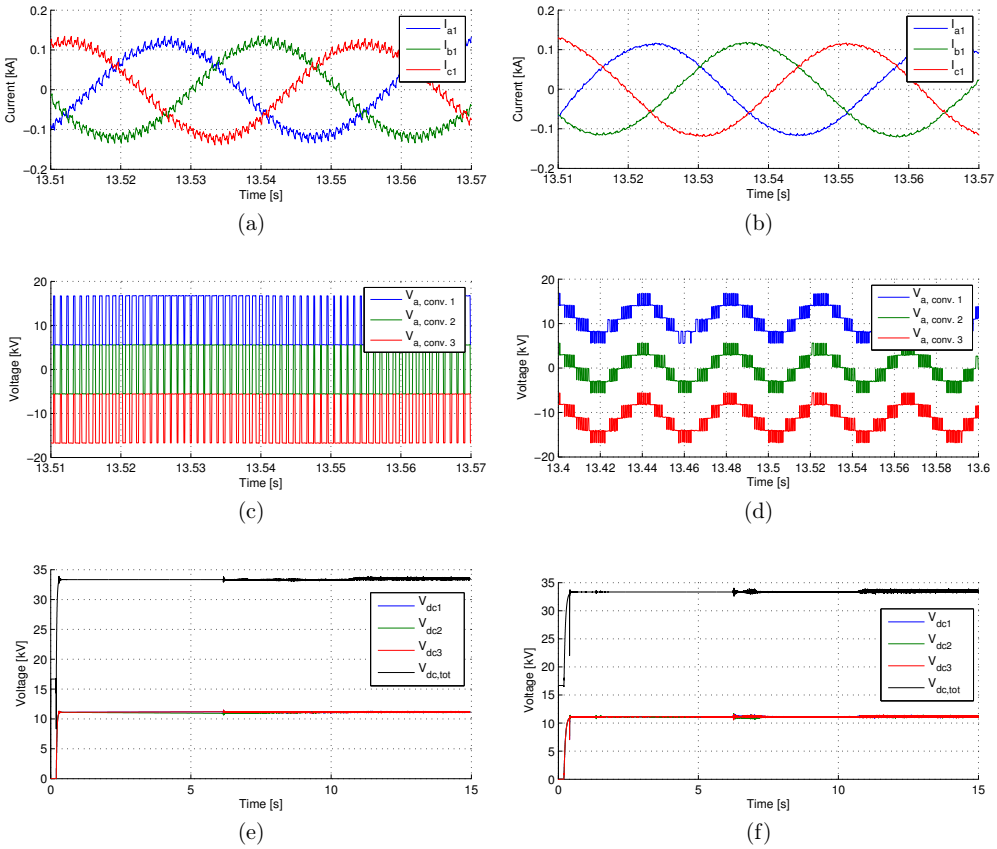

Figure 10: Simulations of the full system models with 2-level VSC (to the left) and 5 level MMC (to the right): a) Line currents with 2-level b) Line currents with MMC c) Phase voltage a in all three converter modules, with 2-level. d) Phase voltage a in all three converter modules, with MMC. e) DC output from 2-level modules, and total DC-link voltage. f) DC output from 5-level MMC modules, and total DC-link voltage.

capacitor voltage drifting. The simulations of the MMC have therefore also included this feature. A voltage balancing strategy was implemented and analysed to ensure correct operation of the converter.

The MMC should have at least five levels to prevent damage to IGBTs because of over voltages in transient periods. This is because of today's limitations in voltage handling of IGBTs. An optimal amount of levels depend upon the desired level of losses, generator specifications, voltage quality and a weighting of reliability versus complexity and cost. This optimization is outside the scope of this work.

The converter has been compared to a conventional two-level converter in a full wind turbine simulation of the proposed generator/converter system. The MMC functioned well in the system, and outperformed the two-level VSC in terms of voltage quality, as was expected. By implementing the features of a multilevel converter into the proposed system, the system can improve in terms of reliability. This is very beneficial in offshore installations where accessibility is limited.

6 Further work

The scope of further work includes laboratory testing of the proposed generator/converter combination, and an optimization to find the ideal number of levels for the MMC. This optimization could also consider the number of converter modules and the total DC-link voltage, which were

set for this work. Economical considerations is also left out for further work. In addition, more practical issues like structural design and detailed weight estimates should be studied.

References

[1] P.K Olsen, S. Gjerde, R.M. Nilssen, J. Holto and S. Hvidsten,*A Transformerless Generator-Converter Concept making feasible a 100 kV Low Weight Offshore Wind Turbine Part I - The Generator*, Accepted for IEEE Energy Conversion Congress & Exposition (ECCE), Raleigh, NC, USA, 2012.

[2] World Wind Energy Association. World Wind Energy Report 2010, accessed sept. 13, 2011. `http:\\www.wwindea.org`

[3] Walford, C. A. *Wind Turbine Reliability: Understanding and Minimizing Wind Turbine Operation and Maintenance Costs*, Sandia National Laboratories, 2006

[4] Zhaoqiang Zhang, Alexey Matveev, Sigurd Ovrebo, Robert Nilssen, and Arne Nysveen. *State of the art in generator technology for offshore wind energy conversion systems*, In Electric Machines Drives Conference (IEMDC), 2011 IEEE International, pages 1131 - 1136, 2011.

[5] J. Ribrant and L. Bertling. *Survey of failures in wind power systems with focus on Swedish wind power plants during 1997-2005*, In Power Engineering Society General Meeting, 2007. IEEE, pages 1 - 8, june 2007.

[6] S. Gjerde and T. Undeland. *Power conversion system for transformer- less offshore wind turbine*, In Power Electronics and Applications (EPE 2011), Proceedings of the 2011-14th European Conference on, pages 1 - 10, sept. 2011.

[7] S. Gjerde and T. Undeland. *A Modular Series Connected Converter for a 10 MW, 36 kV, Transformer-Less Offshore Wind Power Generator Drive*, In Energy Procedia: DeepWind, 19-20 January 2012, Trondheim, Norway, Elsevier Ltd, 2011.

[8] E. Spooner, P. Gordon, and C.D. French. *Lightweight, ironless-stator, PM generators for direct-drive wind turbines*, In Power Electronics, Ma- chines and Drives, 2004. (PEMD 2004). Second International Conference on (Conf. Publ. No. 498), volume 1, pages 29 - 33 Vol.1, march - 2 april 2004.

[9] S. Gjerde and T. Undeland. *Fault Tolerance of a 10 MW, 100 kV Transformerless Offshore Wind Turbine Concept with a Modular Converter System*, In 15th International Power Electronics and Motion Control Conference, EPE-PEMC 2012 ECCE Europe, Novi Sad, Serbia, 2012.

[10] Mohan, N; Undeland, T.M; Robbins, W.P, *Power Electronics: Converters, Applications and Design*, John Wiley & Sons, 2003.

[11] Mitsubishi Electric. *Mitsubishi Electric HVIGBT Module Data Sheets*, accessed June 4rd, 2012. `http://www.mitsubishielectric.com/`

[12] R. Lund. *Multilevel Power Electronic Converters for Electrical Motor Drives*, PhD thesis, NTNU, 2005.

[13] L. Yang, C. Zhao, and X. Yang. *Loss calculation method of modular multilevel HVDC converters*, In Electrical Power and Energy Conference (EPEC), 2011 IEEE, pages 97 - 101, oct. 2011.

[14] A. Nabae, I. Takahashi and H. Akagi. *A New Neutral-Point-Clamped PWM Inverter*, Industry Applications, IEEE Transactions, 1981.

[15] M. Khazraei, H. Sepahvand, K. Corzine, and M. Ferdowsi. *A generalized capacitor voltage balancing scheme for flying capacitor multilevel converters*, In Applied Power Electronics Conference and Exposition (APEC), 2010 Twenty-Fifth Annual IEEE, pages 58 - 62, 2010.

[16] J. Wen and K. Smedley. *Hexagram Rectifier x2014; Active Front End of Hexagram Inverter for Medium-Voltage Variable-Speed Drives*, Power Electronics, IEEE Transactions on, 23(6): 3014 - 3024, nov. 2008.

[17] H. Iman Eini, Sh. Farhangi, and J.L. Schanen. *A modular AC/DC rectifier based on cascaded H-bridge rectifier*, In Power Electronics and Motion Control Conference, 2008. EPE-PEMC 2008. 13th, pages 173 - 180, sept. 2008.

[18] A. Lesnicar and R. Marquardt. *An innovative modular multilevel converter topology suitable for a wide power range*, In Power Tech Conference Proceedings, 2003 IEEE Bologna, volume 3, page 6 pp. Vol.3, june 2003.

[19] M. Hagiwara and H. Akagi. *PWM control and experiment of modular multilevel converters*, In Power Electronics Specialists Conference, 2008. PESC 2008. IEEE, pages 154 - 161, june 2008.

[20] P. M. Meshram and V. B. Borghate. *A novel voltage balancing method of Modular Multilevel Converter (MMC)*, In Energy, Automation, and Signal (ICEAS), 2011 International Conference on, pages 1 - 5, 2011.